

**DEVELOPMENT OF NANO BIO-SORBENT  
COMPOSITE FOR REMOVING HEXAVALENT  
CHROMIUM FROM INDUSTRIAL EFFLUENT**

Thesis Submitted for the Award of the Degree of

**DOCTOR OF PHILOSOPHY**

**in**

**Biotechnology**

**By**

**Shashank Garg**

**Registration Number: 41800493**

**Supervised By**

**Dr. Jastin Samuel (22757)**

**Department of Microbiology (Assistant Professor)**

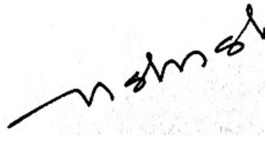
**Lovely Professional University**



**LOVELY PROFESSIONAL UNIVERSITY, PUNJAB  
2024**

## **DECLARATION**

I, hereby declared that the presented work in the thesis entitled “**Development of nano bio-sorbent composite for removing hexavalent chromium from industrial effluent**” in fulfilment of degree of **Doctor of Philosophy (Ph.D.)** is outcome of research work carried out by me under the supervision of Dr. Jastin Samuel, working as Associate Professor, in the Microbiology Department/School of Bioengineering and Biosciences of Lovely Professional University, Punjab, India. In keeping with general practice of reporting scientific observations, due acknowledgements have been made whenever work described here has been based on findings of other investigator. This work has not been submitted in part or full to any other University or Institute for the award of any degree.



**(Signature of Scholar)**

Name of the scholar: Shashank Garg

Registration No. 41800493

Department/school: Biotechnology/School of Bioengineering and Biosciences

Lovely Professional University,

Punjab, India

## CERTIFICATE

This is to certify that the work reported in the Ph.D. thesis entitled “**Development of nano bio-sorbent composite for removing hexavalent chromium from industrial effluent**” submitted in fulfillment of the requirement for the reward of degree of **Doctor of Philosophy (Ph.D.)** in the Department of Biotechnology/School of Bioengineering and Biosciences, is a research work carried out by Shashank Garg, 41800493, is bonafide record of his/her original work carried out under my supervision and that no part of thesis has been submitted for any other degree, diploma or equivalent course.



**(Signature of Supervisor)**

Name of supervisor: Dr. Jastin Samuel

Designation: Assistant Professor

Department/school: Microbiology Department/School of Bioengineering and Biosciences

University: Lovely Professional University, Punjab, India

## ACKNOWLEDGEMENT

All praises to Almighty for giving me strength and patience for completing this research work. I thank Almighty for providing ways and opportunities and enabling me to overcome difficulties which have constantly motivated me to follow the path towards completion of this project.

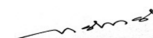
I would like to acknowledge my indebtedness, render my warmest thanks and express my sincere gratitude to my esteemed supervisor **Dr. Jastin Smauel**, Department of Microbiology, School of Bioengineering and Biosciences, Lovely Professional University, for his attentive guidance, constructive criticism, immense knowledge, scientific suggestions and full support in completion of this thesis successfully. It has been a great pleasure and honour to have his as my supervisor. I shall emphasize contribution of **Dr. Joginder Singh** for his immense support and motivation in this entire journey. Without him the work would not have completed.

I prolong my heartfelt thanks to **Dr. Neeta Raj Sharma**, Head of the School of Bioengineering and Biosciences, **Dr. Himanshu Singh**, Head of the Department of Biotechnology, **Dr. M.A. Khan**, Head of Laboratory School of Bioengineering and Biosciences and all other faculty members of the School of Bioengineering and Biosciences I take this opportunity to express warm thanks to **Dr. Ashok Mittal** (Chancellor), **Mrs. Rashmi Mittal** (Pro-Chancellor), **Dr. Loviraj Gupta** (Pro Vice-Chancellor), **Dr. Monica Gulati** (Registrar) for providing an opportunity to work in such a prestigious university. The matter would have not completed without unconditional gesture of my dear friend **Dr. Amit Jaiswal**, Associate Professor, IIT Mandi, who helped me with nanoparticle procurement and characterization. I also want to give my special appreciation to our lab technician **Mr. Kuldip**, **Mr. Varinder**, **Mr. Sandeep** for providing support required at every stage of my research work. I cannot forget the encouragement, support and help of my friends and colleagues **Mr. Sanjeev Singh**, **Dr. Prabhjot Singh Jassal**, **Dr. Joydeep Dutta**, **Dr. Anand Mohan**, **Dr. Anupam Kumar**, **Dr. Ajay Kumar** throughout this journey.

I would like to dedicate this thesis to my parents, **Dr. Madan Gopal Garg**, and **Smt. Aruna Garg**, my wife, **Smt. Jaspreet Kaur Garg**, my little ones, **Advika** and **Viraj** who made the life simpler for me and who were constantly willing to provide everything I needed during the journey of this research and their endless sacrifice have helped me reach where I stand today. I am forever thankful to God for giving me such parents who are always supportive of my dreams and for their unconditional love.

Lastly, I would like to thanks all whom I have not mentioned by name, but directly or indirectly helped me to complete my experimental work and thesis.

Date: 12/04/24



Shashank Garg



## ABSTRACT

This thesis addresses the removal of hexavalent chromium from water. The existing solutions for hexavalent chromium remediation from water often involve physical, chemical, and biological techniques. Combining these methods has a high probability of a better solution to the problem. Physical treatment involves adsorption, ion exchange, and filtration. The methods are simple and economical but are generally rate-limited and thermodynamically controlled, which may lead to a longer time of operation and also may not be able to convert Cr(VI) to a less toxic form. Disposal of adsorbent creates further problems. Chemical and electrochemical methods are found to be faster, but these are not economical, require expertise for operation, and generate lots of secondary sludge.

In the current study, a new composite adsorbent was prepared by combining zero-valent iron nanoparticles and Cr(VI) tolerant bacteria immobilized into calcium alginate beads. Composites of nZVI nanoparticles (which have high adsorption and reduction capacities) with Cr(VI) tolerant bacteria have advantages of both elements.

Cr(VI) tolerant bacteria were isolated from wastewater streams receiving inputs from leather and rubber industries. The bacteria were screened for Cr(VI) tolerance, and the MIC of Cr(VI) for this organism was found to be 400 ppm. Morphological characterization of bacteria revealed that it was a gram-positive, rod-shaped bacteria. Molecular characterization was performed by sequencing 16s rRNA. The amplified product was sequenced, and the sequence was aligned using the BLAST and MSA tools. A phylogenetic tree was constructed, which revealed that this organism was *Bacillus subtilis*.

nZVI was purchased from Sigma Aldrich and was characterized in the lab for its shape, size distribution, purity, and zeta potential. SEM and TEM analysis revealed that the particles are homogenous in shape and found to be spherical. XRD results were compared with JSPDS card no 060696. It showed that the powder was pure and the particles had high crystallinity. The position of the peak revealed metallic iron in the powder, justifying its zero-valent nature. Zeta potential in water at pH 7 was 12.09 mV, suggesting that it achieved moderate stability at the aforementioned pH. DLS experiments were performed, which exhibited that most of the particles were of similar size, corroborating with SEM and TEM results.

Nano-bio-adsorbents (NBA) were simultaneously synthesised with blank (without any nZVI and bacteria). Each combination was used in further experiments. Batch experiments were performed by varying initial pH (5-9), initial Cr(VI) concentration (10-50 ppm), time of

incubation (30-150 min), and adsorbent dosage (0.5-2.5 g) keeping all factor constant but one-factor variable at one time. The effect of these parameters was observed on % Cr(VI) removal and adsorption capacity. pH 7 was found to be most favourable for the adsorption of Cr(VI) on the prepared adsorbent. An adsorbent with both nZVI and bacteria (BNCA) achieved maximum removal (93%) among the different combinations. While varying the initial Cr(VI) concentration, it was found that % removal decreased while adsorption capacity increased with increasing initial Cr(VI) concentration, with maximum removal observed in the case of BNCA. Higher adsorbent dosage gives more % removal which gets saturated at larger dosages. Adsorption capacity was found to be maximum at the lowest adsorbent dosage. % Cr(VI) removal and adsorption capacities were found to increase with time of incubation and remain unchanged after 90 min of incubation.

Isotherm data suggests that the isotherm is most likely to be modelled as per the Sips isotherm or Freundlich isotherm. The Sips isotherm is well-suitable for current adsorption systems as this model assumes that adsorption occurs in a non-ideal, reversible manner that is not limited to monolayer adsorption. The Sips isotherm is a sound model used to study heterogeneous systems. The operating parameters of the isotherm are a relative measure of the heterogeneity of the adsorbent.

Removal kinetics in batch systems was studied and modelled in the current work. The Vermeulen model is the better fitting model for fitting the kinetic data with an  $R^2$  value of 0.995, followed by the PSO model ( $R^2=0.993$ ). The low value of the Y-intercept (0.011) in the Vermeulen model fit revealed that IPD shall be the major rate-limiting step in the entire adsorption process

Fixed bed column studies were performed to evaluate the scope of application of the technology on an industrial scale. The breakthrough curve and its modelling were performed to evaluate the removal parameters. Three different bed heights of columns (4, 8, 12 cm at a constant flow rate of 1 ml/min) and three flow rates (0.5, 1, 1.5 ml/min at constant bed height of 8 cm) were used in this study. From the breakthrough curves for varying flow rates, the breakthrough time (50%) was found to be 380 min, 220 min, and 130 min and breakthrough time (10%) were 115, 90, and 45 min, respectively, for a flow rate of 0.5, 1.0, and 1.5 mL/min. With varying bed heights, the breakthrough time (50%) was found to be 170 min, 220 min, and 270 min and breakthrough time (10%) were 60, 90, and 130 min respectively, for bed heights of 4, 8, and 12 cm respectively. Breakthrough curves were modelled using the Yoon Nelson model and Adams Bohart model, and predicted v/s actual comparisons were

performed, which revealed a good correlation in the initial time of operation, suggesting some heterogeneity in the adsorption onto the bed with due course of time. Fixed bed studies were also performed for real wastewater spiked with Cr(VI). For this, the breakthrough curves for varying flow rates, the breakthrough time (50%) was found to be 230 min, 150 min, and 120 min and breakthrough time (10%) was 110, 70, and 45 min, respectively, for a flow rate of 0.5, 1.0, and 1.5 mL/min. With varying bed heights, the breakthrough time (50%) was found to be 125 min, 150 min, and 180 min and breakthrough time (10%) were 55, 70, and 85 min, respectively, for bed heights of 4, 8, and 12 cm.

The reuse of the spent adsorbent was studied by regenerating it and using it again for adsorption for up to 4 cycles. No significant loss of removal capacity and adsorption capacity was observed for 4 cycles of regeneration and adsorption. The maximum % Cr(VI) removal at the adopted conditions was 89% and adsorption capacity at these conditions was found to be 0.223 mg/g in batch studies.

## TABLE OF CONTENT

1. Introduction.....	1
2. Review of Literature & research gap identification.....	6
2.1 Contamination sources.....	7
2.2 Toxicity to biological systems.....	8
2.3 Remediation technologies.....	9
2.4 Mechanisms involved.....	14
2.5 Mechanism involved in combination of microorganism and nanoparticles.....	14
2.6 International status.....	15
2.7 National status.....	17
2.8 Research Gap.....	19
3. Objectives.....	20
4. Methodology.....	22
5. Materials and methods.....	24
5.1 Screening, isolation and characterization of Cr(VI) tolerant bacteria.....	25
5.1.1 Screening and isolation of bacteria.....	25
5.1.2 Morphological characterization.....	26
5.1.3 Molecular characterization.....	26
5.1.4 Determination of Minimum Inhibitory concentration (MIC) of Cr(VI) .....	31
5.2 Procurement and characterization of zero valent iron nanoparticle (nZVI).....	32
5.2.1 Scanning Electron Microscopy (SEM) and Transmission electron Microscopy (TEM) analysis. ....	32

5.2.2 X Ray Diffraction (XRD) analysis.....	32
5.2.3 Zeta Potential measurement and Dynamic Light Scattering (DLS) analysis.....	32
5.3 Analytical methods to estimate Cr(VI) .....	33
5.4 Development of nanobiosorbent (NBA) .....	33
5.5 Batch studies to evaluate the performance of developed NBA for adsorption of Cr(VI).....	34
5.5.1 Effect of pH on the percentage removal of Cr(VI) .....	34
5.5.2 Effect of initial Cr(VI) concentration on the percentage removal of Cr(VI) .....	35
5.5.3 Effect of time on the percentage removal of Cr(VI) .....	35
5.5.4 Effect of adsorbent dosage on the percentage removal of Cr(VI).....	36
5.5.5 Isotherm modeling and parameter estimation.....	36
5.5.6 Mathematical modeling of the kinetics of batch removal....	37
5.6 Packed Bed Column (PBC) studies for removal of Cr(VI) .....	37
5.6.1 Effect of bed height on percentage removal of Cr(VI) .....	39
5.6.2 Effect of flow rate on percentage removal of Cr(VI) .....	39
5.6.3 Breakthrough curves and its modeling.....	39
5.7 Evaluation of performance of selected NBA in real water matrix under PBC.....	40
5.8 Evaluation of reuse of the adsorbent.....	41
5.9 Disposal of the spent adsorbent.....	41
6. Result and Discussions.....	43
6.1 Water sample collection, bacterial isolation and characterization.....	43
6.1.1 Water sample collection, bacterial isolation and characterization.....	42

6.1.2	Molecular characterization.....	46
6.1.3	Determination of MIC of isolated organism.....	48
6.2	Characterization of nZVI.....	49
6.2.1	Scanning Electron Microscopy and Transmission Electron Microscopy.....	49
6.2.2	X Ray Diffraction study.....	52
6.2.3	Zeta Potential measurement.....	54
6.2.4	Dynamic Light Scattering.....	55
6.3	Standard curve for Cr(VI) by DPC method.....	56
6.4	Characteristics of the developed NBA.....	57
6.5	Batch removal of Cr(VI) .....	60
6.5.1	Effect of pH on the percentage removal of Cr(VI) .....	61
6.5.2	Effect of initial Cr(VI) concentration on the percentage removal of Cr(VI) .....	63
6.5.3	Effect of time on the percentage removal of Cr(VI) .....	65
6.5.4	Effect of adsorbent dosage on the percentage removal of Cr(VI).....	66
6.5.5	Isotherm plotting and modeling.....	69
6.5.6	Mathematical modeling of the kinetics of batch removal.....	71
6.6	Packed Bed Column studies.....	75
6.6.1	Effect of flow rate on breakthrough time.....	78
6.6.2	Effect of bed height on breakthrough time.....	79
6.7	Modeling of breakthrough curves.....	80
6.8	Modeling of PBC under real wastewater matrix spiked with Cr(VI) ..	84
6.9	Reuse of the spent adsorbent.....	86
7.	Summary and Conclusion.....	89

8. Bibliography.....	96
Appendices.....	107
List of publication.....	123
List of conferences.....	126

## List of Figures

Figure 1.1: Predicted growth in market size of chromium in Asia Pacific region .....	2
Figure 1.2: Eh-pH diagram for Chromium.....	3
Figure 5.1: Geographical location of the point of collection of wastewater sample for the study.....	25
Figure 5.2: Experimental design for measurement of MIC.....	31
Figure 6.1: Water sample collected from the effluent stream for studies.....	43
Figure 6.2: Microbes grown over nutrient agar supplemented with 400 ppm Cr(VI) .....	44
Figure 6.3: Brightfield microscopic images of isolated bacteria from tannery effluent.....	45
Figure 6.4: Dendogram pattern obtained after the hierarchical clustering of the sequence.....	47
Figure 6.5: Growth of the isolate in increasing concentration of Cr(VI) supplemented nutrient broth for MIC determination. ....	48
Figure 6.6: Photograph of nZVI powder.....	49
Figure 6.7: SEM image of the nZVI particle	
Figure 6.8: TEM image of the nZVI particle .....	52
Figure 6.9: XRD pattern of the nZVI powder and its comparison with standard JCDPS card no 06-0696.....	53
Figure 6.10: Zeta potential of the nZVI at pH 7.....	54
Figure 6.11: Size distribution pattern of the nZVI particles as per Dynamic Light Scattering experiment.....	55
Figure 6.12: Standard curve for measurement of Cr(VI) in aqueous solution.....	56
Figure 6.13: Slurry obtained after mixing Cr(VI) tolerant bacteria and nZVI. The slurry appears black in color.....	57
Figure 6.14: Setup to prepare beads for different experiments. The picture is of formation of beads with slurry containing Cr(VI) tolerant bacteria and nZVI.....	58



Figure 6.15: Beads of calcium alginate used as immobilization matrix.....	58
Figure 6.16: SEM image of an individual CA bead.....	59
Figure 6.17: SEM image of CA bead. ....	59
Figure 6.18: SEM image of CA bead with nZVI particle immobilized inside it. ....	60
Figure 6.19: Graph representing change in % Cr(VI) removal with varying pH.....	62
Figure 6.20: Graph representing change in % Cr(VI) removal with varying initial Cr(VI) concentration.....	64
Figure 6.21: Graph representing change in % Cr(VI) removal with varying time.....	66
Figure 6.22: Graph representing change in % Cr(VI) removal with varying adsorbent dosage.....	68
Figure 6.23: Isotherm for adsorption of Cr(VI) on BNCA.....	69
Figure 6.24 Non linear fit of isotherm to (A) Langmuir model, (B) Freundlich model, (C) Sips model.....	71
Figure 6.25: Graphs of kinetic data of the adsorption process.....	73
Figure 6.26: Fixed columns made of BNCA beads.....	76
Figure 6.27: Column setup to run the experiments of fixed bed column studies.....	77
Figure 6.28: Breakthrough curves for adsorption with constant bed height and variable flow rate.....	78
Figure 6.29: Breakthrough curves for adsorption with constant flow rate and variable bed height.....	79
Figure 6.30: Modeling of breakthrough curve .....	83
Figure 6.31: Breakthrough curve for adsorption of Cr(VI) from spiked real WW under variable height and constant flow rate.....	84
Figure 6.32: Breakthrough curve for adsorption of Cr(VI) from spiked real WW under variable flow rate and constant bed height.....	85
Figure 6.33: Removal percentage of Cr(VI) in batch mode upon reusing the adsorbent after 4 cycles of regeneration.....	88
Figure 6.34: Equilibrium adsorption capacity of adsorbent for removal of Cr(VI) in batch mode upon reusing the adsorbent after 4 cycles of regeneration.....	88

## List of tables

SN	Title	Page no.
Table 2.1	Conventional and advances methods of reducing chromium content in the effluents	14
Table 2.2	Some important work at international level related to Cr(VI) removal from wastewater	17
Table 2.3	Some recent work at national level for removal of Cr(VI) from wastewater	18
Table 6.1	Modeled equations of isotherms with their parameters and coefficient of determination	70
Table 6.2	Modeled equations of adsorption kinetics with its parameters and coefficient of determination	74
Table 6.3	Change in the breakthrough time (10% and 50%) with change in flow rate	78
Table 6.4	Change in the breakthrough time (10% and 50%) with change in bed height	79
Table 6.5	Model and analysis of breakthrough curve for Adams-Bohart equation with varying bed height and constant flow rate (1 ml/min)	81
Table 6.6	Model and analysis of breakthrough curve for Adams-Bohart equation with varying bed height and constant bed height (8 cm)	81
Table 6.7	Model and analysis of breakthrough curve for Yoon Nelson equation with varying bed height and constant flow rate (1 ml/min)	82
Table 6.8	Model and analysis of breakthrough curve for Yoon Nelson equation with varying bed height and constant bed height (8 cm)	82
Table 6.9	Breakthrough time (10% and 50%) for adsorption of Cr(VI) in PBC using spiked real WW with variable flow rate and constant bed height	86
Table 6.10	Breakthrough time (10% and 50%) for adsorption of Cr(VI) in PBC using spiked real WW with variable flow rate and constant bed height	86
Table 7.1	Adsorption capacities of similar adsorbents	94

### List of abbreviations

1	ANOVA	Analysis of variance
2	Cr(III)	Trivalent chromium species
3	Cr(VI)	Hexavalent chromium species
4	DLS	Dynamic Light Scattering
5	DPC	Diphenyl Carbazide
6	ID	Internal Diameter
7	IPD	Intra Particle Diffusion
8	l	Liter
9	mg	Milligram
10	MIC	Minimum Inhibitory Concentration
11	min	Minutes
12	mL	Milliliter
13	mM	Millimolar
14	NB	Nutrient Broth
15	NBA	Nano-bio Adsorbent
16	nm	Nanometer
17	nZVI	Zero Valent Iron Nanoparticle
18	OD	Optical Density
19	PBC	Packed Bed Column
20	PEG	Poly Ethylene Glycol
21	PPM	Parts per Million
22	RPM	Revolutions per Minute
23	SEM	Scanning Electron Microscope
24	SSE	Sum of Square of Errors
25	TEM	Transmission Electron Microscopy
26	WW	Wastewater
27	XRD	X ray Diffraction
28	µg	Microgram

## **List of Appendices**

1. Table A.1: Cr(VI) removal percentage for different adsorbents in study under varying pH.
2. Table A.2: Cr(VI) removal percentage for different adsorbents in study under varying initial Cr(VI) concentration
3. Table A.3: Cr(VI) removal percentage for different adsorbents in study with time
4. Table A.4: Cr(VI) removal percentage for different adsorbents in study under varying adsorbent dosage
5. Table A.5: Two way ANOVA analysis for effect of pH and adsorbent type on Cr(VI) removal percentage
6. Table A.6: Two way ANOVA analysis for effect of initial Cr(VI) concentration and adsorbent type on Cr(VI) removal percentage
7. Table A.7: Two way ANOVA analysis for effect of time and adsorbent type on Cr(VI) removal percentage
8. Table A.8: Two way ANOVA analysis for effect of adsorbent dosage and adsorbent type on Cr(VI) removal percentage
9. Table A.9: Variation of  $C/C_0$  with time for fixed bed column under variable bed height with synthetic wastewater
10. Table A.10: Variation of  $C/C_0$  with time for fixed bed column under variable flow rate with synthetic wastewater
11. Table A.11: Variation of  $C/C_0$  with time for fixed bed column under variable bed height with spiked real wastewater
12. Table A.12: Variation of  $C/C_0$  with time for fixed bed column under variable flow rate with spiked real wastewater
13. Table A.13: Cr(VI) removal percentage under four cycles of adsorbent regeneration
14. Table A.14: ANOVA table for effect of adsorbent reuse on Cr(VI) removal percentage

**Chapter 1**  
**INTRODUCTION**

## 1. Introduction

With an increasing population, there is an unprecedented increment in the demand for products which demands a higher number of industrial units, which has resulted in a increase in the various detrimental pollutants released by the industries (Kumar et al. 2020, Singh et al. 2020). A group of such pollutants is salts containing chromium, which are used and released along with effluents from various industries like leather processing (Chowdhury et al. 2015, Sivaram and Barik 2019), electroplating (Sibi 2016, Alvarez et al. 2021), printing (Jangra 2016), dyeing (Varjani et al. 2021), and metallurgy (Coetzee et al. 2020). As per the research by Precedence Research, the chromium market size is expected to increase 1.8 times in next 10 years (Fig .1.1).



Fig 1.1: Predicted growth in market size of chromium in Asia Pacific region. (report fetch on 28 April 2024 from <https://www.precedenceresearch.com/chromium-market>)

There are various chromium-containing chemical species which are produced during different unit operations (Pradhan et al. 2017). Among the most commonly found species in the natural environment, the oxidation state of chromium is found to be trivalent chromium Cr(III) and hexavalent chromium Cr(VI) as they are comparatively stable forms. These species are interconvertible to each other depending on the pH and redox potential of the environment. The Eh-pH diagram can predict this conversion (Fig: 1.2).

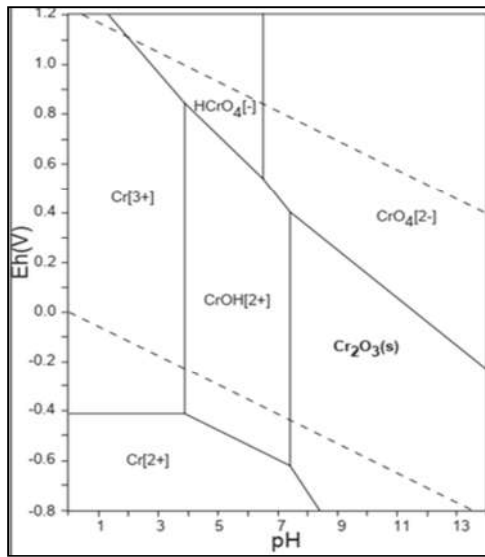


Fig. 1.2 Eh-pH diagram for Chromium (The Atlas of Eh-pH Diagrams, Geological Survey of Japan, Open File Report No. 419 (2005))

The salts from industries are spent in effluent wastewater, which eventually reaches the human and animal systems through various matrices and pathways (Engwa et al. 2019). Improper disposal of effluent water in these industries is leading to serious health issues for soil and aquatic ecosystems. The water released to natural sources like rivers and ponds accumulates the compounds which eventually leach to groundwater. The people living in the nearby regions of the industries are inadvertently exposed to heavy doses of Cr compounds. The consequences are fatal for plants and animals as chromium is carcinogenic and mutagenic beyond a certain limit (DesMarias and Costa 2019, Pavesi and Moreira 2020).

To reduce the amount of chromium in the effluent water, industries adopt various methods which generally immobilizes Cr(VI) and/or reduce it to Cr(III), the latter being a less toxic form as compared to the former (Dong et al. 2017, Jobby et al. 2018). Immobilization although reduces the Cr(VI) content from wastewater but suffers from the limitation that it does not remove the metal ion from the environment (Crini and Lichtfouse 2019, Younas et al. 2021). To alleviate this, adsorption and simultaneous reduction to Cr(III) shall be performed. This form (Cr(III)) is less toxic and can be recovered easily from wastewater giving a better solution for the environmental toxicity issues.

According to literature, various synthetic and natural materials have been used as adsorbents for Cr(VI) (Islam et al. 2019). Several methods including electroplating (Jin et al. 2016), chemical (Peng and Guo 2020), and biological methods (Malaviya and Singh 2016, Sharma et al. 2022) have been proposed for the reduction of Cr(VI). It has been clearly indicated that electroplating and chemical methods are effective but produce a large amount of sludge which requires additional strategies for disposal (Peng and Guo 2020).

There are different mechanisms that facilitate the removal of chromium related to different methods. Chemical methods mostly rely on conversion of Cr species into insoluble form like chromium hydroxide that is precipitated as insoluble form. In chemical precipitation, calcium hydroxide and sodium hydroxide are generally employed to reduce Cr(VI) to Cr(III) and further conversion of same to hydroxide form that is precipitated out (Ramakrishnaiah and Prathima 2012). Photocatalytic reduction generally reduces Cr(VI) to Cr(III) in presence of visible light and a catalyst and does not produce any sludge (Wang et al. 2020). Electrocoagulation of Cr(VI) may lead to different products depending on the pH of the reaction (Kabdaşlı and Tünay 2023).

Physical methods employed utilize adsorption principle, filtration (ultrafiltration, reverse osmosis), or electrostatic interactions (ion exchangers, electrodialysis) for their working.

Biological methods for Cr(VI) removal are complex as these employ combination of mechanisms like electrostatic attraction followed by adsorption and chemical reaction for either conversion of Cr(VI) to metallic form or reduce it to Cr(III) (Chen and Tian 2021). The reduction can be mediated by extracellular enzymes, membrane bound enzymes or intracellular enzymes (Rahman and Thomas 2021).

Nanomaterials like nZVI can do simultaneous adsorption and reduction of Cr(VI) but is limited by dispersal problems and formation of oxide layer on its surface which stops its further activity. Regenerating the surface may increase the capacity of nanomaterial for reduction of Cr(VI).

Taking these issues into account, the current study hypothesized to produce a novel adsorbent with the combined attribute of *simultaneous adsorption and reduction of*



*hexavalent chromium*. This will be a combination of nanoparticles and bacteria as adsorbent which can synergistically reduce and remove Cr(VI) from the environment.

**Chapter 2**  
**REVIEW OF LITERATURE**

## **2. Review of Literature**

The contamination of the environment is increasing day by day and is progressively becoming more severe. Heavy metals, pesticides, halogenated and aromatic hydrocarbons, chlorinated solvents and salts are the major widespread toxic contaminants of soil, air and water (Mansour and Gad 2010). Heavy metals are the elements in the periodic table that have an atomic weight higher than 20 and associated properties such as conductivity, ductility, and specificity. Among a total of 118 naturally occurring elements, 90 are heavy metals, but all are not biologically significant. Based on the solubility and availability to the living cells, only 17 heavy metals are important and essential to the living system (Mahurpawar 2015). Out of these 17 metals, iron, manganese, and molybdenum are the essential micronutrients whereas cobalt, chromium, copper, nickel, zinc, tungsten and vanadium are toxic at elevated concentrations (Jyothi 2020).

### **2.1 Contamination sources**

The natural occurrences and anthropogenic activities are the primary sources of heavy metal contamination in the environment. Anthropogenic sources of heavy metal contamination include mining, agrochemicals, metal processing industries, battery manufacturing industries, paint and preservatives, fossil fuel combustion, bio-solids and automobile exhausts. Effluent from various industries is one of the key sources, polluting the majority of water bodies, which in turn directly or indirectly pollutes nearby agricultural fields and soil. Industrial wastewater is a reservoir of recalcitrant organic and inorganic substances and metal ions, depending on the type of industry. Industrial effluent from different industries such as fertilizer and pesticide, mining, smelting, metallurgy, surface finishing, iron and steel, electroplating, electrical equipment manufacturing, leather and textile industry, photography, atomic energy installation, fuel and energy production, aerospace and many more are discharging metals as the major contaminants (Hanchang 2009). Chromium is released into the environment through effluents from electroplating, leather tanning, wood preservation, pulp processing, steel manufacturing, and industries. Hexavalent chromium is highly soluble in water and carcinogenic to humans (Holmes et al. 2008). Because of the ill effects of these metals on life forms, several limits have been included to release chromium into the environment (Breida et al. 2019, Vaiopoulou

and Gikas 2020). As per General Standards for Discharge Of Environmental Pollutants of Central Pollution Control Board, the permissible limit of Cr(VI) in WW leaving to inland surface and public sewers are 0.1 and 2.0 mg/L. Because chromium compounds were used in leather tanning, paints, and dyes, they are frequently detected in soil and groundwater at former industrial sites. As with brownfield land, these sites require environmental cleanup and remediation.

## **2.2 Toxicity to biological systems**

The toxicity of chromium and other heavy metals towards animal systems is strongly linked to its oxidation state. These elements may be conjugated to proteins and DNA to form stable, bio-toxic compounds. In a recent study by Shaw et al., it has been shown that chromium concentration as low as 2 mg/L can induce oxidative stress in zebrafish (Shaw et al. 2019). Oxidative stress is a well-known factor for the induction of various abnormal situations through oxidation of cellular proteins and lipids mediated by Reactive Oxygen Species (ROS). Jindal et al. also have concluded the same remarks in a separate work done performed on expression of Nrf2 and MT2 genes in the bronchial tissue of *Ctenopharyngodon idellus* (Jindal and Handa 2019). Des Marais et al. (2019) have reviewed the mechanisms of chromium-induced toxicity and have concluded that complex mechanisms, including oxidative stress, epigenetic changes, chromosome and DNA damage, and mutagenesis, are responsible for its toxicity (DesMarias and Costa 2019). Similar results have been published by Zablon et al. (2019), which reported that Cr(VI) induces direct macromolecular damage, changes transcription factor function, and disrupts epigenetic signatures, which results in changes in gene expression in a variety of cell signaling pathways. (Zablon et al. 2019).

A study on inhabitants of Kanpur, India (an area with lot of tanneries and chromium salts manufacturing industries), have revealed that high levels of Cr (VI) in groundwater is associated with gastrointestinal and dermatological complaints and abnormal hematological function (Sharma et al. 2012).

### **2.3 Remediation technologies**

To safeguard the environment from hazards of Cr(VI), it is required to reduce the amount of chromium (VI) in the effluent water by treating it through certain processes. The following Table 2.1 comprehends the conventional and advances methods of reducing chromium content in the effluents.

<b>Method</b>	<b>Gap</b>	<b>Proposed Technology</b>	<b>Reference</b>
Adsorption	<ol style="list-style-type: none"> <li>1. No reduction of Cr(VI), only accumulation.</li> <li>2. Dispensing the spent adsorbent</li> </ol>	<ol style="list-style-type: none"> <li>1. Reduction by nZVI and microorganism</li> <li>2. Spent matrix can be easily utilized in fabrication of roads and structures or can be reutilized after washing.</li> </ol>	<p>(Enniya et al. 2018)</p> <p>(Vakili et al. 2018)</p>
Ion exchange	<ol style="list-style-type: none"> <li>1. No reduction of Cr(VI), only accumulation.</li> <li>2. Dispensing the spent adsorbent and regeneration of column causes secondary pollution.</li> <li>3. Costly</li> </ol>	<ol style="list-style-type: none"> <li>1. Reduction by nZVI and microorganism</li> <li>2. Spent matrix can be easily utilized in fabrication of roads and structures or can be reutilized after washing.</li> <li>3. Cheap</li> </ol>	(Fu and Wang 2011)
Membrane filtration	<ol style="list-style-type: none"> <li>1.No reduction of Cr(VI), only accumulation.</li> <li>2.Dispensing the spent adsorbent</li> <li>3.Costly</li> <li>4.Labor intensive</li> </ol>	<ol style="list-style-type: none"> <li>1. Reduction by nZVI and microorganism</li> <li>2. Spent matrix can be easily utilized in fabrication of roads and structures or can be reutilized after washing.</li> <li>3. Cheap</li> <li>4. Not much labor and expertise required as the matrix will be available as a general adsorbent</li> </ol>	(Fu and Wang 2011, Kargar and Zolfaghari 2018)
Reverse osmosis	<ol style="list-style-type: none"> <li>1. No reduction of Cr(VI), only accumulation.</li> <li>2. Dispensing the spent adsorbent</li> <li>3. Costly</li> </ol>	<ol style="list-style-type: none"> <li>1. Reduction by nZVI and microorganism</li> <li>2. Spent matrix can be easily utilized in fabrication of roads and structures or can be</li> </ol>	(Kazemi et al. 2018)

		reutilized after washing. 3. Cheap	
Granular activated carbon	1.No reduction of Cr(VI), only accumulation. 2. Dispensing the spent adsorbent 3. Costly	1. Reduction by nZVI and microorganism 2. Spent matrix can be easily utilized in fabrication of roads and structures or can be reutilized after washing. 3. Cheap	(Fu and Wang 2011)
Floatation	1. High cost of operation 2. Maintenance cost is high	1. Low cost of operation after scaling up. 2. Low maintenance	(Fu and Wang 2011)
Electrokinetic methods	1. Costly. 2. Scale up is difficult	1. The proposed technology will be cheaper. 2. Scale up with sorption technology is comparatively easy.	(Cherifi et al. 2016)
Electrocoagulation	1. Costly. 2. Scale up is difficult, 3. Electrodes are sacrificed regularly.	1.The proposed technology is cheaper as, (a) the sorbent is green synthesized, (b) biocomposite and the immobilization matrix are cheap. 2. Scale up with sorption technology is comparatively easy. 3. No depletion of sorbent as microbe is immobilized along with nZVI in a matrix.	(Jin et al. 2016)
Electrochemical reduction	1. Costly 2. Lead oxide electrodes are used	1. Cheaper 2. No secondary pollution is created.	(Jin et al. 2016)

Electrodialysis	<ol style="list-style-type: none"> <li>1. No reduction of Cr(VI), only accumulation.</li> <li>2. Costly</li> <li>3. poor stability of membrane</li> <li>4. polarization.</li> </ol>	<ol style="list-style-type: none"> <li>1. Reduction by nZVI and microorganism</li> <li>2. Cheap</li> <li>3. No membrane involved</li> <li>4. No problems related to polarization</li> </ol>	(Jin et al. 2016)
Electrodeionization	<ol style="list-style-type: none"> <li>1. Costly</li> </ol>	<ol style="list-style-type: none"> <li>1. No power required, cheap</li> </ol>	(Zhao et al. 2018)
Hydrogen sulfide	<ol style="list-style-type: none"> <li>1. Secondary pollution,</li> <li>2. Not species specific,</li> <li>3. Sludge disposition adds to cost.</li> </ol>	<ol style="list-style-type: none"> <li>1. Secondary pollution is not created as synthesis is eco-friendly and reduction of chromium takes place.</li> <li>2. Less sludge is formed that too non toxic</li> </ol>	(Pena-Caballero et al. 2016)
Sodium dithionite	<ol style="list-style-type: none"> <li>1. Secondary pollution,</li> <li>2. Not species specific,</li> <li>3. Sludge disposition adds to cost.</li> </ol>	<ol style="list-style-type: none"> <li>1. Secondary pollution is not created as synthesis is eco-friendly and reduction of chromium takes place.</li> <li>2. Less sludge is formed that too non toxic</li> </ol>	(Li et al. 2017)
Sodium metabisulfite, Calcium metabisulfite, Ferrous sulphate	<ol style="list-style-type: none"> <li>1. Secondary pollution,</li> <li>2. Not species specific,</li> <li>3. Sludge disposition adds to cost.</li> </ol>	<ol style="list-style-type: none"> <li>1. Secondary pollution is not created as synthesis is eco-friendly and reduction of chromium takes place.</li> <li>2. Less sludge is formed that too non toxic</li> </ol>	(Tsybulskaya et al. 2019)
Photocatalysis	<ol style="list-style-type: none"> <li>1. Secondary pollution,</li> <li>2. Not species specific,</li> <li>3. Sludge disposition adds to cost.</li> </ol>	<ol style="list-style-type: none"> <li>1. Secondary pollution is not created as synthesis is eco-friendly and reduction of chromium takes place.</li> <li>2. Less sludge is formed that too non toxic</li> </ol>	(Gan et al. 2018)



Chemical precipitation	<ol style="list-style-type: none"> <li>1. Sludge formation,</li> <li>2. Secondary pollution</li> </ol>	<ol style="list-style-type: none"> <li>1. Secondary pollution is not created as synthesis is eco-friendly and reduction of chromium takes place.</li> <li>2. Less sludge is formed that too non toxic</li> </ol>	(Mella et al. 2015)
Biotransformation	<ol style="list-style-type: none"> <li>1. Slow process,</li> <li>2. Higher loads may be toxic to live species</li> </ol>	<ol style="list-style-type: none"> <li>1. Faster as it contains nZVI.</li> <li>2. Higher loads may be tolerated by microorganisms as it is immobilized</li> </ol>	(Pradhan and Sukla 2019)
Biosorption	<ol style="list-style-type: none"> <li>1. Only accumulation, no reduction,</li> <li>2. Disposal issues,</li> <li>3. Higher loads may be toxic to live species</li> <li>4. Chromium may be secreted out</li> </ol>	<ol style="list-style-type: none"> <li>1. Reduction by nZVI and microorganism</li> <li>2. Spent matrix can be easily utilized in fabrication of roads and structures or can be reutilized after washing.</li> <li>3. Higher loads may be tolerated by microorganisms as it is immobilized</li> <li>4. Chromium secreted is of non toxic form</li> </ol>	(Franguelli et al. 2019)
Biomining	<ol style="list-style-type: none"> <li>1. Slow process, higher loads may be toxic to live species</li> </ol>	<ol style="list-style-type: none"> <li>1. Faster as it contains nZVI.</li> <li>2. Higher loads may be tolerated by microorganisms as it is immobilized</li> </ol>	(Maity et al. 2019)
Extracellular precipitation	<ol style="list-style-type: none"> <li>1. Slow process, higher loads may be toxic to live species</li> </ol>	<ol style="list-style-type: none"> <li>1. Faster as it contains nZVI.</li> <li>2. Higher loads may be tolerated by microorganisms as it is immobilized</li> </ol>	(Kumar and Dwivedi 2019)

Table 2.1: Conventional and advances methods of reducing chromium content in the effluents

## **2.4 Mechanisms involved**

**2.4.1 Physical Methods:** Major mechanism for this mechanism is found in adsorption where the solute moves from liquid phase to solid phase till an equilibrium is achieved. Other mechanisms include ion exchange between a resin and solvent, sieving as in filtration, reverse osmosis, ultrafiltration. Electrodialysis involves movement of solute under an electric field.

**2.4.2 Chemical Methods:** Chemical methods involve a chemical reaction that convert the form of solute either mediated by chemicals or electrode based electron donors. Photocatalytic procedures involve visible light for mediating the reactions.

**2.4.3 Biological Methods:** It mainly involves use of biological cells including bacteria, fungi, and plants to perform the function. The mechanisms mainly is a combination of physical attachment followed by chemical reaction in most cases but not always.

## **2.5 Mechanism involved in combination of microorganism and nanoparticles**

Studies has been performed using combination of bacteria and nanoparticle for treatment of wastewater containing Cr(VI) and other metals species. These studies have evaluated the performance of these composite systems over removal of Cr(VI) as well as some studies were pertaining to study the mechanisms behind the combinatorial effect as well. In the study conducted by Nemecek et al. they combined nanotechnology with biotechnology to observe the effect of this combination in remediating a Cr(VI) contaminated site. With a scientifically designed experimental procedure, they are able to conclude that nZVI was able to remove the Cr(VI) from the site significantly. They also proved that the oxidized product of the reaction between iron and Cr(VI) was partly regenerated by microbes. Also, the partial reduction of Cr(VI) was attributed to the microbial processes (Němeček et al. 2016).

Dong et al. in their study have emphasized that the oxidation of iron nanoparticles in these systems generate an environment of low oxidation reduction potential that benefits the growth of anaerobic bacteria which are helpful in reducing the pollutants (Dong et al. 2019). Also, it was proposed that another mechanism that may lead to

increase in the efficiency of the system to reduce metal ions is the generation of hydrogen which is a potent supplier of electron to bacteria which survive on hydrogen donated electron. These bacteria utilize the electrons donated by hydrogen to remove the pollutants (Xiu et al. 2010, Honetschlägerová et al. 2018). Kocur et al. have successfully shown that abundance of a particular bacterial species is immediately populated after addition of nZVI loaded on carboxymethyl cellulose the simultaneously the load of pollutants were reduced suggesting coupling of biotic and abiotic removal (Kocur et al. 2015).

In a very recent study, passivation of lone ZVI particles during Cr(VI) removal were subsided by using these particles in combination with sulfur reducing bacteria. This combination resulted in sulfidated ZVI particles which had improved reactivity and rate of removal of Cr(VI). This thin layer of iron sulfide over ZVI that is responsible for better electron conduction and reaction processes (Xu et al. 2024).

## **2.6 International status**

Several groups round the world are involved in development of technologies for removal and/or reduction of Cr (VI) from effluent released from industrial site before it enters in natural waters as once it gets into natural water system it becomes diluted and its volume also increasing to unmanageable levels. The major findings have been comprehended in Table 2.2 and 2.3.

SN	Important findings	Reference
1.	<ul style="list-style-type: none"> <li>• Magnesium and iron-based hydrotalcite-like compound (MFHT), can remove Cr(VI) and Cr(III) efficiently.</li> </ul>	(Yoshinaga et al. 2018)
2.	<ul style="list-style-type: none"> <li>• Zero valent iron nanoparticle and <i>Aeromonas hydrophila</i> HS01 were put together to form new composite system with sustained reactivity of nZVI and improved removal of Cr(VI) under anoxic condition.</li> </ul>	(Shi et al. 2019)
3.	<ul style="list-style-type: none"> <li>• Physiochemical process of electrocoagulation was found to remove 97.76% of Cr(VI),</li> <li>• Chromium metal was recovered from water of tanning process by electrocoagulation with Cu electrodes.</li> </ul>	(Mella et al. 2015)
4.	<ul style="list-style-type: none"> <li>• Polyethylene glycol was used as an agent to perform photo-reduction of Cr(VI) to Cr(III). PEG was recovered using salting out and Cr(III) was removed by adding into another high-salt wastewater, so that the high-salt wastewater could also be treated.</li> </ul>	(Liu et al. 2016)
5.	<ul style="list-style-type: none"> <li>• nZVI-Biochar biocomposite was found to remove aqueous Cr(VI) (43%)</li> <li>• Process was found to be simultaneous reduction and adsorption.</li> <li>• Composite was found to be converted to a magnetic material during removal.</li> </ul>	(Fan et al. 2019)
6.	<ul style="list-style-type: none"> <li>• Removal performance of composite material was found similar to that of natural materials</li> <li>• These composite materials can be recovered, regenerated and used again for metal removal with similar efficiency.</li> </ul>	(Toli et al. 2016)
7.	<ul style="list-style-type: none"> <li>• Cr(VI) removal was found to be as high as 84% in suitable conditions.</li> <li>• No secondary pollution was observed.</li> </ul>	(Fu et al. 2013)
8.	<ul style="list-style-type: none"> <li>• Cr(VI) removal was monitored by regenerating the adsorbent.</li> <li>• Efficiency was 68% with five cycles of regeneration.</li> </ul>	(Mortazavian et al. 2018)

Table 2.2: Some important work at international level related to Cr(VI) removal from wastewater

## 2.6 National status

SN	Findings	Reference
1.	<ul style="list-style-type: none"> <li>• Upto 98% removal of Cr(VI) was observed in about 30 min even at low adsorbent dosage</li> </ul>	(Madhavi et al. 2013)
2.	<ul style="list-style-type: none"> <li>• <math>\text{Cu}_2(\text{OH})_2\text{CO}_3</math> nanoparticles removed Cr(VI) by adsorption with high capacities and 99% removal from real wastewater.</li> </ul>	(Srivastava et al. 2015)
3.	<ul style="list-style-type: none"> <li>• Conversion of Cr(VI) to trivalent form (Cr(III) ) was done by reduction with Fe nanoparticles entrapped in sweet lemon peels</li> </ul>	(Dalal and Reddy 2019)
4.	<ul style="list-style-type: none"> <li>• Removal of Cr(VI) by <math>\text{Fe}_3\text{O}_4@n\text{-SiO}_2</math> is done via adsorption</li> <li>• Maximum removal was achieved at pH 2.0.</li> </ul>	(Srivastava and Sharma 2014)
5	<ul style="list-style-type: none"> <li>• Maximization of adsorption of Cr(VI) happens with low pH</li> <li>• Maximum adsorption capacity (124.11 mg/gwas reported at pH 2</li> </ul>	(Debnath et al. 2016)
6	<ul style="list-style-type: none"> <li>• Removal of Cr(VI) was done via adsorption.</li> <li>• Near neutral pH(6) was found to be favorable for the same.</li> </ul>	(Arthy and Phanikumar 2016)

Table 2.3: Some recent work at national level for removal of Cr(VI) from wastewater

It can be inferred from above studies that the hexavalent chromium remediation processes developed until now have limitations which affect their field application potential. Although, physical techniques are simple and economic, they do not degrade or reduce (detoxify) Cr(VI). Similarly, chemical techniques change the oxidation state of Cr(VI), but in doing so lot of energy and consumable compounds are utilized which adds to generation of excessive amount of toxic sludge, disposal of which in itself a question.

## **2.7 Research gap**

1. The modern application of nanomaterial for adsorption allows high adsorption capacities but dispersal of bare nanoparticle in environmental matrix is a limitation.
2. Composites of nanomaterial like nZVI (with high adsorption capacities and reducing capacities) with biofilm of Cr(VI) reducing microbes (or iron reducing bacteria) were tested in earlier reported studies yielding very high removal capacity but having the limitation of integrity and sustainability of the surface biofilm on sorbent in large scale field applications which in turn affects the technology transferability to the industry.

Current study focuses on developing a robust system using nZVI and Cr(VI) tolerant bacteria, which can completely remove (simultaneously adsorb and reduce Cr(VI)) and can sustain the real water matrix conditions enhancing its field application potential.

# Chapter 3

## OBJECTIVES



### **3. Objectives**

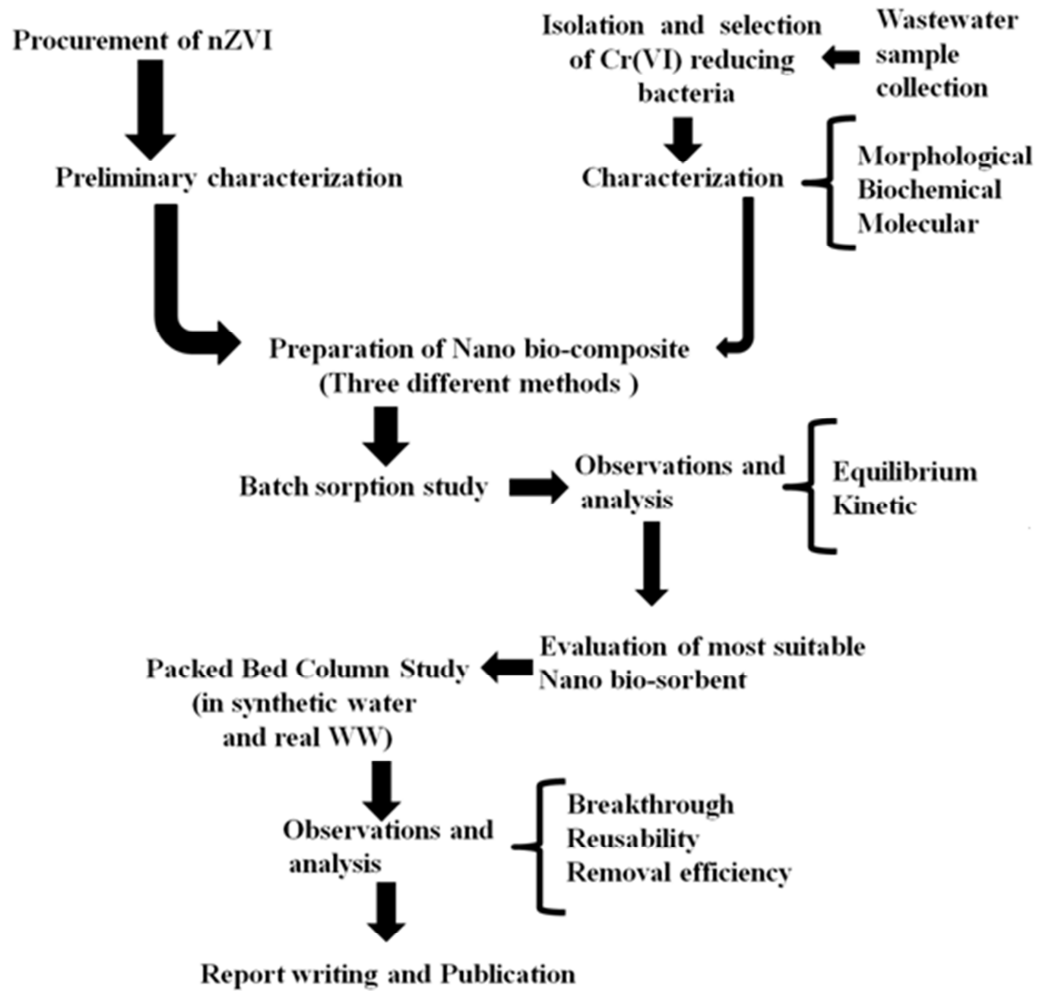
The major objectives of the present work are summarized as follows

1. To isolate and characterize Cr(VI) reducing bacteria from tannery effluent contaminated water bodies.
2. To develop different combinations of nano-biosorbent composite and screening of the sorbent with maximum batch sorption capacity.
3. To evaluate the performance of selected nano bio-sorbent in packed bed column (PBC) reactor under variable factors.
4. To test the performance of selected nano bio-sorbents in different real water matrix under optimized condition of PBC.
5. To evaluate the reuse cycle and disposal of the effective nano-biosorbent.

# Chapter 4

## METHODOLOGY

#### 4. Methodology



# Chapter 5

MATERIALS AND

METHODS

## 5. Material and Methods

### 5.1 Sample collection, and bacterial isolation and characterization.

The water sample which is prospected to be populated by Cr(VI) tolerant bacteria is procured from a location which is receiving wastewater from the industries processing leather and rubber (Fig 5.1). These industries are located in “Leather Complex” in Jalandhar district. Water sample was collected as per the standard procedure from stream near to Common Effluent Treatment Plant (CETP) at Leather Complex, Jalandhar. 100 ml of water sample was collected in dark colored glass bottles and brought to lab on ice and was processed on same day. The initial characterization of the effluent was done for pH and Cr(VI) concentration determination.

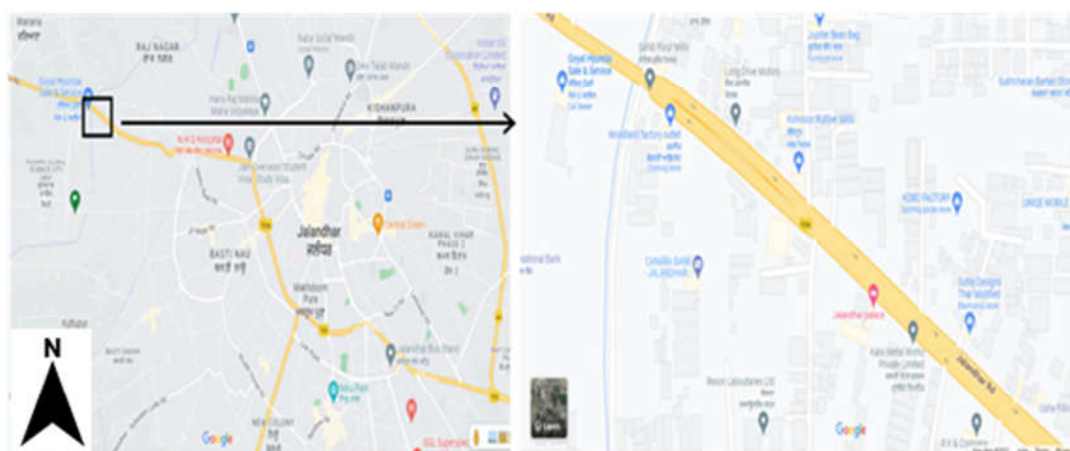


Fig 5.1: Geographical location of the point of collection of wastewater sample for the study.  
(31.34° N, 75.528° E)

#### 5.1.1 Screening and isolation of bacteria

Isolation and screening were performed simultaneously using nutrient agar supplemented with 400 ppm Cr(VI). Agar was prepared, autoclaved, and poured on sterilized and dried petriplates under laminar air flow chamber for growth of Cr(VI) tolerant bacteria. 20  $\mu$ l of wastewater sample was spread on the plates and the plates were incubated at 37 $\pm$ 2°C and were periodically observed for growth of organism till

36 h. The observed colonies were further sub cultured on the same medium to make pure cultures.

#### 5.1.2 Morphological characterization

Gram staining was performed to observe the morphological characteristics of the isolated bacteria. Briefly, a loopful of pure colony was grown in 400ppm Cr(VI) appended nutrient broth for 12 h at 37°C. A small drop of this culture was taken on a clean glass slide and spread for appropriate time to separate the bacterial cells. The slide was fixed by moving the slide on flame of a burner. Small amount of crystal violet dye was poured onto the fixed culture followed by Gram's iodine which was allowed to react and subsequently washed in stream of clean water to drain off excess unabsorbed dye. Further, absolute alcohol was poured on the slide to (decolorisation) and finally the slide was stained with counter stain (safranin). The slide was observed under bright field microscope at varying magnification.

#### 5.1.3 Molecular characterization

Molecular characterization was performed to identify the organisms through its 16s rRNA sequence. Characterizing bacteria using 16S rRNA gene sequencing is a widely used method in microbiology for identifying and classifying bacterial species. The 16S rRNA gene is a segment of the ribosomal RNA that is highly conserved among all bacteria but contains variable regions that can be used to differentiate between different bacterial species. The steps of the process are as follows:

DNA Extraction: The first step is to extract DNA from the bacterial sample. The extracted DNA will contain the 16S rRNA gene among other genetic material. The following protocol was performed for isolation of DNA.

Lysis/Homogenization: 1-3 colonies were picked up aseptically and mixed with 450  $\mu$ L of lysis buffer in a 2 ml microcentrifuge tube.



4  $\mu$ l of RNase A and 250  $\mu$ l of neutralization buffer were added to mixture



Contents were mixed and tubes were incubated at 65°C for 30 min. in water bath. To minimize shearing, contents were mixed by inversion



Tubes were centrifuged at 14000 RPM for 15 min. at 10°C



Supernatant was carefully transferred to a fresh tube without disturbing the pellet



600  $\mu$ l of "B Cube" binding buffer was added to the content, was mixed thoroughly, and incubated at room temperature for 5 min



The contents was transferred to a spin column placed in 2 ml collection tube



The content was centrifuged at 14000 RPM for 2 min and flow through was discarded




The spin column and collection tube were reassembled and remaining lysate was transferred.




The content was centrifuged at 14000 RPM for 2 min and flow through was discarded







500  $\mu$ L washing buffer I was added to the spin column. The content was centrifuged at 14000 RPM for 2 min and flow through was discarded




The spin column was reassembled. The content was centrifuged at 14000 RPM for 2 min and flow through was discarded




The spin column was transferred to a sterile 1.5-ml microcentrifuge tube




100  $\mu$ l of elution buffer was added at the middle of spin column. Care should be taken to avoid touch with the filter



The tubes were incubated for 5 minutes at room temperature and centrifuged at 6000 rpm for 1 min.



The above 2 steps were repeated for complete elution. The buffer in the microcentrifuge tube contains the DNA



DNA samples were quantified by Agarose Gel Electrophoresis and stored at -20°C.



PCR Amplification: It is used to amplify the 16S rRNA gene from the extracted DNA. Primers are designed to target conserved regions at the beginning and end of the gene, allowing for the amplification of the entire gene. The PCR product will contain both conserved and variable regions of the 16S rRNA gene.

The composition of Taq Mater Mix used in the reaction is dNTPs (0.4 mM), MgCl<sub>2</sub>(3.2 mM), bromophenol blue (0.02%) in a buffer

Primers used in amplification and protocol of PCR are as follows:

Primer Name	Sequence	Number of bases
27F	AGAGTTTGATCMTGGCTCAG	20
1492R	TACGGYTACCTTGTTACGACTT	22

5 µL of isolated DNA was added in 20 µL of PCR reaction solution (1.5 µL of Forward Prime and Reverse Primer, 5 µL of deionized water, and 12 µL of Taq Master Mix



**Denaturation**: The DNA template is heated to 94°C for 3 minutes. This breaks the weak hydrogen bonds that hold DNA strands together in a helix, allowing the strands to separate creating single stranded DNA.



**Annealing**: The mixture is cooled to anywhere from 94°C for 30 sec, 50°C for 60 sec, and 72°C for 60 sec. This allows the primers to bind (anneal) to their complementary sequence in the template DNA.



**Extension**: The reaction is then heated to 72° C for 10 mins, the optimal temperature for DNA polymerase to act. DNA polymerase extends the primers, adding nucleotides onto the primer in a sequential manner, using the target DNA as a template.

Purification and sequencing of PCR product

Montage PCR Clean up kit (Millipore) was used to remove the remaining unincorporated primers and dNTPs. Sequencing reactions were performed using a ABI PRISM® BigDye™ Terminator Cycle Sequencing Kits with AmpliTaq® DNA polymerase (FS enzyme) (Applied Biosystems).

Single-pass sequencing was performed on each template extended with the cited 16S rRNA universal primers. An ethanol precipitation was performed to purify the fluorescent-labeled fragments. The samples were resuspended in distilled water and subjected to electrophoresis in an ABI 3730xl sequencer (Applied Biosystems)

Sequence Analysis, Taxonomic classification, and phylogenetic analysis: The obtained sequence was then analyzed using bioinformatics tools. The sequence is typically compared to databases containing known 16S rRNA gene sequences, such as the NCBI GenBank database or the Ribosomal Database Project (RDP), using algorithms like BLAST. This comparison helps identify the closest matches to known bacterial species or genera.

Based on the similarity of the sequence to known sequences in the database, the bacteria can be classified taxonomically. This includes identifying the genus and species of the bacteria. Sometimes, if the sequence is very similar to a known sequence, the identification can be quite precise. In other cases, the identification might be at a broader taxonomic level.

The sequences can also be used to construct phylogenetic trees that show the evolutionary relationships between different bacterial species. This can provide insights into the evolutionary history and relatedness of different bacteria.

1. BLAST tool of NCBI was used to perform the phylogenetic analysis of query sequence with the sequence present in NCBI database. Pairwise alignment was followed by multiple sequence alignment.

2. Multiple Sequence Comparison by Log-Expectation (MUSCLE 3.7) was used to perform multiple sequence alignments (Edgar 2004). Another computer program, Gblocks 0.91b was used to cure the aligned sequences by eliminates poorly aligned positions and divergent regions (removes alignment noise) (Talavera and Castresana

2007). Finally, the program PhyML 3.0 aLRT was used for phylogeny analysis and HKY85 as Substitution model.

#### 5.1.4 Determination of Minimum Inhibitory concentration (MIC) of Cr(VI)

As per definition “MIC is the lowest concentration of an antibacterial agent expressed in mg/L ( $\mu\text{g}/\text{mL}$ ) which, under strictly controlled in vitro conditions, completely prevents visible growth of the test strain of an organism”(Phillips et al. 1998). In current study, MIC was determined to analyze the potential of growth of microbe under Cr(VI) stressed condition. Higher MIC will suggest a prospective advantage of organism to be used in the further experiments. The experimental setup to determine MIC is given in Fig 5.2. Nine different test tubes were taken and 10 ml of nutrient broth (NB) was taken in each of these. Further these were supplemented with different amount of dichromate solution (2000 ppm) to make final concentration of Cr(VI) to be 0, 200, 300, 400, 500, 600, 700, 800, 1000 ppm. Volume was adjusted to 10ml in each tube by removing equivalent amount of NB from each tube before addition of dichromate solution. The tubes were autoclaved and kept overnight for observing any contamination. The tubes were further used by inoculating 100 $\mu\text{l}$  of 12 hr grown culture of SG1 to each tube separately under aseptic conditions. The tubes were kept in shaker incubator (REMI CIS 24, India) at 37°C and observed at periodic intervals upto 48 h for growth.

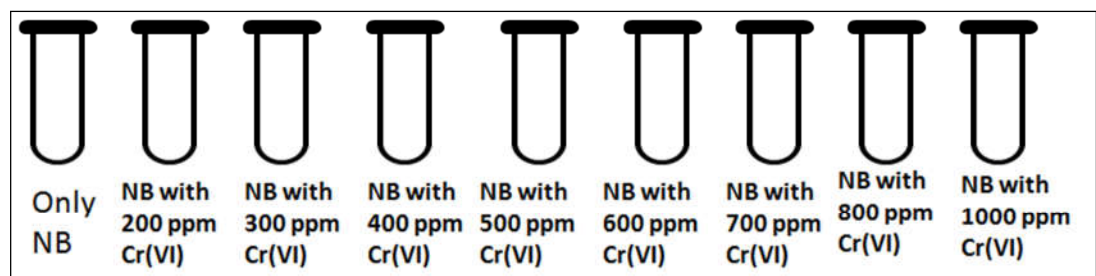


Figure 5.2 : Experimental design for measurement of MIC

## 5.2 Procurement and characterization of zero valent iron nanoparticle (nZVI)

nZVI was purchased from SIGMA ALDRICH (CAS Number: 7439896). The particle was kept in dry air tight conditions and was characterized for size, morphology, charge, and aggregation before being used in experiments.

### 5.2.1 Scanning Electron Microscopy (SEM) and Transmission electron Microscopy (TEM) analysis.

SEM was performed to observe the shape, size and homogeneity of nZVI (Make: JFEI company Of USA(S.E.A.) PTE LTD Model: Nova Nano SEM-450). The particles were observed at different magnifications of 8000X, 35000X, 80000X, and 120000X to look into different features of the material. TEM was performed with High Resolution Transmission Electron Microscope (Make: FEI company Of USA Model: FP 5022/22-Tecnai G2 20 S-TWIN) and images at different magnifications were obtained.

### 5.2.2 X Ray Diffraction (XRD) analysis

XRD was performed X-ray Diffractometer (Make: Rigaku Corporation Model: SmartLab 9kW rotating anode x-ray diffractometer) to analyze the purity of the sample. The sample was kept in the sample holder and X ray was incident on the material. The intensity of diffracted X rays at different 2theta were recorded and plotted.

### 2.2.3 Zeta Potential measurement and Dynamic Light Scattering (DLS) analysis

For measurement of zeta potential, the nZVI was suspended in water (pH7) by stirring the solution on a magnetic stirrer. It is used to analyze the surface charge of nZVI at this pH. It is a measure of stability of any colloidal system at given state conditions. The size of the zeta potential represents the strength of electrostatic attraction between adjacent particles with similar charges in dispersion. DLS analysis relies on the fact that diffusivity of particles in solution is related to its size. The hydrodynamic size of the matter is thus can be obtained from DLS measurements. Zetasizer Nano ZS (MALVERN INSTRUMENTS LTD.) was used to collect the scattering data (details

in appendix) and the same was analyzed using NTA 3.2 Dev Build 3.2.16 software in built in machine.

### 5.3 Analytical methods to estimate Cr(VI)

To estimate the amount of Cr(VI) in the aqueous solution, standard method of reaction with Diphenyl carbazide (DPC) was used (Lace et al. 2019). For this standard solution of DPC reagent was prepared by dissolving 250 mg of DPC in 100 ml of pure acetone. Standard solutions containing 0.5, 1.0, 1.5, 2.0, 2.5 ppm of Cr(VI) were prepared by diluting 10 ppm of stock accordingly. Distilled water was taken as blank. 1ml of each of these standards was mixed with 330  $\mu$ l of 6M H<sub>2</sub>SO<sub>4</sub> and mixed well with vortex mixer. To this 400 $\mu$ l of DPC reagent was added the mixed well. The optical density of pink colored solutions thus obtained is measured at 540nm against water treated with DPC as blank. The data obtained is used to plot standard curve and this was further used to interpolate the concentrations of unknown test solutions. The test solutions were diluted when and as required to get the optical densities between 0.2-0.9 and the concentration deduced is then multiplied with appropriate dilution factor.

### 5.4 Development of nanobiosorbent (NBA)

For the preparation of NBA, calcium alginate (CA) beads were used as immobilization matrix for encapsulating bacteria and nZVI. Four different types of beads were produced to perform the experiments. Bacterial cells were grown in 500ml conical flask at 37°C for 12h. High inoculum density was used as we require high biomass after 12 h in active phase. The cells were separated by centrifuging at 3500g in a bench top centrifuge (REMI). The pellet was washed with distilled water and centrifuged again. This step was repeated three times. The cells in pellet were re-suspended in distilled water and used in experiment at the same time. First, blank beads (CA) were formed which does not contain any bacteria and nZVI. Second, beads with 0.5% (w/w) bacteria only designated as BCA. Then, beads with 0.1% nZVI (w/w) alone called as NCA and finally beads with 0.5% bacteria+0.1% nZVI (w/w) named as BNCA. For preparation of beads, 2% sodium alginate (Hi Media) solution was prepared with respective concentration of different components and

beads of CA were prepared by dropping this solution in 0.2 M Calcium Chloride solution with 20 gauge needle. Beads were formed instantaneously. Beads were cured for 4 h in CaCl<sub>2</sub> before being used in experiment.

Beads were characterized for size and morphology by observing directly and under scanning microscope. SEM was performed to observe the shape, size and homogeneity of nZVI (Make: JFEI company Of USA(S.E.A.) PTE LTD Model: Nova Nano SEM-450). The particles were observed at different magnifications of 350X, and 800X to look into different features of the material.

### 5.5 Batch studies to evaluate the performance of developed NBA for adsorption of Cr(VI)

The developed NBA were used separately in batch experiments to evaluate the effect of certain factors on the removal efficiency for Cr(VI). The data obtained through these experiments was further used to calculate percent Cr(VI) removal and adsorption capacity. % Cr(VI) removal and adsorption capacity are calculated as follows:

$$\% Cr(VI) Removal = \frac{(C_0 - C_t) \times 100}{C_0}$$

$$q = \frac{(C_0 - C_t) \times V}{m}$$

Where: C<sub>0</sub>= Initial Cr(VI) concentration in solution ,C<sub>t</sub>= Cr(VI) concentration in solution at any time “t”, V=Volume of the test solution, m= mass of adsorbent in the test solution.

All the experiments were performed in triplicates.

#### 5.5.1 Effect of pH on the percentage removal of Cr(VI)

Percentage of Cr(VI) removal from the aqueous solution by the four different types of NBA was determined by incubating each type of NBA at different pH values of 5,6,7,8, and 9. This is done to determine the favorable pH range of the adsorption process as mostly the pH of real WW lies in a bit acidic region (nearly 6). A higher

variation in optimum working pH may be unfavorable for the process. For this, 2g (wet weight) of each NBA was kept in 50 ml of 10 ppm Cr(VI) solution for 90 min with constant stirring to keep the beads suspended. pH of the solution was set with concentrated NaOH and concentrated HCl. After 90 min, the residual Cr(VI) concentration was measured with DPC reagent method and % Cr(VI) removal was calculated.

#### 5.5.2 Effect of initial Cr(VI) concentration on the percentage removal of Cr(VI)

Initial adsorbate concentrations have a profound effect on the rates of adsorption process. Here, for this, we incubated 2g of each NBA separately with 10, 20, 30, 40, and 50 ppm of Cr(VI) solution with initial pH of 7 for 90 min. The solutions were constantly stirred on a magnetic stirrer. Samples were drawn after 90 min and analyzed for Cr(VI) concentrations.

#### 5.5.3 Effect of time on the percentage removal of Cr(VI)

To analyze the progression of adsorption process with time, the experiment was designed where the samples from the adsorption systems were collected at different time intervals viz. 30, 60, 90, 120, and 150 min. The experiment was run at pH7, initial Cr(VI) concentration of 10 ppm, and adsorbent dosage 2 g. The samples were stored at 4°C and analyzed for residual Cr(VI) concentration.

#### 5.5.4 Effect of adsorbent dosage on the percentage removal of Cr(VI)

50 ml solution (10ppm) of Cr(VI) at pH7 was constantly stirred with different amount of adsorbent separately for 90 min and samples were analyzed for residual Cr(VI) concentration by method of DPC described earlier. The adsorbent dosage taken were 0.5, 1.0, 1.5, 2.0, 2.5 g.

#### 5.5.5 Isotherm modeling and parameter estimation

Isotherms for the adsorption process were developed by scatter plot of  $q_e$  v/s  $C_e$ . Here residual concentration at equilibrium ( $C_e$ ) can be determined by running the adsorption for a suitable time so that saturation of adsorption occurs and no more adsorption is allowed. For our case, we have taken the time to be 180 min. The

concentration of Cr(VI) at this time in the solution will be the measure of  $C_e$ . Adsorption capacity at equilibrium ( $q_e$ ) was calculated as follows:

$$q_e = \frac{(C_0 - C_e) \times V}{m}$$

Where:  $C_0$ = Initial Cr(VI) concentration in solution,  $V$ =Volume of the test solution,  $m$ = mass of adsorbent in the test solution. Graphpad PRISM V 8.0 was used to plot the scatter graph.

Adsorption isotherm occupies an important space in adsorption studies. They are useful in providing several insights into the adsorption mechanisms and mode of adsorption. To model this, we require model equation of the process for which the data is fitted. The fitting process is carried out by using the method of linear non linear regression using minimization of Sum of Squares of Errors (SSE). MS Excel (2018), and Graphpad PRISM V 8.0 are used as and where required to perform modeling. we have plotted adsorption isotherms and then have tried to fit these isotherms to three different isotherm models viz. Langmuir, Freundlich, and Sips (Foo and Hameed 2010). The model form of each of these in non linear form is given below.

$$q_e = \frac{Q_0 b C_e}{1 + b C_e} \dots \dots \dots (Langmuir)$$

$$q_e = K_F C_e^{\frac{1}{n}} \dots \dots \dots (Freundlich)$$

$$q_e = \frac{K_s C_e^{\beta_s}}{1 + a_s C_e^{\beta_s}} \dots \dots \dots (Sips)$$

Here, “ $Q_0$ ” is maximum monolayer coverage capacities (mg/g), “ $b$ ” is Langmuir isotherm constant (mL/mg), “ $K_F$ ” is Freundlich isotherm constant (mg/g) (mL/g)<sup>n</sup> related to adsorption capacity, “ $n$ ” is adsorption intensity, “ $K_s$ ” is Sips isotherm model constant (L/g) , “ $\beta_s$ ” is Sips isotherm model exponent , “ $a_s$ ” is Sips isotherm model constant (L/mg).



Coefficient of Determination ( $R^2$ ) was used to estimate the goodness of fit. From the fits obtained by regression modeling, the relevant isotherm parameters were estimated and the same were used to decipher changes in the adsorption process as the type of adsorbent changes.

#### 5.5.6 Mathematical modeling of the kinetics of batch removal

Data obtained from the experiment done for measurement of % reduction with time was used to perform modeling of kinetics batch studies. Same procedure of minimization of SSE was used to perform regression modeling. 50 mL, 20 ppm Cr(VI) solution was incubated with 0.5 g of BNCA. Samples were drawn after every 30 min up to 180 min and analyzed for residual Cr(VI) concentration. Adsorption capacity ( $q$ ) was plotted against time to perform kinetic analysis. The plots obtained were then fitted to Vermeulen model (equation given below). This model is used to model kinetics in case of intra particle diffusion (Tan and Hameed 2017). It is used to describe the diffusion of adsorptive in a spherical particle. As we have a CA bead which is macro particle with pores inside it, we find this as a suitable model to understand the kinetics of adsorption process.

$$\frac{\bar{q}}{q_e} = \sqrt{1 - e\left(\frac{-D\pi^2 t}{R^2}\right)}$$

The linear form of the equation is

$$\ln\left(1 - \left(\frac{\bar{q}}{q_e}\right)^2\right) = \frac{-D\pi^2 t}{R^2}$$

Here, “D” is diffusion coefficient,  $\bar{q}$  is the average value of  $q$  in the spherical particle of radius  $R$  at any particular time.

#### 5.6 Packed Bed Column (PBC) studies for removal of Cr(VI)

PBC columns were utilized further to batch studies to access the practical application of the process. It is often utilized to evaluate the adsorbent for its efficiency in real systems so that we can be put in practice. In contrast to batch, where the concentration gradient between adsorbent and adsorbate decreases over time, columns maintain a

continuous flow over a fixed bed, increasing the adsorbent capacity. For large-scale applications, the continuous process or column study is preferred over the batch process due to its simplicity of use, flexibility in design, consistency in product quality, and low capital and operating costs per unit of product. One of the most popular and effective methods for removing heavy metals from waste water is adsorption using a column. However, it is important to note that adsorption isotherm studies, such as batch experiments, were carried out to determine the maximum adsorption capacity of the adsorbent before evaluating the effectiveness of the adsorbent in fixed-bed adsorber. By using fixed-bed columns, separation issues between the biosorbent and the effluent can be avoided. Since the adsorption reactions do not limit the process due to the fast kinetics, the limiting step in this experimental procedure is the mass transfer of metal from solution to the biosorbent.

For our studies we have utilized glass column (ID 1 cm) and this column is packed with adsorbent according to the experimental requirement. The column is held stable with a burette and fed with Cr(VI) solution of concentration 10 ppm with the help of a variable flow peristaltic pump (Galaxy Instruments, India). The solution passes through the adsorbent and is collected at the bottom in eppendorf tubes at certain time intervals. The samples are centrifuged and stored at 4°C and analyzed for Cr(VI) with standard method of DPC.

To analyze the data obtained from column experiments, Breakthrough curve are generally employed as they are useful in understanding the capacity of an adsorption system in continuous and long run. The size, location, and shape of breakthrough curves are influenced by a variety of macroscopic, mesoscopic, and microscopic factors. Here is a summary of the top few parameters and their effects. A breakthrough curve is helpful for a realistic estimation of an adsorbent's performance because it depicts the concentration profile in the adsorption column.

The position of the breakthrough curve is significantly influenced by the sorption capacity. The breakthrough curve will shift to longer breakthrough times (to the right) as the sorption capacity increases because more adsorptive molecules will be held back by the adsorbent. If a spontaneous breakthrough occurs as a result of too slow

sorption kinetics on the sample, then this is not the case. The sorption kinetics have an impact on the shape of the breakthrough curve as opposed to the sorption capacity. The mass transfer zone will be smaller and the breakthrough curve will become steeper (sharper) for faster kinetics. Short local equilibrium times are caused by a rapid mass transfer from the gas phase to the adsorption sites, which results in a smaller expansion of the concentration front. A further factor that contributes to the expansion of the mass transfer zone is the axial dispersion. This parameter is also in charge of the breakthrough curves' increasing asymmetry.

#### 5.6.1 Effect of bed height on percentage removal of Cr(VI)

Bed height of the column is an important parameter that affects the shape and nature of breakthrough curve. Generally, as the bed height increases the breakthrough curve is shifted towards increasing X axis. To perform this experiment, glass columns (ID 1 cm) are packed with BNCA to height of 4 cm, 8 cm, and 12 cm separately and the column are fed with solution of Cr(VI) with constant concentration (10 ppm) and constant flow rate of 1.0 ml/min. Effluent samples are collected at the bottom at an interval of every five min and further centrifuged (5500g, 5 min) and stored at 4°C before being analyzed for Cr(VI). The Cr(VI) concentration was measured with DPC reagent method and scatter curve was plotted between fraction of Cr(VI) eluted v/s Time. Fraction Cr(VI) eluted was calculated as follows:

$$\text{Fraction eluted} = \frac{C_t}{C_0}$$

#### 5.6.2 Effect of flow rate on percentage removal of Cr(VI)

To analyze the effect of flow rates on the breakthrough curve and adsorption process, the BNCA column with bed height 8 cm is fed with 10 ppm Cr(VI) at constant flow rates of 0.5, 1.0, and 1.5 ml/min. The samples were collected, analyzed and data was plotted in the same way as stated in previous section.

#### 5.6.3 Breakthrough curves and its modeling

Kinetic modeling of breakthrough curves relies on solving three types of balances simultaneously viz. mass balance, energy balance, and momentum balance. Only

addressing mass balance will resolve the issue because heat effects and pressure drops are insignificant when a liquid column is involved, which is the situation here. Common models which are utilized in modeling breakthrough curves are Bohart-Adams model, and Yoon-Nelson model (Tan and Hameed 2017). The mathematical linear equations of these models are given as follows:

$$\ln\left(\frac{C_0}{C} - 1\right) = \frac{k_{BA}N_0Z}{u} - k_{BA}C_0 t \dots\dots\dots \text{Bohart-Adams model}$$

$$\ln\left(\frac{C}{C_0 - C}\right) = k_{YN}(t - \tau) \dots\dots\dots \text{Yoon Nelson model}$$

Linear regression utilizing minimization of SSE was used to fit the obtained data to the given mathematical models. Coefficient of determination was used to assess the goodness of fit. Graphpad PRISM v8.0 and MSeExcel V 2014 were used as and when required to perform regression.

#### 5.7 Evaluation of performance of selected NBA in real water matrix under PBC.

BNCA was used to evaluate its performance under real WW. For this, WW from influent of CETP, Leather complex was taken and brought to lab on ice pack and processed immediately. The WW was centrifuged to settle colloidal particles and the supernatant was then filtered through 0.2 micron membrane filter to remove bacteria. The filtrate thus obtained was used as source of WW in further experiments. The Cr(VI) content in this processed WW (PWW) was measured by standard colorimetric method using DPC reagent. Then this WW was spiked with  $K_2Cr_2O_7$  to produce a final Cr(VI) concentration of 10 ppm. pH of PWW was set to 7 with concentrated NaOH before being used in experiments. The PBC column studies were performed by passing PWW through a bed of BNCA with bed heights 4 cm, 8 cm, and 12 cm with flow rates of 0.5, 1.0, and 1.5 ml/min. The eluent was collected at regular intervals and data was represented and analyzed as done earlier.

### 5.8 Evaluation of reuse of the adsorbent

To evaluate reusage of the spent adsorbent (BNCA), it is treated with 0.1 M  $\text{HNO}_3$  (Yang, Niannian, et al. 2019) to desorb the attached ions. It is then washed with distilled water and soaked in 0.1 M  $\text{CaCl}_2$  to regenerate the adsorbent. This regenerated adsorbent is then again used in batch mode adsorption to measure its removal efficiency.

Experimentally, 2 g of spent adsorbent (BNCA) is placed in contact with 0.1 M  $\text{HNO}_3$  at a biosorbent concentration of 1g/l for 60 min to achieve maximum desorption. The acid was reported to be an effective eluent of several other ions. The metal ion concentration in the solution was monitored with time and beads were filtered after the equilibrium has reached. After separation beads were washed to remove trace of acid. After desorption the beads were regenerated by soaking in 1 M  $\text{CaCl}_2$  for 6 h. This process repair the damaged linkages make the beads stiffer. The beads were again washed thrice with distilled water. The regenerated beads are then used as adsorbent to estimate removal of Cr(VI) as per the settings in given in section 2.5.3. 50 ml of 10 ppm Cr(VI) solution at pH 7 was prepared and 2 g of regenerated BNCA were stirred with it for 120 min. to achieve adsorption equilibrium. Solution was analyzed for residual Cr(VI) by standard DPC method. Cr(VI) removal % was calculated as in previous experiments. The desorption, regeneration, and adsorption cycle was repeated 4 times to evaluate the recyclability of the prepared BNCA.

### 5.9 Disposal of the spent adsorbent.

Safe disposal of the spent adsorbent is much required as the adsorbent is mainly removing the Cr(VI) ions from wastewater and its conversion to less toxic stable form is still not conformed. Even though it is stabilized we need to dispose it safely so that it does not cause harm to life forms. For this, the spent adsorbent was incinerated and the ash was packed in standard bags and was sent for landfills.

# Chapter 6

## RESULTS

AND

## DISCUSSIONS

## 6 Results and Discussions

### 6.1.1 Water sample collection, bacterial isolation and characterization.

The geographical location of the stream from where the samples were collected is shown in Figure 5.1. The collected sample is shown in Figure 6.1. The water was turbid and brownish in color with suspended solids. pH of the water was found to be 6.7 and Cr(VI) concentration was found to be  $2.54 \pm 0.2$  mg/l



Figure 6.1 Water sample collected from the effluent stream for studies

The colonies observed on NA supplemented with 400 ppm Cr(VI) are shown in fig: 6.2. Gram staining of the pure culture reveals gram positive rod shaped bacteria (Fig: 6.3). The culture was represented by SG1 in further literature.

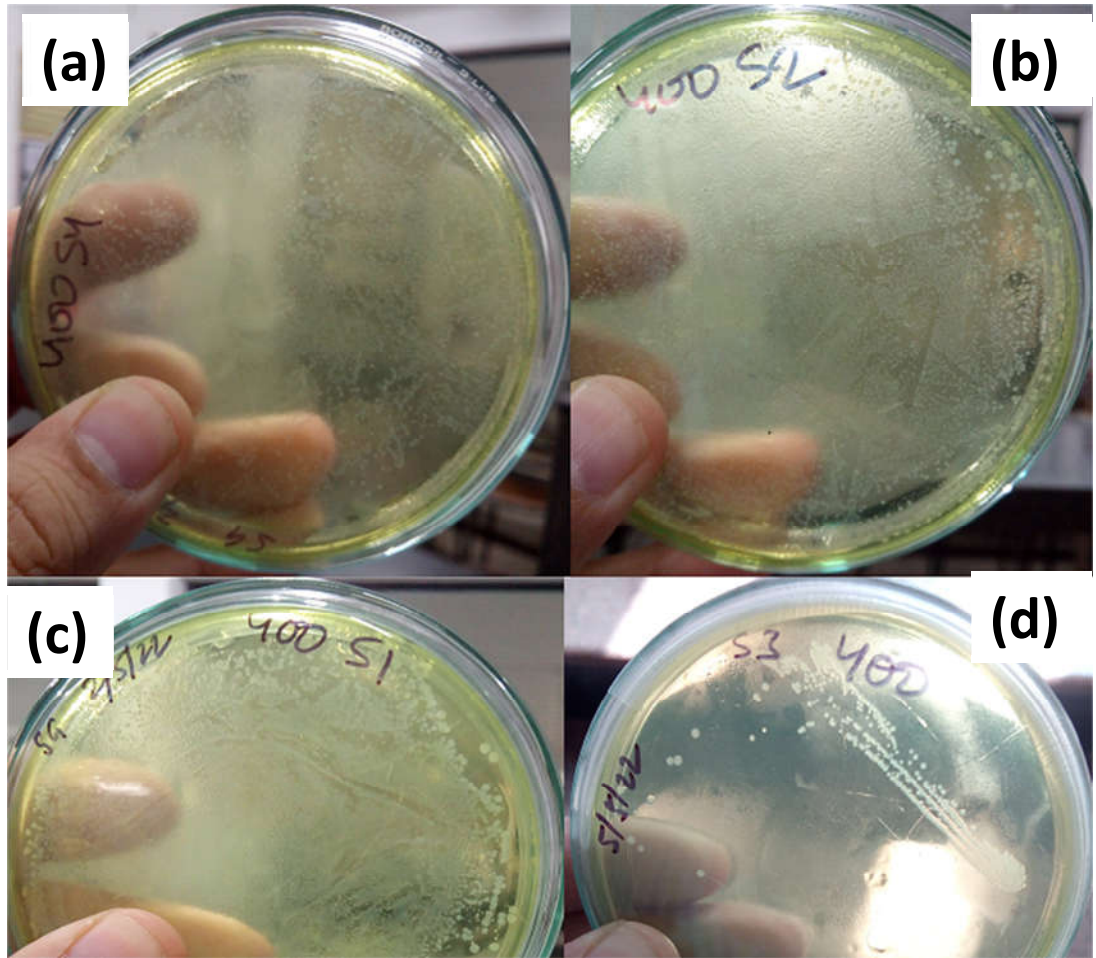


Figure 6.2 Microbes grown over nutrient agar supplemented with 400 ppm Cr(VI)



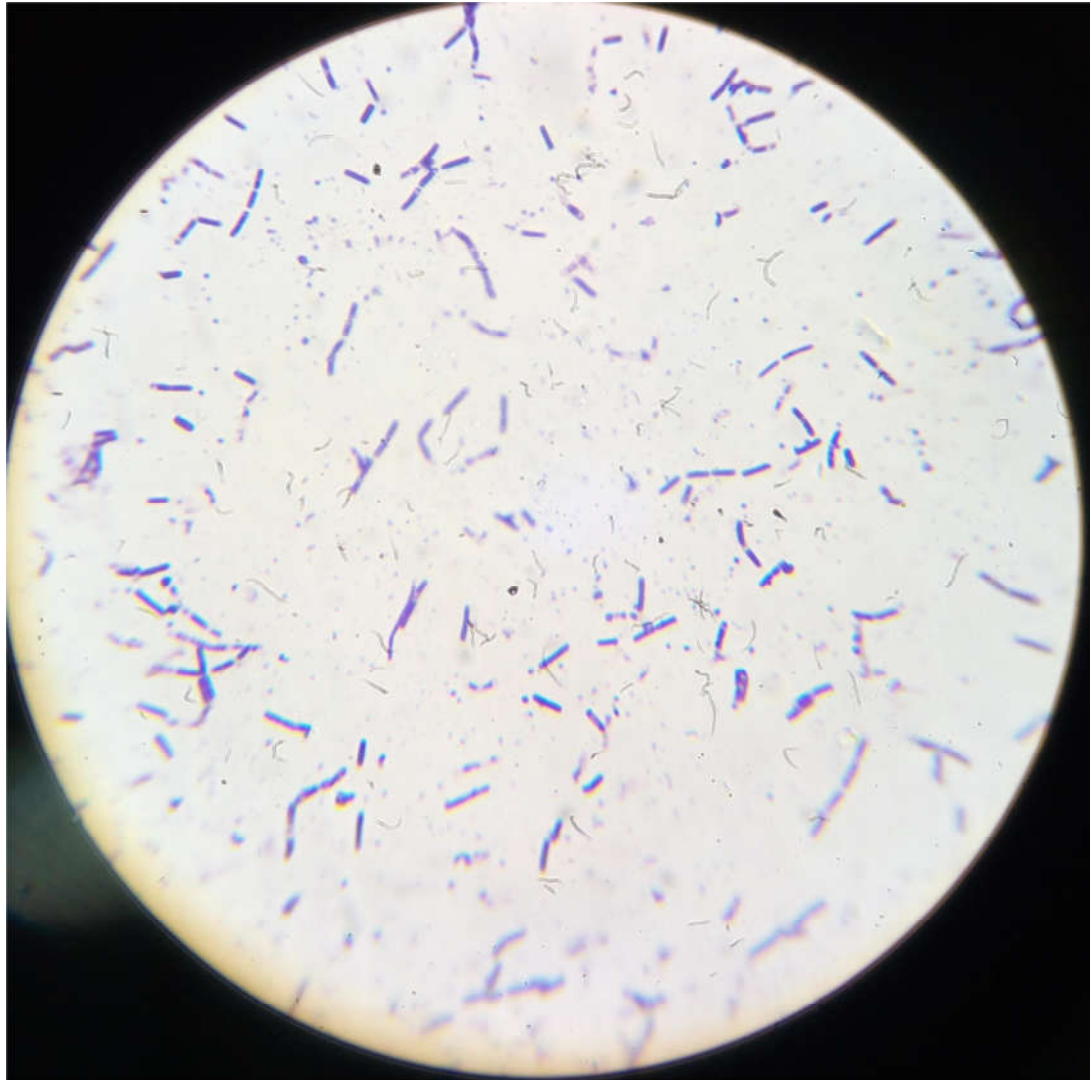


Figure 6.3: Brightfield microscopic images of isolated bacteria from tannery effluent.  
(Magnification 100X)

### 6.1.2 Molecular characterization:

The sequence of the 16s rRNA of the organisms is given below. The sequence is 1249 bases long which contain the constant and variable region.

```
CCAAATCTTCTTCCTTCATTCCATGCTGTGCGAGCGGACAGATGGGAGCTTG
CTCCCTGATGTTAGCGGCGGACGGGTGAGTAACACGTGGGTAACCTGCCT
GTAAGACTGGGATAACTCCGGGAAACCGGGGCTAATACCGGATGGTTGTT
TGAACCGCATGGTTCAAACATAAAAGGTGGCTTCGGCTACCACTTACAGA
TGGACCCGCGGCGCATTAGCTAGTTGGTGAGGTAATGGCTCACCAAGGCA
ACGATGCGTAGCCGACCTGAGAGGGTGATCGGCCACACTGGGACTGAGAC
ACGGCCCAGACTCCTACGGGAGGCAGCAGTAGGGAATCTTCCGCAATGGA
CGAAAGTCTGACGGAGCAACGCCGCGTGAGTGATGAAGGTTTTCGGATCG
TAAAGCTCTGTTGTTAGGGAAGAACAAGTACCGTTCGAATAGGGCGGTAC
CTTGACGGTACCTAACCAGAAAGCCACGGCTAACTACGTGCCAGCAGCCG
CGGTAATACGTAGGTGGCAAGCGTTGTCCGGAATTATTGGGCGTAAAGGG
CTCGCAGGCGGTTTTCTTAAGTCTGATGTGAAAGCCCCGGCTCAACCGGG
GAGGGTCATTGGAAACTGGGGA ACTTGAGTGCAGAAGAGGAGAGTGGAA
TTCCACGTGTAGCGGTGAAATGCGTAGAGATGTGGAGGAACACCAGTGGC
GAAGGCGACTCTCTGGTCTGTA ACTGACGCTGAGGAGCGAAGCGTGCGGA
GCCAACAGGATTAGATACCCTGGTAGTCCACGCCGTAAACGATGAGTGCT
AAGTGTTAGGGGGTTTTCCGCCCTTAGTGCTGCAGCTAACGCATTAAGCA
CTCCGCCTGGGGAGTACGGTCGCAAGACTGAAACTCAAAGGAATTGACGG
GGGCCCCGCACAAGCGGTGGAGCATGTGGTTTAATTCGAAGCATCGCGAGA
ACCTTACCAGGTCTTGACATCCTCTGACAATCCTAGAGATAGGACGTCCCC
TTCGGGGGCAGAGTGACAGGTGGTGCATGCTGTCGTCAGCCGTGTCGTGA
GATGTTGGGTTAGTCCCGCAACGAGCGCATCCCTTGATCTTAGTTGCCAGC
AATTCAGTGGTACTCTAGGTGACTTGCCGGTGACATACGAGAGTGGGATG
ACGTCAATCATCATGCCCTTATGACTGGCTACACACCTCTACATTGACGGA
CATGGCATCGTAACCGCGGAGGTTAAGCCAATCCCACAAACTCTGG
```

The dendrogram pattern obtained after the hierarchical clustering is shown in fig 6.4. The pattern reveals that the organism is most likely to be *Bacillus subtilis*.

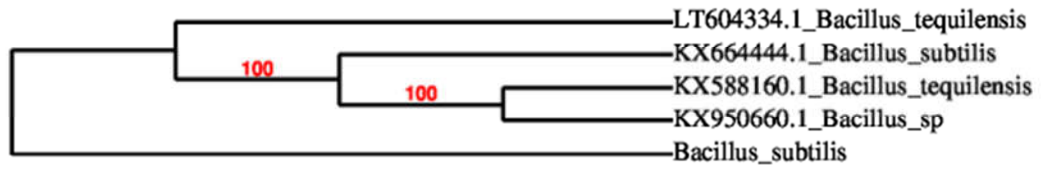


Figure 6.4: Dendrogram pattern obtained after the hierarchical clustering of the sequence

### 6.1.3 Determination of MIC of isolated organism

MIC of Cr(VI) for SG1 was found to be 400 ppm. It can be observed that the culture tube beyond 400 ppm have not shown any visible growth. The actual images of the culture tubes for the experiment are shown in fig 6.5. The tube having 0, 100, 200, and 400 ppm of Cr(VI) can be seen to have received growth of bacteria while tubes with Cr(VI) of 500 ppm and above are having no visible turbidity.



Figure 6.5: Growth of the isolate in increasing concentration of Cr(VI) supplemented nutrient broth for MIC determination. Growth can be observed upto 400 ppm

## 6.2 Characterization of nZVI

The nZVI powder is amorphous and black in color (Fig 6.6) and was delivered in dark colored bottle.



Figure 6.6: nZVI powder

### 6.2.1 Scanning Electron Microscopy and Transmission Electron Microscopy

The SEM images of the nZVI particles reveal its shape, size and aggregation properties. It can be seen that the particles are having a tendency to form aggregates as depicted in fig 6.7 (A) and 6.7 (B). Clumping of these particles is natural and well predicted as the particles are metallic in nature with no net charge (zero-valent). The similar results are obtained by other workers as well who have extensively characterized iron nanoparticles (Sun et al. 2006). The particles can be seen to have almost similar size with some variation as observed in fig 6.7 (C). A similar observation is made with the TEM images as well. Fig. 6.8 is the TEM micrographs of the nZVI particles taken at different magnifications. These images confirm the uniform shape, quite homogeneous size, and aggregates of the material in the powder.

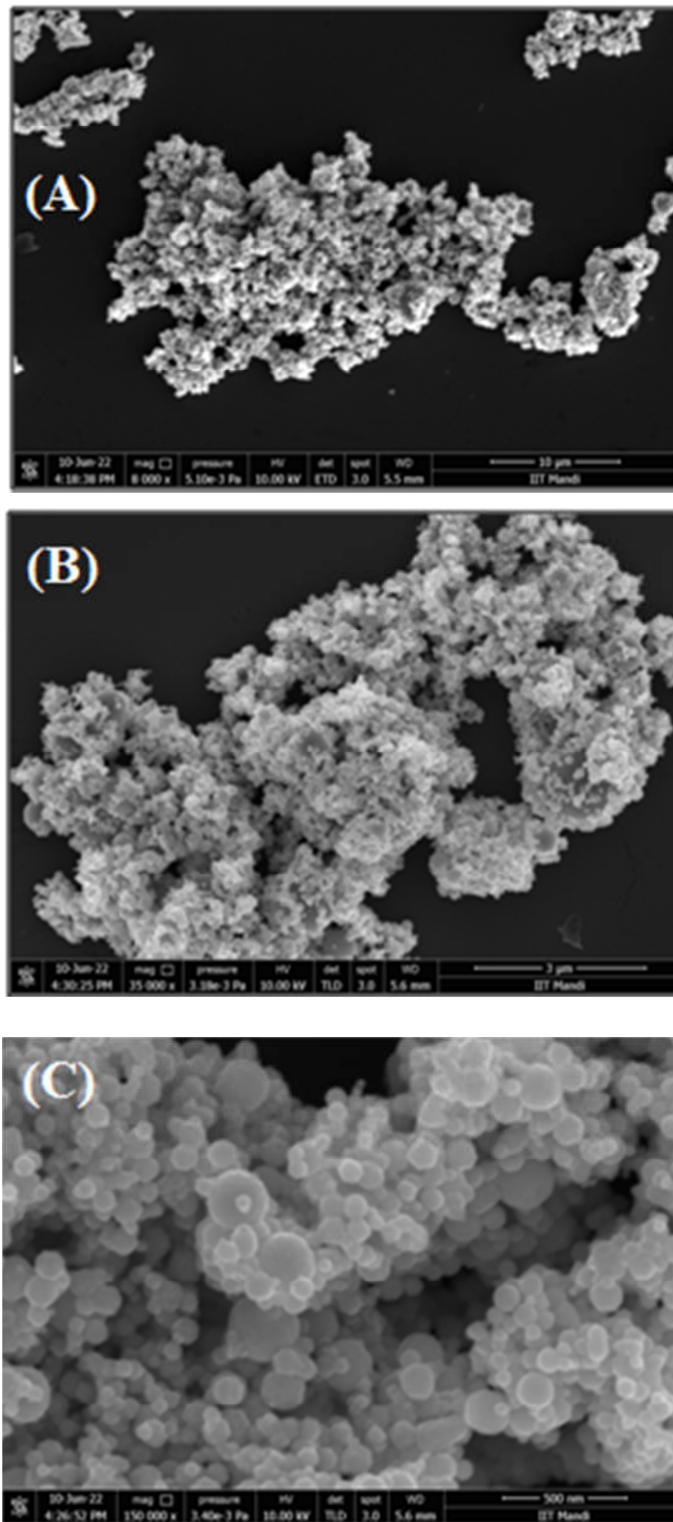


Figure 6.7: SEM image of the nZVI particle at a magnification of (A) 8000X, (B) 35000X, and (C) 150,000

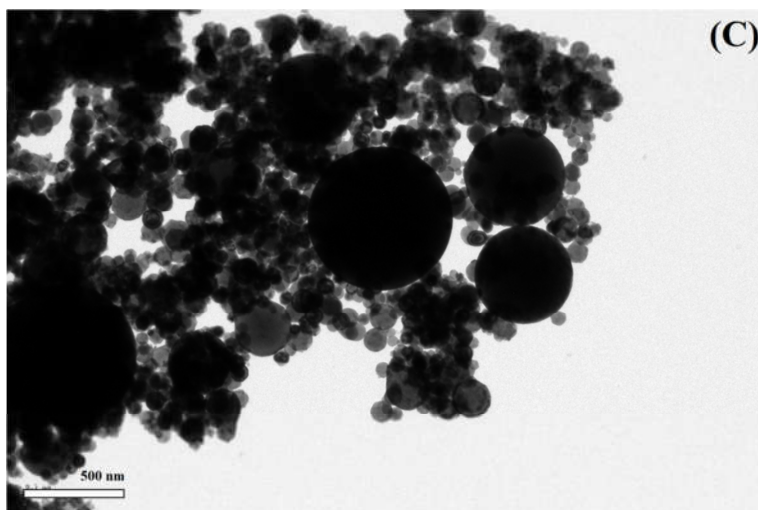
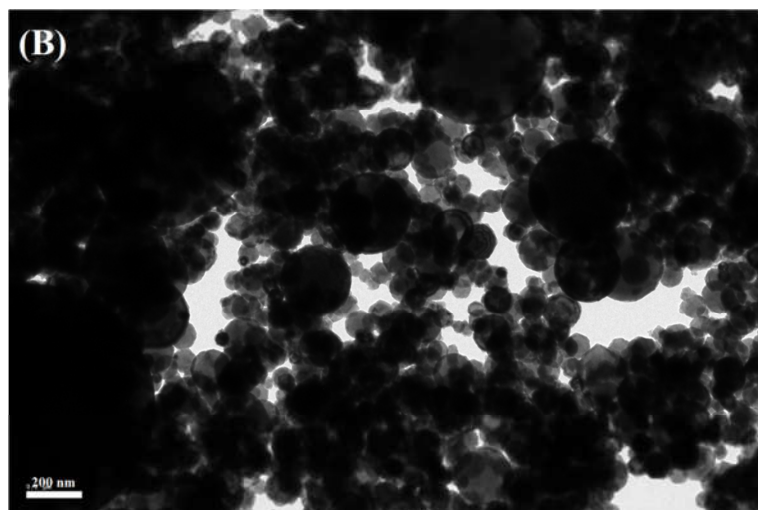
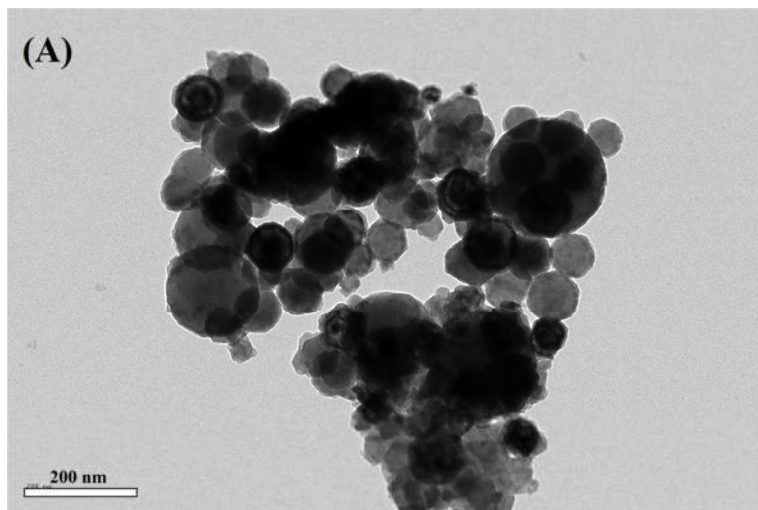


Figure 6.8 TEM image of the nZVI particle showing size distribution

### 6.2.2 X Ray Diffraction study

XRD pattern of the nZVI powder is shown in fig 6.9. The JCPDS (card no 06-0696) pattern is placed along with it for comparison. It is clear from the nature of the pattern that the sample is highly pure in nature as there is no irrelevant peak present in the pattern. The lack of noise in the pattern and sharp peaks represents the crystallinity of the material being analyzed. So, it can be seen from the experimental XRD pattern that the nZVI powder is highly pure and crystalline in nature. The position of peaks suggests that the material is metallic iron only with strong and clear peaks around 2 theta values of 45, 65, and 83 degrees. These positions are matching well with the JCPDS card pattern of metallic iron.



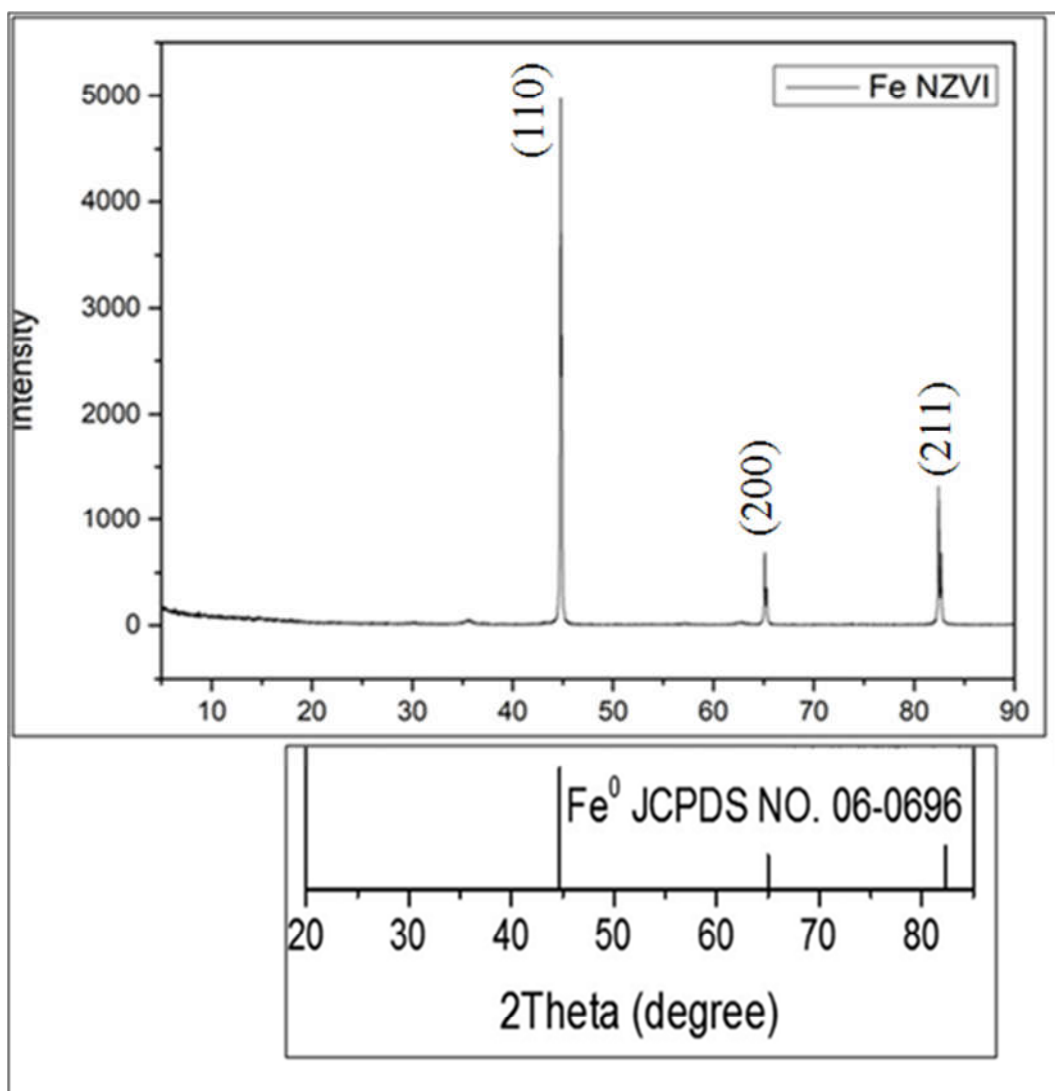


Figure 6.9: XRD pattern of the nZVI powder and its comparison with standard JCPDS card no 06-0696 ((Mao et al. 2014)

### 6.2.3 Zeta Potential measurement

Zeta potential of the powder in water (pH 7) as solvent was found to be 12.09 mV (Fig: 6.10). This value is a representative of incipient stability that may be lost with time. Lower value of zeta potential (10-30) suggests low stability (Sun et al. 2006). This is quite good that SEM, TEM results are matching well with this evidence which is suggesting that agglomeration will happen because of lower stability.

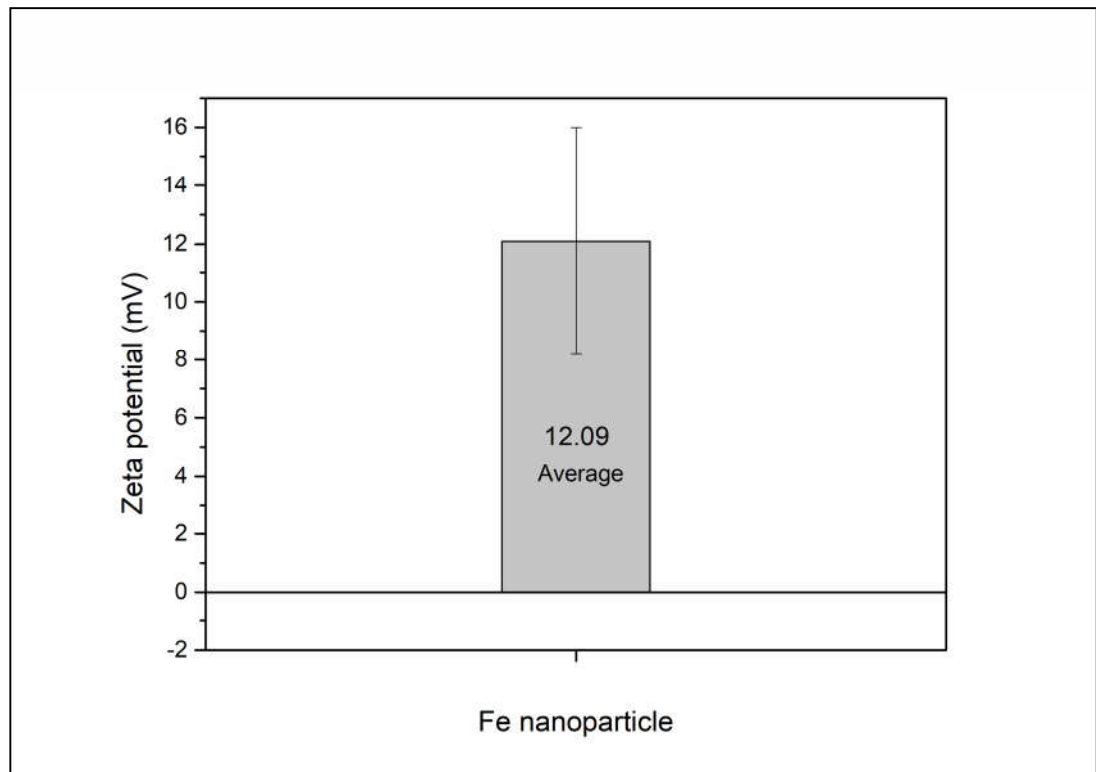


Figure 6.10: Zeta potential of the nZVI at pH 7

#### 6.2.4 Dynamic Light Scattering

DLS experiments yielded the distribution of size of the particles in the powder and the same is represented in fig: 6.11. The mean and modal values of the particle diameter were found to be 190.4 and 190.7 nm respectively. This data is well correlated with values of size that can be interpreted from SEM and TEM micrographs. The variation of size of the particles in mixture is 45.3 nm. This data suggests that the particles are mostly homogeneous in size.

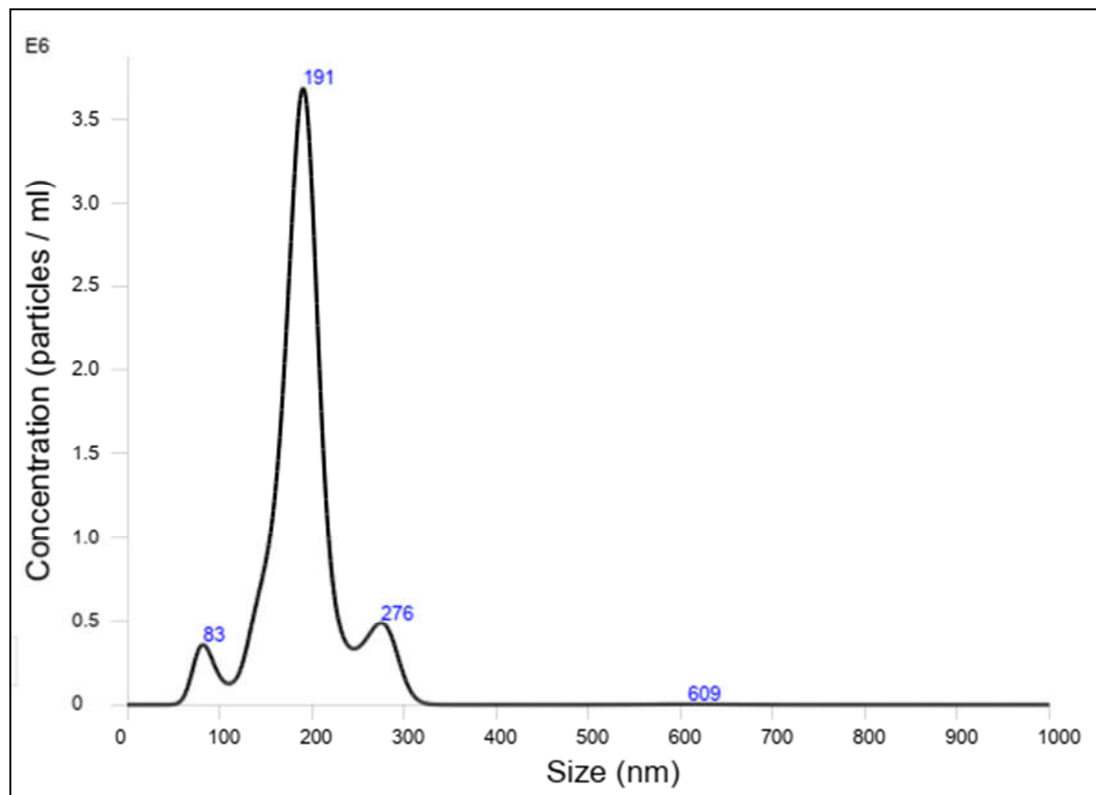


Figure 6.11: Size distribution pattern of the nZVI particles as per Dynamic Light Scattering experiment

### 6.3 Standard curve for Cr(VI) by DPC method

The measurement of Cr(VI) in the aqueous solutions is done by interpolating the OD values obtained by treating the samples with standard DPC method as described earlier. For that, the model equation was obtained by linear regression of the standard curve which is shown fig 6.12. Linear regression yields the following model equation. Coefficient of determination of the fit was found to be 0.99 suggesting a very good fit.

$$y = 0.3154x - 0.0061$$

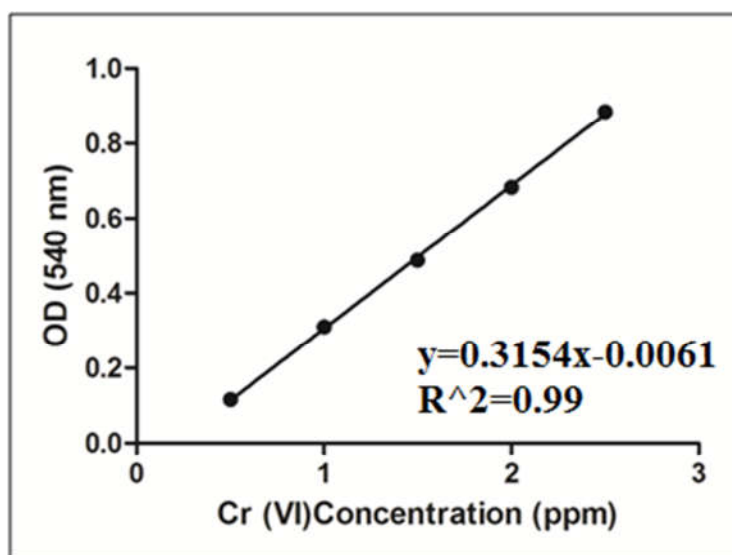


Figure 6.12: Standard curve for measurement of Cr(VI) in aqueous solution

#### 6.4 Characteristics of the developed NBA

The slurry (mixture) of nZVI in water is shown in fig 6.13. The setup used to prepare the beads is shown in fig 6.14. The four types of NBA were found to have size nearly 2 mm and found to be homogenous in size and shape. Its shape was found to be almost spherical. The NBAs are shown in fig 6.15. The strength of these was found to be enough to bear the shear forces experienced during different experiments in shake flask and packed bed reactor. The dry weight of the NBA was found to be 0.1% of the wet weight of NBA bead. The beads with nZVI were black in color while the rest were white. Observation of beads under SEM revealed the regular size and shape of the beads as shown in fig 6.16. At higher magnification, the surface clearly reveals some cracks corresponding to pores in the structure of bead fig 6.17. These pores are aiding the transport of ions into and out of the bead. It can be seen that for NBA having cells immobilized inside it (fig 6.18), the surface is not smooth as in other cases. This may be attributed to the presence of cells in the bead which are protruding from some parts of the surface.

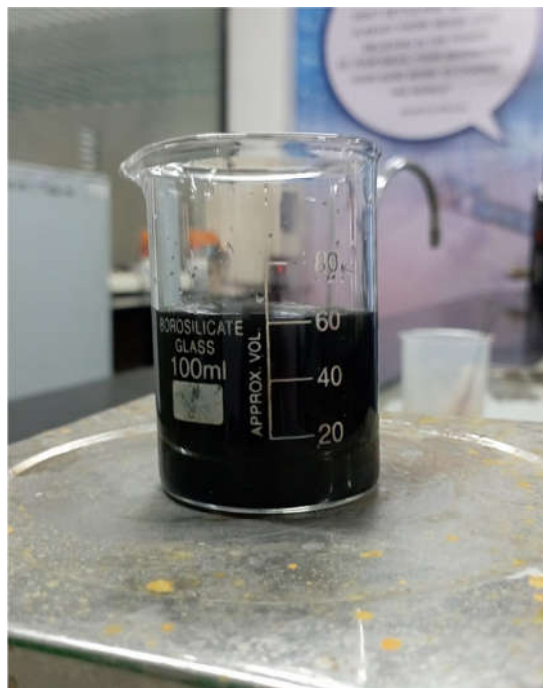


Figure 6.13: Slurry obtained after mixing Cr(VI) tolerant bacteria and nZVI. The slurry appears black in color.

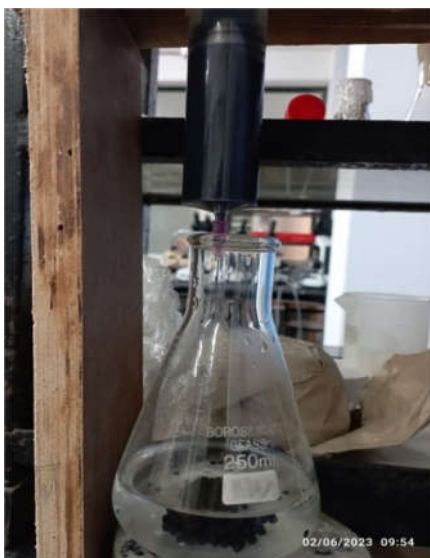


Figure 6.14: Setup to prepare beads for different experiments. The picture is of formation of beads with slurry containing Cr(VI) tolerant bacteria and nZVI.

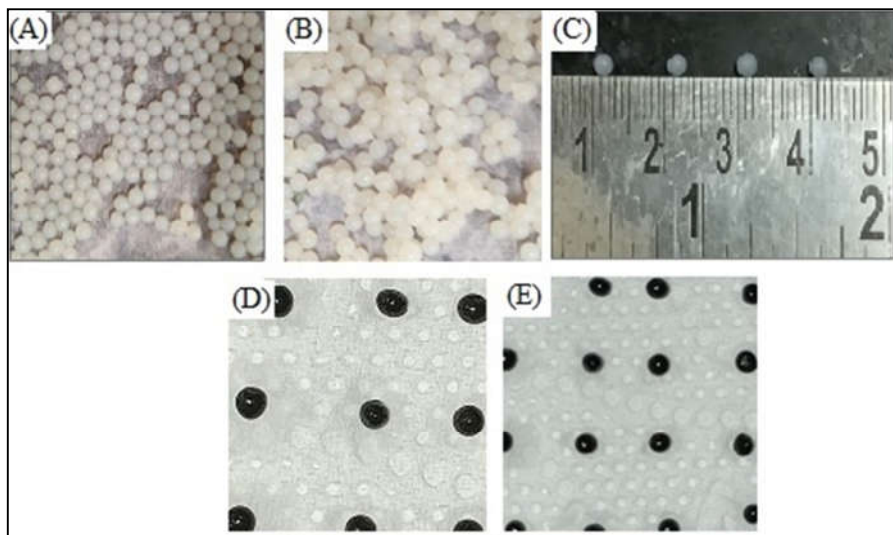


Figure 6.15: Beads of calcium alginate used as immobilization matrix (A) Blank CA beads, (B) CA beads with cells, (C) Size visualization of CA beads, (D) CA Beads with nZVI, (E) CA Beads with cells and nZVI

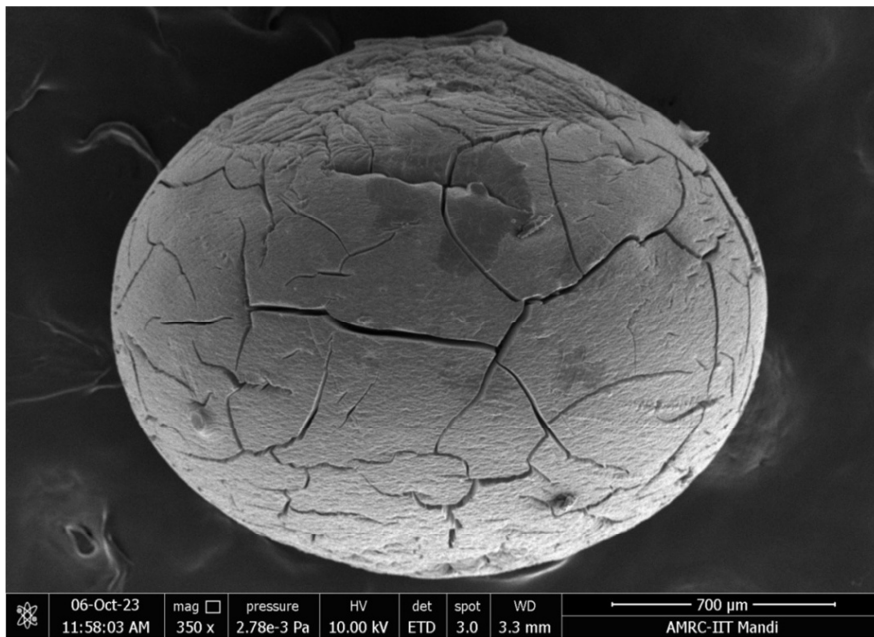


Figure 6.16: SEM image of an individual CA bead

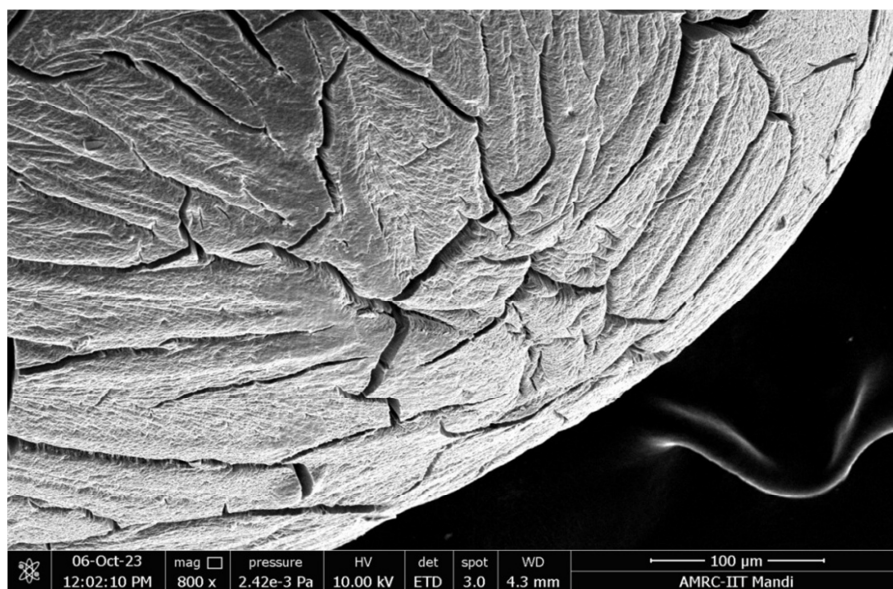


Figure 6.17: SEM image of CA bead. Pores are visible in the bead structure which are routes for transfer of solutes.

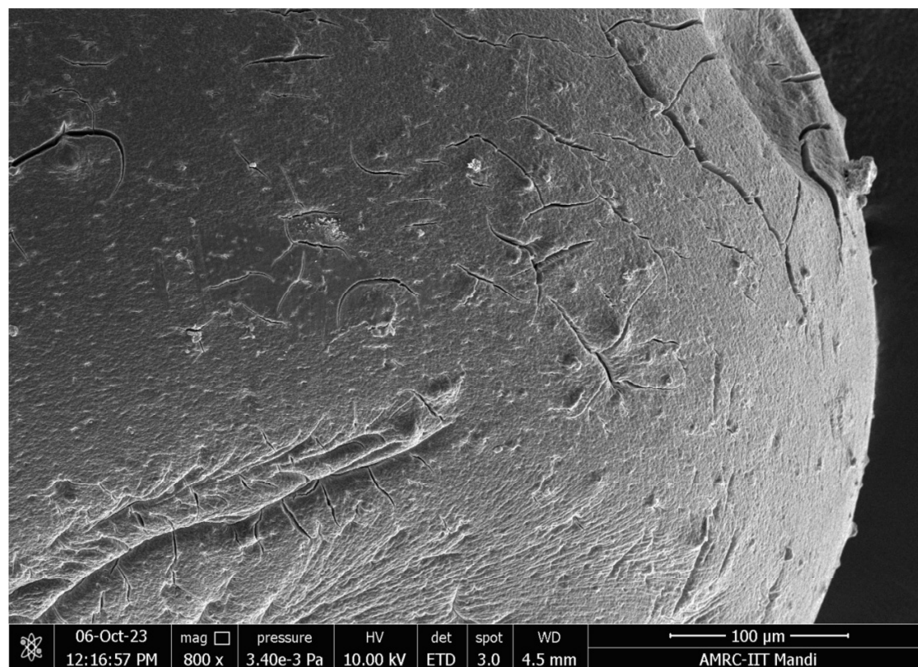


Figure 6.18: SEM image of CA bead with nZVI particle immobilized inside it. The surface blisters are impressions of impregnated nZVI particles.

### 6.5 Batch removal of Cr(VI)

Batch adsorption studies provide important data and parameters on the removal of adsorbate. The small-scale experiment from the batch study can provide crucial details on the parameter used for fixed bed column adaptation in industrial scale. Continuous column is more advantageous than batch adsorption because it is simple to operate, has a quicker adsorption process, and is easier to scale up. Because batch adsorption uses less material and takes less time, it is preferred by researchers conducting laboratory scale research. However, batch adsorption is practical for small-scale research but unsuitable for large-scale implementation. The ability to predict an adsorbent's performance prior to application on a larger scale is made possible by the study of adsorption by equilibrium in batch mode. Additionally, the equilibrium study offers crucial details about the effectiveness of specific.

The effect of pH, time, initial Cr(VI) concentration, and adsorbate amount over removal are presented first. Following that, equilibrium studies and kinetics studies including isotherm and kinetic modeling are presented.



### 6.5.1 Effect of pH on the percentage removal of Cr(VI)

The removal percentage of the analyte is found to be affected by change in pH. Fig 6.19 depicts the change in % removal of Cr(VI) at different pH considered in the study. It has to be noted that this is the initial pH of the solution. When the initial pH is low, the adsorption was low and this increased as the pH was raised up to 7 and it was found to decrease after that. The removal percentages were found to be highest for BNCA at every pH value in consideration. The highest removal percentages were 89%, 79%, 62%, and 14.5% for BNCA, NCA, BCA, and CA respectively. In other studies, it has been observed that lower pH is more favorable for adsorption of Cr(VI), which is contrast to this. Like, Lin et al. have observed that the solution with initial pH 3 was most favorable to remove Cr(VI) by their resin supported nZVI adsorbent (Fu et al. 2013). Another study involving nZVI supported on biochar used as adsorbent to remove Cr(VI) shows that lower pH (pH=2) is favorable for removal of Cr(VI) (Fan et al. 2019). They argued that at lower pH the adsorbent species are going to be positively charged as against the adsorbate i.e  $\text{Cr}_2\text{O}_7^{2-}$ . For our case, the solution pH will not affect the adsorbent because it is immobilized, so we can very well justify the decrease in removal percentage at higher pH as ZVI tends to bear negative charge at much higher pH range (Tarekegn et al. 2021). A two way ANOVA of the experimental data gives a clear effect of adsorbent type and pH on the removal percentages. Post Hoc analysis by Bonferroni test that the effect of pH on the % Cr(VI) removal is clearly pronounced in each of the combination received with a low P value ( $P < 0.001$ ). However, the effect was less remarkable between removal by BCA and NCA where the removal percentages were not found to be significantly different in pH range 8-9.

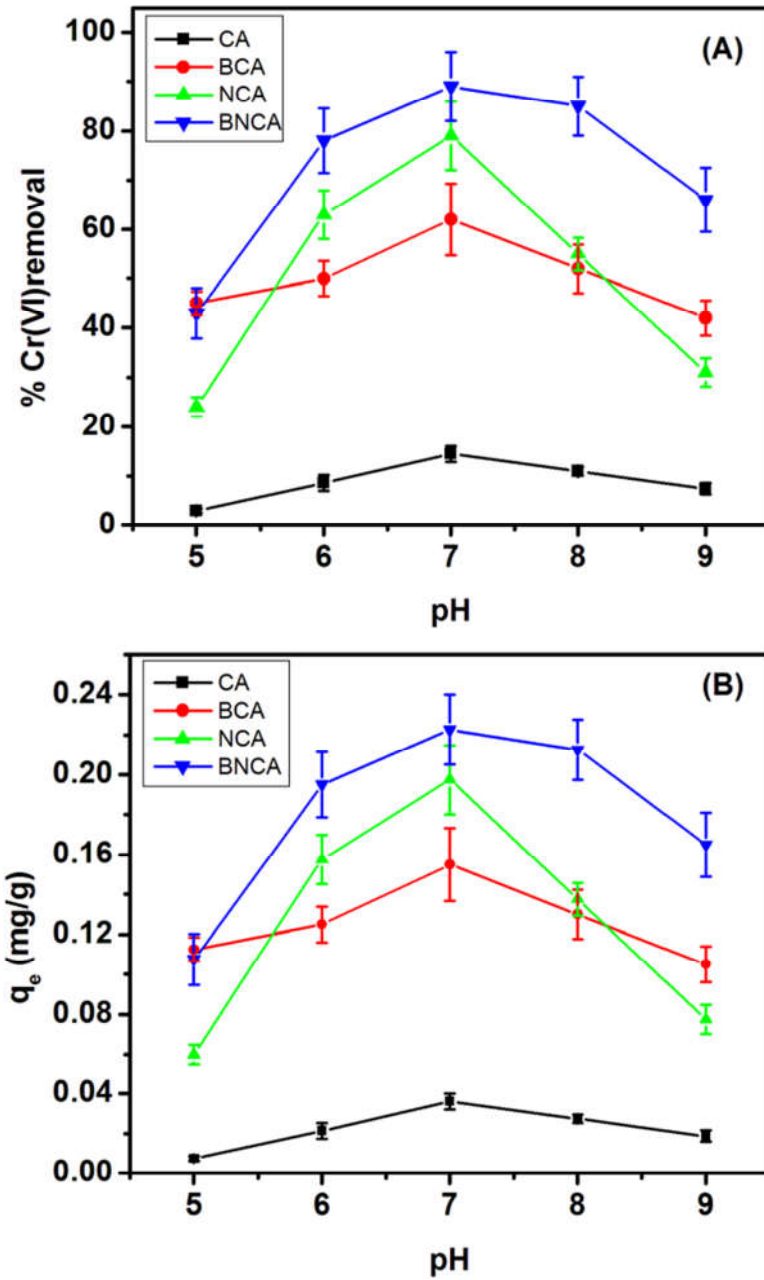


Figure 6.19: Percentage Cr(VI) removal (A) and  $q_e$  (B) as a function of pH for different types of adsorbents (adsorbent dosage= 2 g/l, time=90 min, initial Cr(VI) concentration=10 ppm, n=3)

### 6.5.2 Effect of initial Cr(VI) concentration on the percentage removal of Cr(VI)

The studies of effect of initial adsorbate concentrations are helpful in understanding the saturation behavior and provide some insights about the kinetics of adsorption process. In current study, the highest removal percentage was observed for BNCA at all the given concentrations. The removal percentage were found to decrease with increase in initial Cr(VI) as the adsorbent is getting saturated much faster with higher concentrations of Cr(VI). The removal percentages for different adsorbents at initial Cr(VI) of 10 ppm were found to be 91%, 82%, 66%, and 14% for BNCA, NCA, BCA, and CA respectively. The variation of removal percentages are represented in fig 6.20. The increase in solid-state phase concentration could be attributed to the utilization of more active sites available for adsorption at higher initial metal ion concentrations. A lack of available active sites for adsorption could be the cause of the decline in percent removal. Beyond a specific concentration limit of adsorbate, these active sites become saturated. As the metal concentration rises, no more adsorption occurs, and the ion remains in the final solution.

These trends are well consistent with similar studies. Tow et al. have also observed same trend of decreasing removal percentage with increase in initial metal ion concentration (Ayob et al. 2015). In another similar study, the same trend was observed which is justifying the hypothesis stated above regarding this (Bharagava and Mishra 2018). Two way ANOVA results proves a good and significant effect of adsorbent type and initial Cr(VI) concentration on the removal percentages ( $P < 0.0001$ ). Post-Hoc test revealed that the difference of outcome becomes insignificant for BCA versus NCA. However with both elements the result is pronounced with a higher value on addition of nZVI.

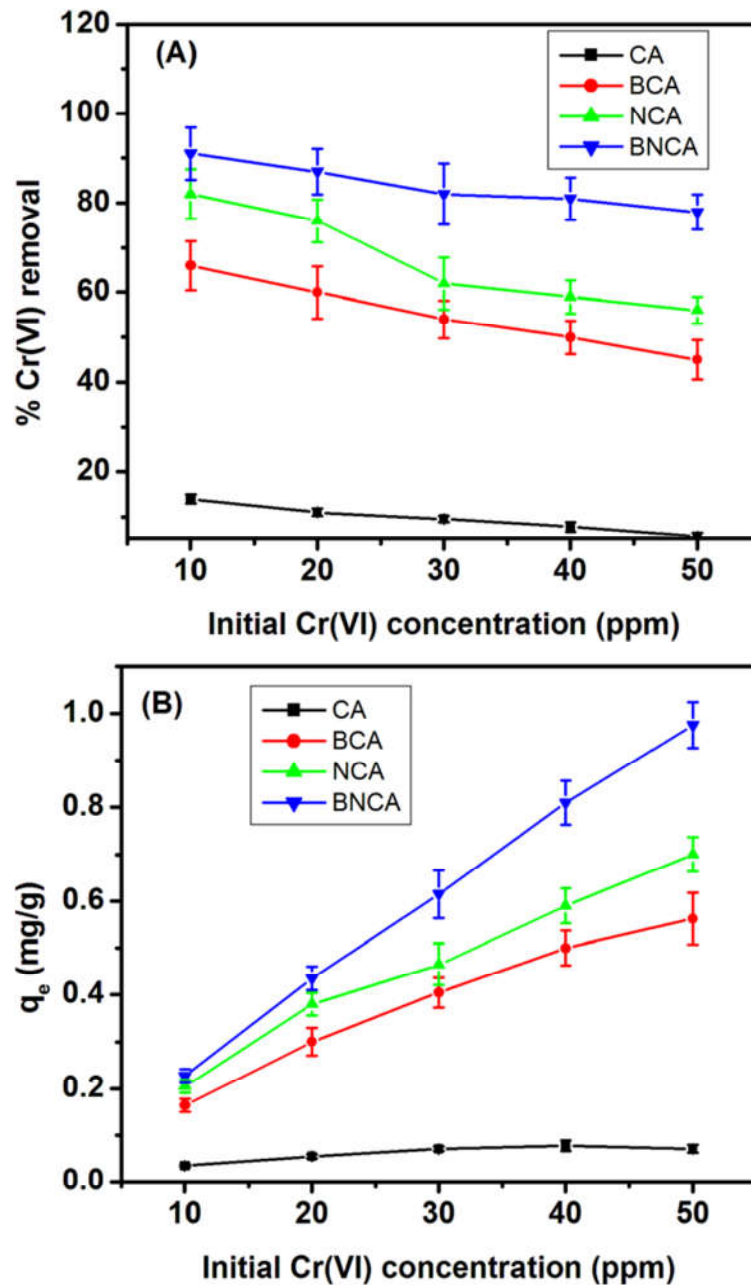


Figure 6.20: Percentage Cr(VI) removal (A) and  $q_e$  (B) as a function of initial Cr(VI) concentration for different types of adsorbents (adsorbent dosage= 2 g/l, pH=7, time=90 min, n=3)

### 6.5.3 Effect of time on the percentage removal of Cr(VI)

The increment in the removal percentage of Cr(VI) with time for different systems is depicted in fig 6.21. It is clearly observed that with time the removal percentage is increasing and it becomes constant at later stages. It can be well explained with the fact that with time the adsorption sites are getting over so with time due hindrance the rate of adsorption eventually falls to zero (saturation stage). As all the sites are occupied, the % removal gets constant. It is worthy to note that the curve is not falling in later stages which suggest that there is no net desorption taking place in the given solution. In this experiments as well, the highest removal % was obtained for BNCA (91%) suggesting a synergistic role of both the components in the adsorption process. The NCA, BCA, and CA beads adsorbed 78%, 65%, and 15.8% at maximum respectively. Two way ANOVA suggest that % removal changes significantly upon time available for adsorption in the range of study ( $P < 0.0001$ ). Post-Hoc tests shows that for all the combinations under study, time is showing significant effect but for NCA versus BNCA the effect did not remain significant suggesting that NCA and BNCA are giving almost same effect on response variable. Addition of bacteria is not favoring the adsorption process in initial stages of adsorption, but became significant in later stages.

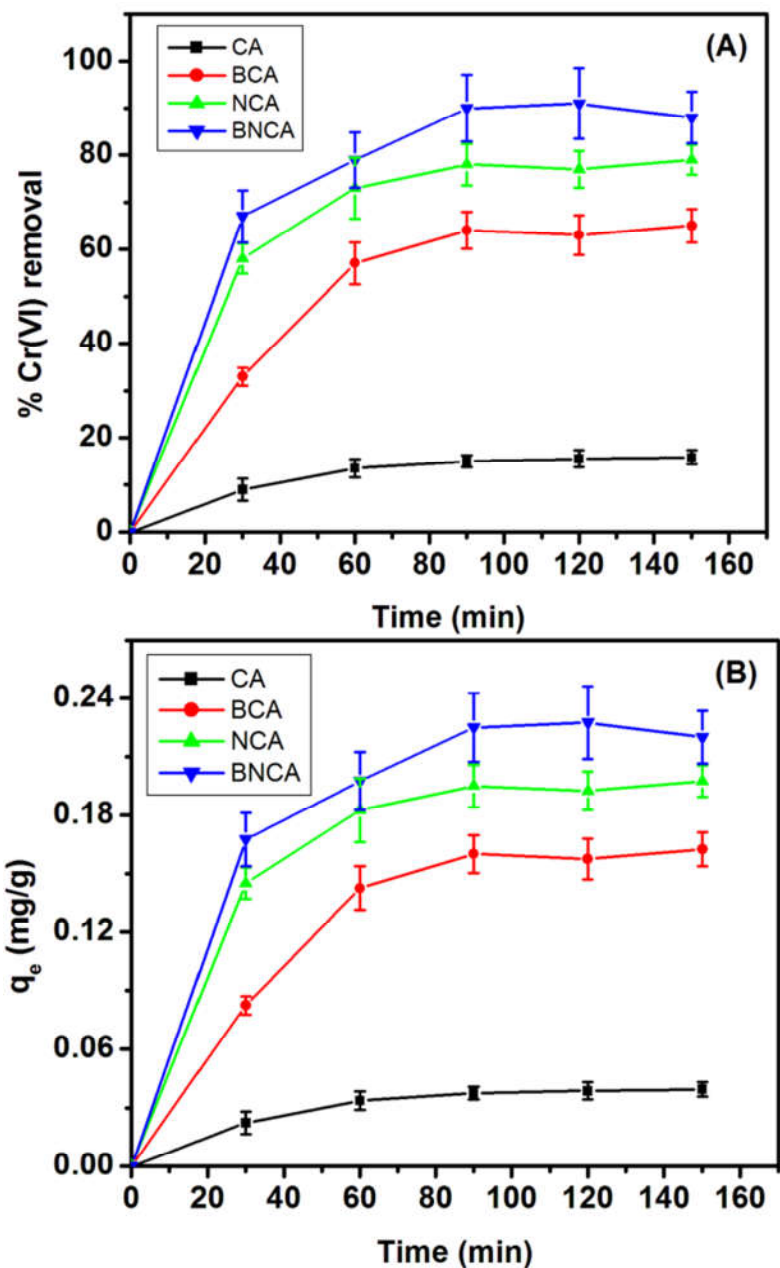


Figure 6.21: Percentage Cr(VI) removal (A) and  $q_e$  (B) as a with time of incubation for different types of adsorbents (adsorbent dosage= 2 g/l, pH=7, initial Cr(VI) concentration=10 ppm, n=3)

#### 6.5.4 Effect of adsorbent dosage on the percentage removal of Cr(VI)

Adsorbent dosage is found to affect the rate and amount of Cr(VI) from the aqueous solutions. More amount of adsorbent naturally means higher availability of adsorption sites which definitely affects the process output variable. Fig 6.22 depicts the variation in % Cr(VI) removal from aqueous solution with change in adsorbent dosage. The BNCA beads are found to give highest removal (93%) followed by NCA (80%), BCA (63%), and then CA (15%). Principally, the adsorption percentage shall keep on increasing with higher dosage of adsorbent without getting saturated till 100% removal is attained, but that is not the observed case in the experiment. It was found that the removal gets saturated even with higher adsorbent dosage. This is attributed towards increasing mass transfer problems in the given volume due to increasing adsorbent load. Two way ANOVA and Post Hoc tests revealed that addition of more adsorbent gives a significant change in the removal percentages for all the combinations but for NCA versus BNCA, the response is less significant ( $P < 0.05$ ) and some even not significant sometimes ( $P > 0.05$ ). This gives an impression that bacterial synergism is not much pronounced in current study. We may need to add more amounts of bacteria or search for another species which may give even a better result.

It is analyzed from above experiments that BNCA is best among the tested model systems (BNCA, NCA, BCA, and CA) for removing Cr(VI) from the water systems. So, in further experiments only BNCA is utilized for studies.

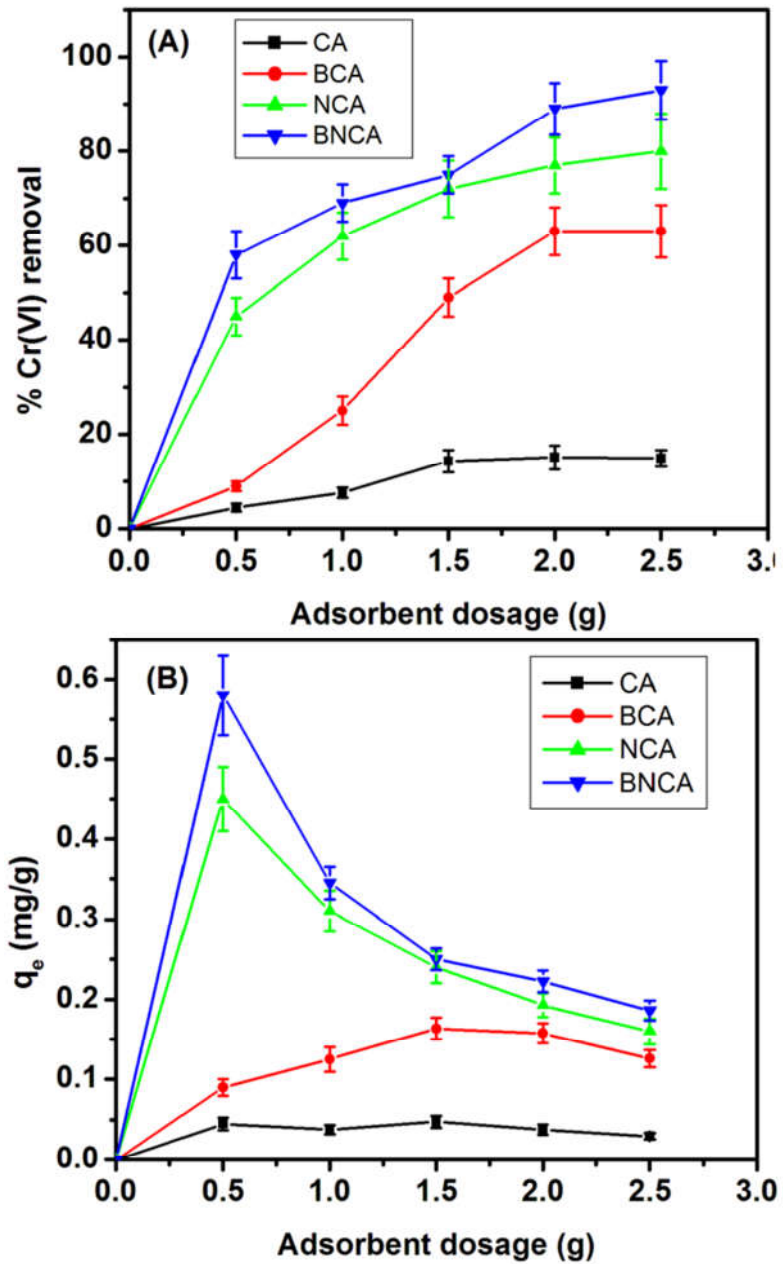


Figure 6.22: Percentage Cr(VI) removal (A) and  $q_e$  (B) as a function of adsorbent dosage for different types of adsorbents (pH=7, time=90 min, initial Cr(VI) concentration=10 ppm, n=3)



### 6.5.5 Isotherm plotting and modeling

The isotherm of adsorption of Cr(VI) onto BNCA beads is represented in fig 6.23.  $q_e$  is found to increase with  $C_e$  which is typical to an isotherm plot.

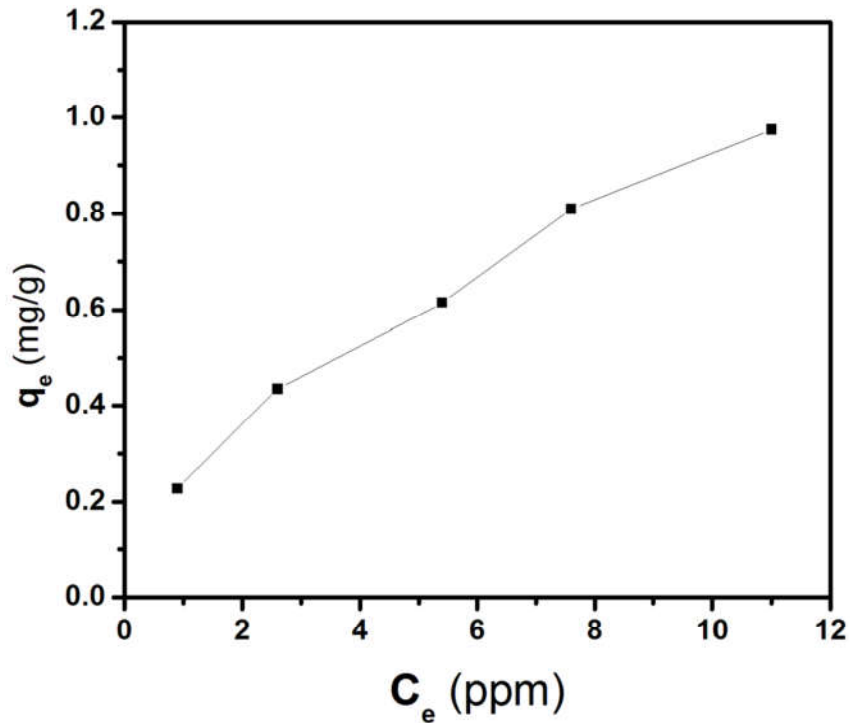


Figure 6.23: Isotherm for adsorption of Cr(VI) on BNCA

Isotherm modeling was performed as per the methods stated in the section 5.5.5 and the non linear modeled curves are represented in fig 6.24 (A) for Langmuir, fig 6.24 (B) for Freundlich, and fig 6.24 (C) for Sips isotherm. The model parameters and coefficient of determination are represented in table 6.1. The data suggests that the isotherm is most likely to be modeled as per Sips isotherm or Freundlich isotherm. Sips isotherm is well suitable for the current adsorption systems as this model makes the assumption that adsorption occur in a non-ideal, reversible manner that is not limited to monolayer adsorption. Sips isotherm is a sound model used to study heterogeneous systems. The operating parameters of the isotherm are a relative measure of the heterogeneity of the adsorbent (Foo and Hameed 2010). Here, the slope value of

around 0.2397 suggests that the surface of adsorbent is more of the homogenous kind, which is attributed towards the homogeneity of size and shape of nZVI. The comparison of values of obtained parameters is not recommended as these are highly annexed to process variables.

Model	Fitting Equation	Corresponding parameters	R <sup>2</sup>
Langmuir	$\frac{C_e}{q_e} = 0.7059C_e + 3.993$	Q <sub>0</sub> =1.417    b= 0.177	0.951
Freundlich	$\ln q_e = -1.413 + 0.5791 \ln C_e$	K <sub>f</sub> = 0.243    n=1.727	0.997
Sips	$q_e = \frac{0.2397C_e^{0.5512}}{1 - 0.022C_e^{0.5512}}$	K <sub>s</sub> = 0.2397    a <sub>s</sub> = -0.022 β <sub>s</sub> =0.5512	0.995

Table 6.1: Modeled equations of isotherms with their parameters and coefficient of determination

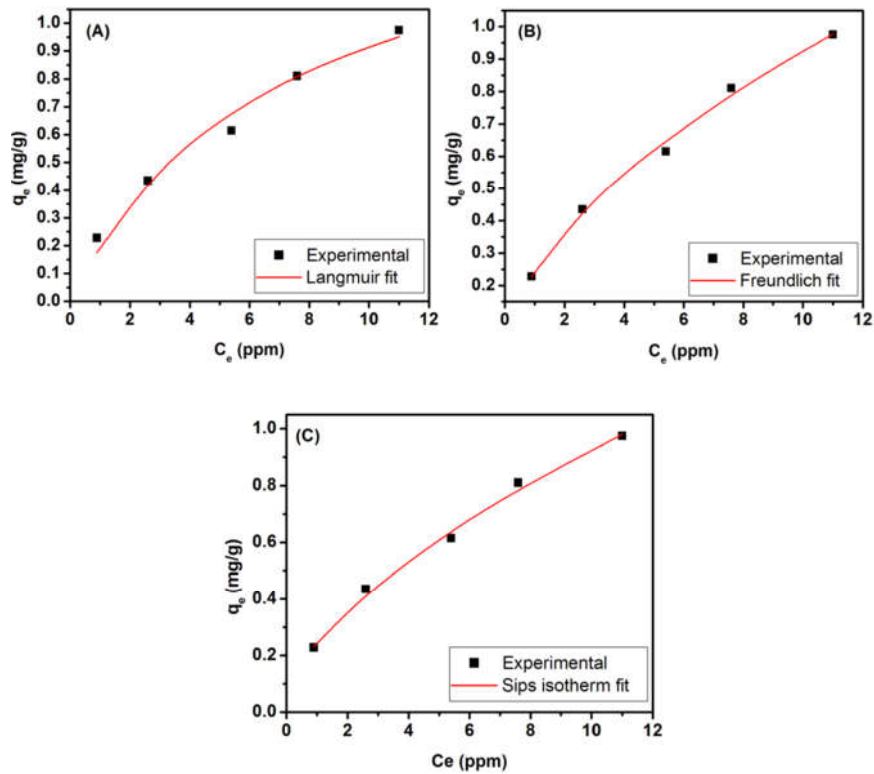


Figure 6.24: Non linear fit of isotherm to (A) Langmuir model, (B) Freundlich model, (C) Sips model

### 6.5.6 Mathematical modeling of the kinetics of batch removal

Kinetics of adsorption is defined as time-dependent behavior of the amount of adsorption. This is a crucial and important parameter to analyze the behavior of adsorption process. Kinetic parameters are useful in evaluating, designing and scaling up of the systems that utilizes adsorption. The intrinsic theoretical complexity of the adsorption process limits the development of understanding of kinetics as adsorption process is mostly an orchestra of several physiochemical processes. The model equations along with coefficients obtained after performing regression, are given in table 6.2. Fig 6.25 (A) depicts the linear fit of kinetic data to PFO model and Figure fig 6.25 (B) exhibits the fitting of the kinetic data to linear form of PSO model equation. The linear fit of the Vermeulen model is shown in fig 6.25 (C). We used Vermeulen model for fitting the kinetic data as our adsorption system being a porous

system follows the assumption of this model. The low value of the Y-intercept of linear form of vermuelen model (0.011 reveals that IPD shall be the major rate-limiting step in the entire adsorption process. Recently, Kulkarni et al. (Kulkarni et al. 2022) have used a modified form of Vermeulen diffusion model to study the kinetics of adsorption of Cu(II) ions onto calcium alginate beads. They argued that the mesoporous nature of their beads requires an intermediate model that will combine the features of fractal-like structure and pore diffusion effects. Yao and Chen (Yao and Chen 2019) have also suggested in their study that the Vermeulen kinetic model is better suitable to describe the cases when IPD is the rate-controlling step.

Kinetics of the batch studies pronounces the performance which holds a great significance for scaling up and pilot studies. The data obtained is useful for determining the solute uptake rate which is one of the indicators of residence time of adsorbent for effective removal. Kinetic analysis also reveals the information related to the size of apparatus required for the actual operation. This is also helpful in predicting the performance of fixed bed adsorption systems.

Fitting the obtained experimental data to the Vermeulen model yielded the following linear equation:

$$y = 0.026x - 0.011$$

The coefficient of determination of the fitted equation was determined to be 0.995 which suggested that the data is fitting well to the model equation. It is to be noted that only data points which are not in the saturated region of the curve were used to get the fit. Using all the data points may cause to the data unnecessarily getting biased towards the saturation region which is not desired. Comparing the fit equation with the linear form of the model yields a low value of y intercept (0.011) which points a strong intraparticle diffusion (IPD) process that is limiting the reaction.

This phenomenon of IPD may cause a problem while putting the matter to column studies and scaling up for pilot studies because the beads will be even be more packed in the column where IPD may become more prominent. This phenomenon may be pronounced at higher flow rates only because at smaller flow rates residence time of

the analyte is enough to equilibrate the mass between in flowing phase and adsorbent. So, it is advised not to run the operation at high flow rates. The same is demonstrated and experienced during the column studies further.

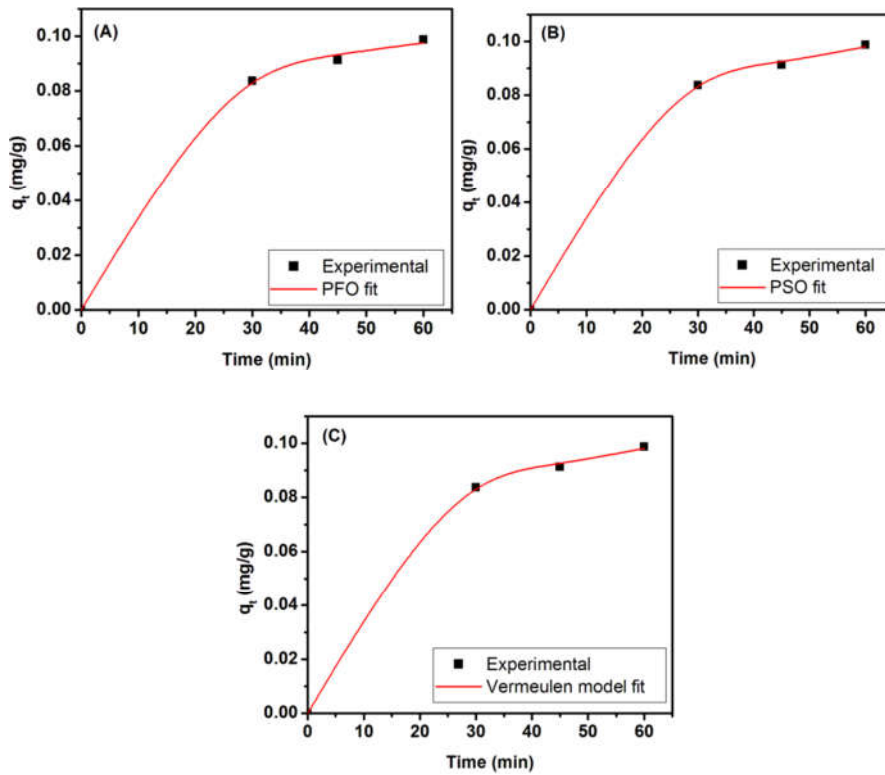


Figure 6.25: Graphs of kinetic data of the adsorption process; (A) Linear fit to the PFO kinetic model, (B) Linear fit to the PSO kinetic model, and (C) Linear fit to the Vermeulen Model

Model	Model Equation	Corresponding parameters	R <sup>2</sup>	SSE
PFO	$q_t = q_e(1 - \exp(-k_1 t))$	$k_1=0.0578\text{sec}^{-1}$ , $q_e=0.1007 \text{ mg/g}$	0.999053	$6.02 \times 10^{-6}$
PSO	$q_t = q_e \left(1 - \frac{1}{1 + q_e k_2 t}\right)$	$k_2=0.6485 \text{ g.mg}^{-1}.\text{sec}^{-1}$ , $q_e=0.1191 \text{ mg/g}$	0.999613	$2.46 \times 10^{-6}$
Vermeulen kinetic model	$\frac{\bar{q}}{q_e} = \sqrt{1 - e^{\left(\frac{-D\pi^2 t}{R^2}\right)}}$	$D=0.0000314 \text{ cm}^2/\text{sec}$ , $q_e=0.1068 \text{ mg/g}$	0.999578	$2.68 \times 10^{-6}$

Table 6.2: Modeled equations of adsorption kinetics with its parameters and coefficient of determination

## 6.6 Packed Bed Column studies

Packed bed studies in wastewater treatment involve the use of packed bed columns to remove contaminants and pollutants from wastewater. The packed bed acts as a filter medium, providing a large surface area for the interaction between the wastewater and the packing material, which may be activated carbon, zeolites, sand, or other suitable materials. The column used in current study is shown in fig 6.26. The setup used in the performing the continuous study is shown in fig 6.27. Here are some important aspects of packed bed studies in wastewater treatment:

1. Adsorption studies: One of the primary mechanisms in packed bed wastewater treatment is adsorption. Contaminants in the wastewater are adsorbed onto the surface of the packing material, effectively removing them from the water. Researchers study the adsorption capacity of the packing material, the kinetics of adsorption, and the effect of various operating parameters like flow rate, pH, and contact time on adsorption efficiency.
2. Breakthrough curves: Breakthrough curves represent the concentration of pollutants in the treated water as a function of time or volume of water treated. These curves help determine the point at which the adsorption capacity of the packed bed is exhausted, indicating the need for replacement or regeneration of the packing material.
3. Regeneration studies: Over time, the adsorption capacity of the packing material decreases as it becomes saturated with contaminants. Researchers investigate different methods of regenerating the packing material to restore its adsorption capacity and extend its lifespan. Common regeneration techniques include backwashing, chemical regeneration, and thermal regeneration.
4. Mass transfer and fluid dynamics: Understanding the mass transfer rates and fluid dynamics within the packed bed is crucial for optimizing the wastewater treatment process. Researchers study the flow patterns, pressure drop, and residence time distribution to improve the efficiency of contaminant removal and avoid channeling or preferential flow paths.
5. Media selection: The choice of packing material is essential in wastewater treatment packed bed columns. Different contaminants require specific packing

materials with suitable adsorption properties. Studies focus on identifying the most appropriate packing material for the targeted pollutants in the wastewater.

6. Scale-up and system design: Laboratory-scale studies play a crucial role in developing an understanding of the packed bed's performance. However, researchers also work on scaling up the system to larger treatment plants. This includes design considerations, hydraulic loading rates, and process optimization for full-scale applications.

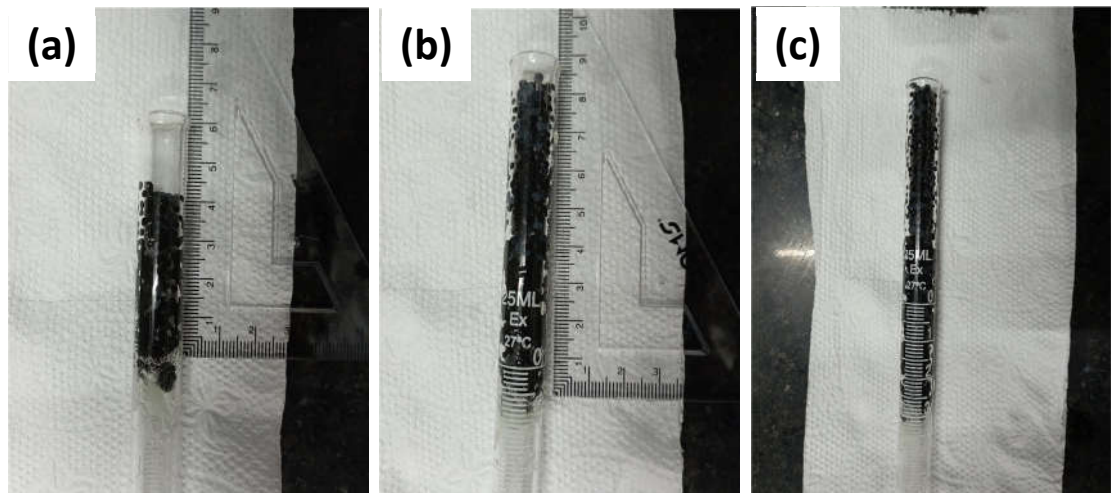


Figure 6.26: Fixed columns made of BNCA beads; (a) 4 cm bed (b) 8 cm bed, (c) 12 cm bed



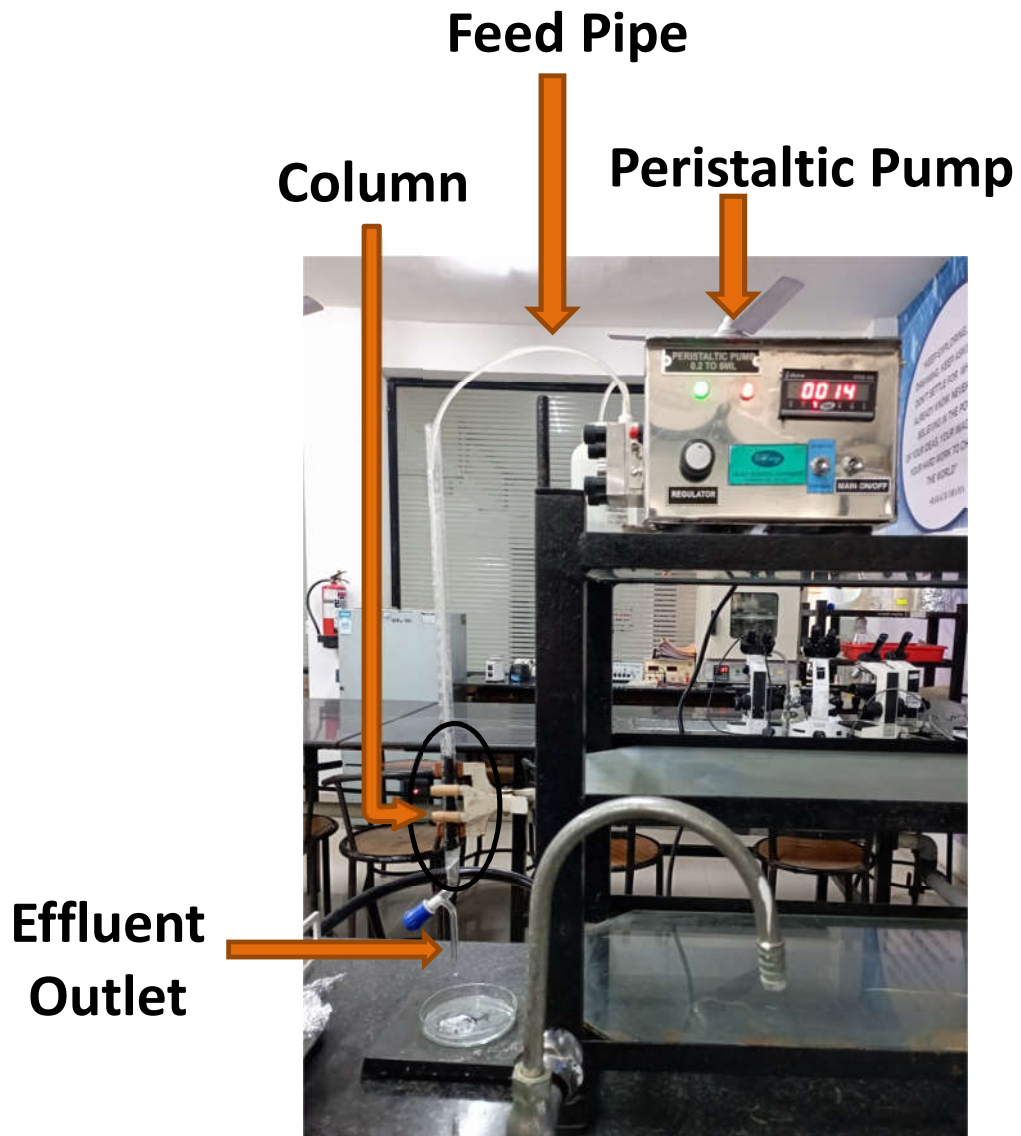


Figure 6.27: Column setup to run the experiments of fixed bed column studies

Breakthrough analysis was performed for the data obtained from column studies and is curve of fraction eluted v/s time is shown in fig 6.28 and fig 6.29.

The general nature of curve can be explained as follows. The adsorbent bed is the region of mass transfer where the transport of the solute (Cr(VI) species here) takes place from liquid phase to solid phase (adsorbent beads). As the liquid phase moves

down the column, the distribution of matter takes place. The solid phase from the top starts adsorbing that solute from the liquid phase and the liquid that reaches the bottom is free of solute. Gradually, the adsorbent starts getting saturated and the adsorption zone start moving downwards. As the adsorption zone reaches to bottom of bed we observe a small increment in the concentration of solute in the eluant. It increases and reaches to maximum ( $F/F_0=1$ ) when the entire bed becomes saturated. Breakthrough time is defined as time required reaching a particular vale of  $F/F_0$ . Like,  $t_{B,50}$  is breakthrough time for  $F/F_0=50\%$ , and  $t_{B,10}$  is breakthrough time for  $F/F_0=10\%$ , or  $F/F_0=0.1$ .

#### 6.6.1 Effect of flow rate on breakthrough time.

The experimental effect of change of flow rate on the nature of breakthrough curve is shown in fig 6.28. It is observed that as the flow rate is increased, breakthrough time decreases table 6.3.

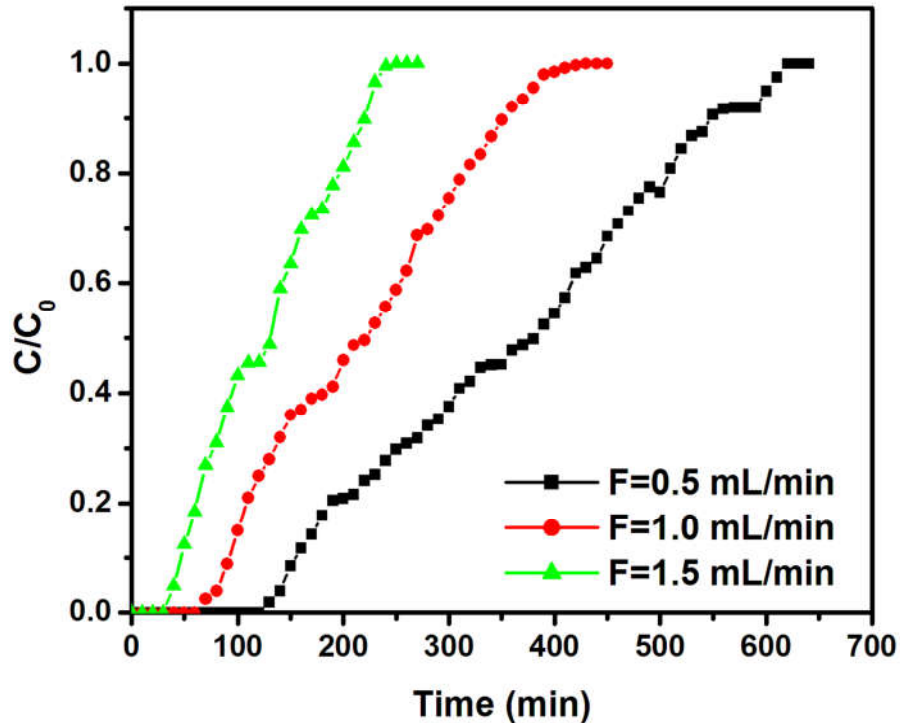


Figure 6.28: Breakthrough curves for adsorption with constant bed height and variable flow rate

Flow rate (mL/min)	$t_{B,50}$ (min)	$t_{B,10}$ (min)
0.5	380	115
1.0	220	90
1.5	130	45

Table 6.3: Change in the breakthrough time (10% and 50%) with change in flow rate

As the flow rate is increased, more amount of solute is fed into the column with time. This makes the column to get saturated earlier and hence the breakthrough is achieved earlier.

#### 6.6.2 Effect of bed height on breakthrough time.

Fig 6.29 reveals the effect of bed height on the breakthrough curves. It is seen that breakthrough time is increased with increase in bed height of the adsorption column (Table 6.4).

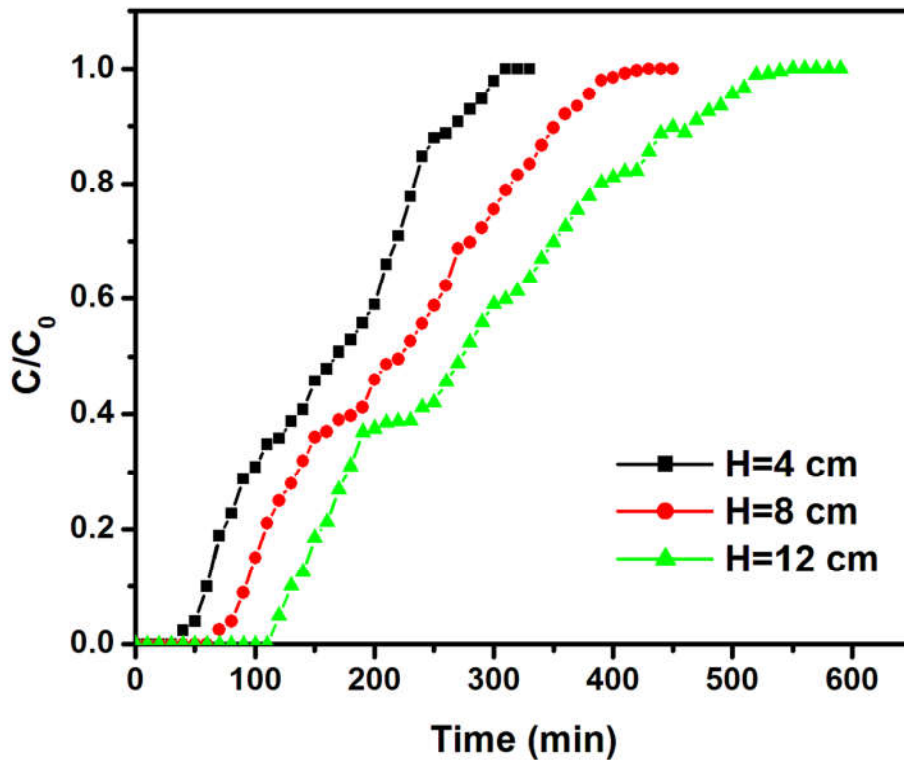


Figure 6.29: Breakthrough curves for adsorption with constant flow rate and variable bed height

Bed Height (cm)	$t_{B,50}$ (min)	$t_{B,10}$ (min)
4	170	60
8	220	90
12	270	130

Table 6.4: Change in the breakthrough time (10% and 50%) with change in bed height

As the bed height is increased we add more adsorbent to the bed. With constant flow rate the amount of solute added to column with time is constant. The larger amount of adsorbate can be retained in larger bed and this makes the breakthrough curve to shift to right side of the curve. The higher the amount adsorbed, higher is the time taken to get it in eluant at a given flow rate.

Similar results of breakthrough were reported by Dorota Kołodyńska et al. (Fila and Kołodyńska 2023). They utilized beads of calcium alginate to remove Lanthanum (III) ions from aqueous systems. They also reported that with increase in bed volume it will take a higher time to reach the breakthrough. Lee et al. performed adsorption of phosphate ions from aqueous solutions using modified biochar calcium-alginate beads (Jung et al. 2017). Their results of fixed column studies were well similar to that obtained by us.

#### 6.7 Modeling of breakthrough curves

Modeling of breakthrough curves was performed to analyze the estimation of parameters that are characteristics of adsorption process. This is helpful in making sensible assumptions about the mechanisms which becomes helpful in scaling up the process.

The obtained data was fitted to the different models as mentioned earlier. The model equations obtained by the fitting procedure are given in table 6.5-6.8.

The fitted models were simulated to give the predicted curves which were plotted against the actual values that are given in fig 6.30. Observation of these graphs revealed that models were working well for initial time but were deviated from the actual values in later stages of PBC operation. This may be attributed to the column packing and handling. If the column is not packed homogenously the breakthrough

may be achieved later as compared to predicted value. This may be even serious issues at large scales where larger volumes and flow rates are to be handled.

Prediction of  $t_{b,50}$  by Yoon Nelson modeling gives a lower value as compared to actual value in all the cases clearly indicating a deviation.

<b>SN</b>	<b>Bed height (cm)</b>	<b>Model Equation</b>	<b>N<sub>0</sub></b>	<b>K</b>	<b>R<sup>2</sup></b>
1	4	$y = 0.0236x - 3.823$	51541.07	0.002361	0.9786
2	8	$y = 0.0151x - 3.238$	34129.04	0.00151	0.9823
3	12	$y = 0.00997x - 2.737$	29126	0.000997	0.985

Table 6.5 Model and analysis of breakthrough curve for Adams-Bohart equation with varying bed height and constant flow rate (1 ml/min)

<b>SN</b>	<b>Flow rate (ml/min)</b>	<b>Model Equation</b>	<b>N<sub>0</sub></b>	<b>K</b>	<b>R<sup>2</sup></b>
1	0.5	$y = 0.0128x - 4.593$	28714.98	0.001273	0.9833
2	1.0	$y = 0.0151x - 3.238$	34129.04	0.00151	0.9823
3	1.5	$y = 0.0189x - 2.173$	27380.95	0.001895	0.9799

Table 6.6 Model and analysis of breakthrough curve for Adams-Bohart equation with varying flow rate and constant bed height (8 cm)

<b>SN</b>	<b>Bed height (cm)</b>	<b>Model Equation</b>	<b>k<sub>YN</sub></b>	<b>τ</b>	<b>R<sup>2</sup></b>
1	4	$y = 0.01895x - 3.068$	0.01895	161.922	0.979
2	8	$y = 0.0151x - 3.238$	0.0151	214.44	0.9823
3	12	$y = 0.01273x - 3.494$	0.01273	274.506	0.985

Table 6.7: Model and analysis of breakthrough curve for Yoon Nelson equation with varying bed height and constant flow rate (1 ml/min)

<b>SN</b>	<b>Flow rate (ml/min)</b>	<b>Model Equation</b>	<b>k<sub>YN</sub></b>	<b>τ</b>	<b>R<sup>2</sup></b>
1	0.5	$y = 0.00997x - 3.597$	0.00997	360.843	0.983
2	1.0	$y = 0.0151x - 3.238$	0.0151	214.439	0.9823
3	1.5	$y = 0.02361x - 2.708$	0.02361	114.693	0.9799

Table 6.8: Model and analysis of breakthrough curve for Yoon Nelson equation with varying flow rate and constant bed height (8 cm)

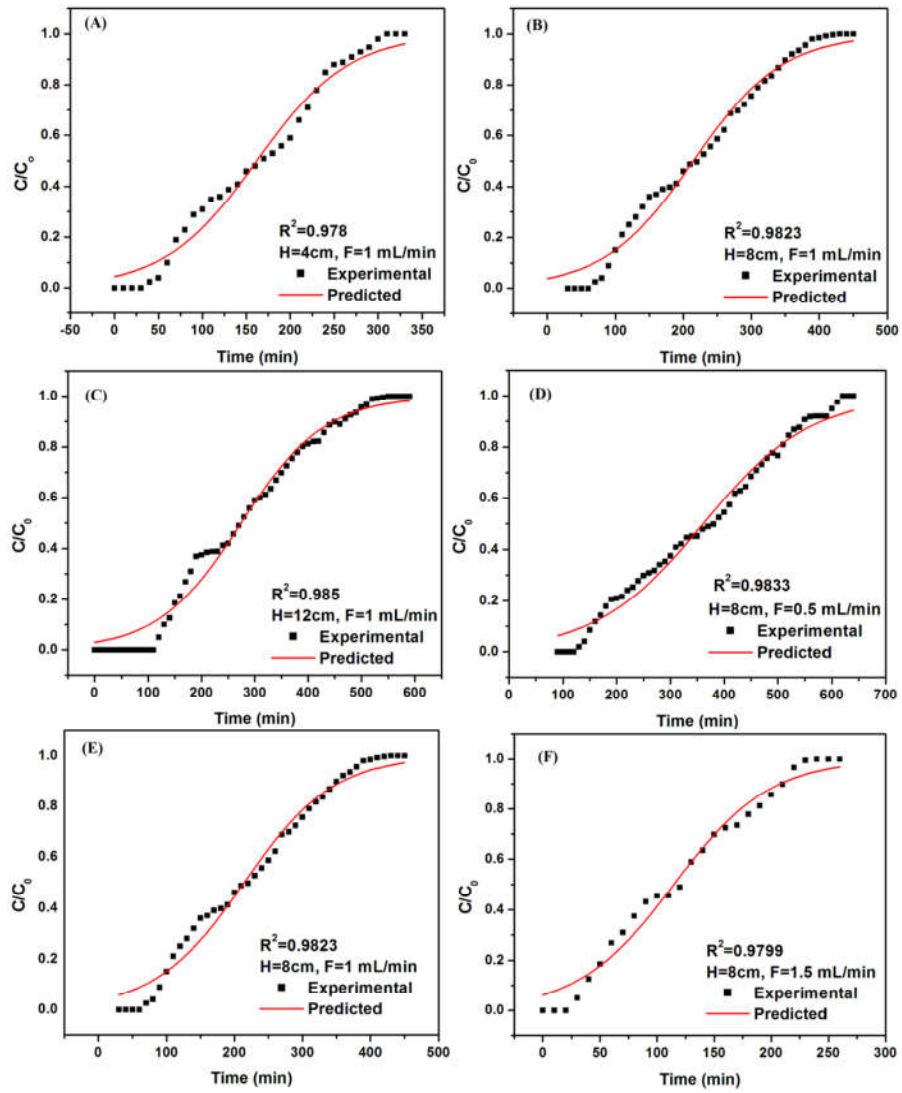


Figure 6.30: Modeling of breakthrough curve; (a)  $H=4\text{ cm}$ ,  $F=1\text{ mL/min}$ ,  $C_0= 10\text{ ppm}$ , (b)  $H=8\text{ cm}$ ,  $F=1\text{ mL/min}$ ,  $C_0= 10\text{ ppm}$ , (c)  $H=12\text{ cm}$ ,  $F=1\text{ mL/min}$ ,  $C_0= 10\text{ ppm}$ , (d)  $H=8\text{ cm}$ ,  $F=0.5\text{ mL/min}$ ,  $C_0= 10\text{ ppm}$ , (e)  $H=8\text{ cm}$ ,  $F=1.0\text{ mL/min}$ ,  $C_0= 10\text{ ppm}$ , (f)  $H=8\text{ cm}$ ,  $F=1.5\text{ mL/min}$ ,  $C_0= 10\text{ ppm}$



## 6.8 Modeling of PBC under real wastewater matrix spiked with Cr(VI)

After performing modeling of the adsorption process under PBC with synthetic WW, we performed the experiment with spiked real WW obtained from effluent stream. The breakthrough curve for variable bed height is shown in fig 6.31.

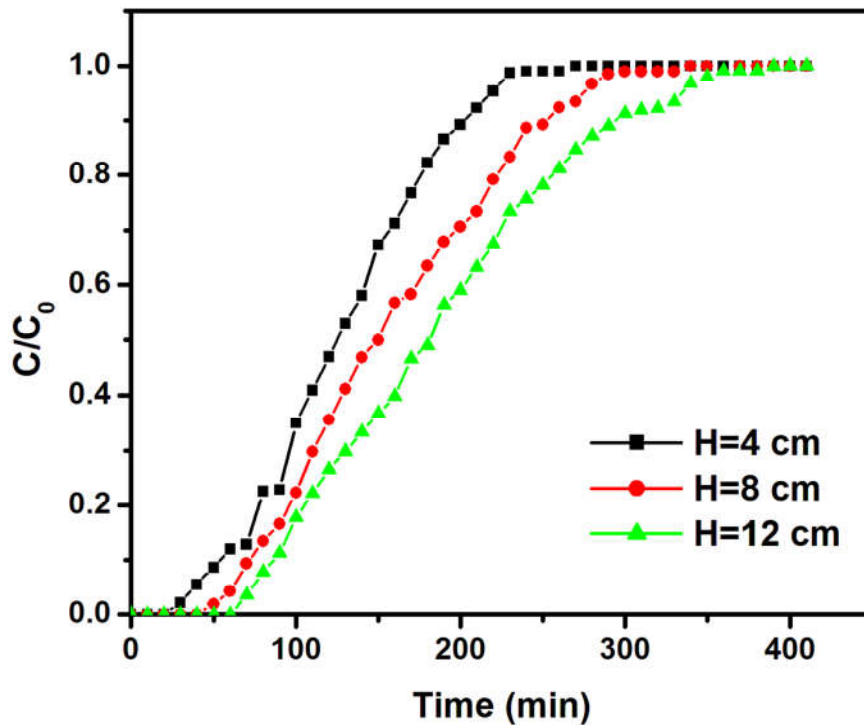


Figure 6.31: Breakthrough curve for adsorption of Cr(VI) from spiked real WW under variable height and constant flow rate

A similar trend of shift in the curve was observed as in the case of synthetic WW. With an increase in bed height there was an increment in the breakthrough time (50%,  $t_{b50}$ ). As more amount of adsorbent was available for adsorption, more amount of analyte was adsorbed which lead to an increment in the breakthrough time.

The breakthrough curves obtained for three different flow rates (while keeping the bed height fixed at 8 cm) are shown in fig 6.32. It is observed that the breakthrough time is decreased as we increase the flow rate. By increasing the flow rate, we are feeding more amount of analyte into the column a given time interval which leads to quicker saturation of the column that causes decrement in breakthrough time.

It is also observed from comparing fig 6.3 with fig 6.9 and fig 6.4 with fig 6.10 that the breakthrough time of the column decreased while using the spiked real WW as compared to synthetic WW. This effect can be attributed to the fact that real WW may contain certain other ions as well which may also be adsorbed and saturates the column faster.

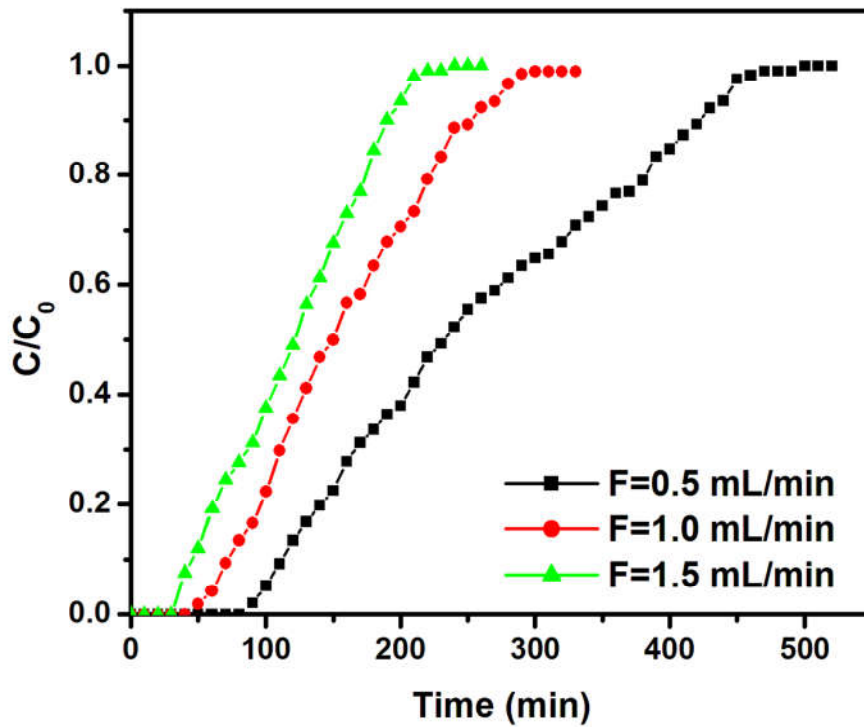


Figure 6.32: Breakthrough curve for adsorption of Cr(VI) from spiked real WW under variable flow rate and constant bed height

Flow rate (mL/min)	$t_{B,50}$ (min)	$t_{B,10}$ (min)
0.5	230	110
1.0	150	70
1.5	120	45

Table 6.9: Breakthrough time (10% and 50%) for adsorption of Cr(VI) in PBC using spiked real WW with variable flow rate and constant bed height

Bed Height (cm)	$t_{B,50}$ (min)	$t_{B,10}$ (min)
4	125	55
8	150	70
12	180	85

Table 6.10: Breakthrough time (10% and 50%) for adsorption of Cr(VI) in PBC using spiked real WW with variable bed height and constant flow rate

### 6.9 Reuse of the spent adsorbent

The reusability of the spent adsorbent was evaluated on the basis of % Cr(VI) removal capacity and  $q_e$  value obtained after each desorption-adsorption cycle. For the desorption step, it was observed that no color was developed after adding DPC reagent which suggested that all the adsorbed Cr(VI) was desorbed. The same kind of observation was made for desorption in all the four cycles. It is observed that the acid was able to elute almost all the ion. This acid is found to be an effective agent which can be used to regenerate the spent adsorbent when it has reached its equilibrium adsorption capacity. Chiew et al. have done a comprehensive work over testing of reusability of such adsorbents for heavy metal removal

(Chiew et al. 2016). They reported a desorption efficiency of over 90% upto 10 cycles of desorption.

The removal capacities of the regenerated adsorbent is shown in fig 6.33 (% Cr(VI) removal) and fig 6.34 ( $q_e$ ). The % Cr(VI) removal in the four subsequent cycles was found to be 92%, 89%, 91%, and 87% respectively. The variation between the removal percentages in the four cycles is quiet low which suggests a significant regeneration of the adsorbent after each regeneration step. ANOVA was performed among the adsorption capacities, and among removal percentages of the four groups involved. A P value $>0.05$  suggested no significant difference among the four cycles involved. The value of  $q_e$  obtained after adsorption in the four cycles was found to be 230, 222.5, 227.5, 217.5 mg/g. These nearness of these values also signifies that the regeneration steps were well successful is retaining the properties of adsorbent. After 4 cycles the mechanical strength of the beads were found to be lost so the regeneration was stopped after that. In similar work the equilibrium adsorption capacities were found to be uniform over the cycles as well. Chiew et al. have shown that the adsorption capacities were uniform upto 10 cycles of regeneration for adsorption of lead ions over calcium-alginate and alginate-halloysite nanocomposite beads (Chiew et al. 2016). Another work led by Y.N. Mata have exhibited that adsorption uptake may reduce if the regeneration step is omitted. They have also shown that the regeneration step is shown to increase the capacity of adsorption in the subsequent cycles (Mata et al. 2010).

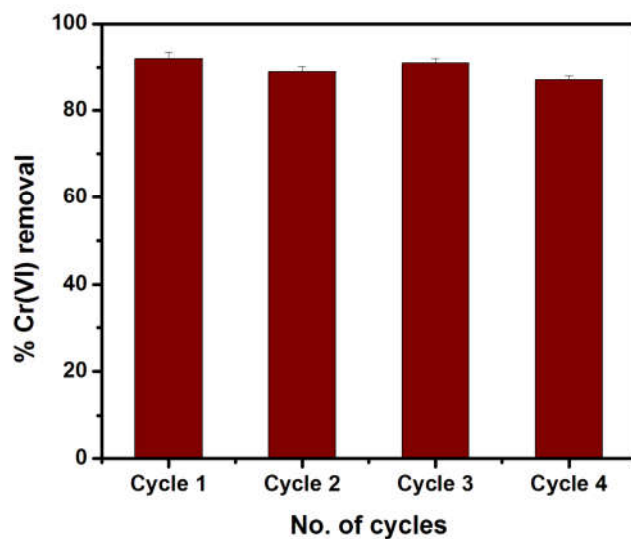


Figure 6.33: Removal percentage of Cr(VI) in batch mode upon reusing the adsorbent after 4 cycles of regeneration

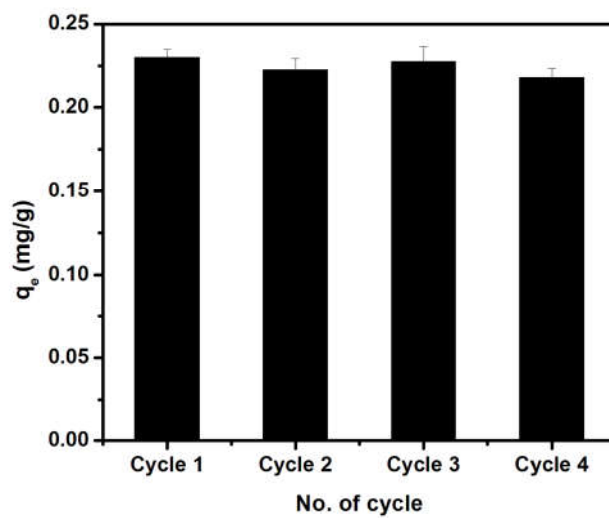


Figure 6.34: Equilibrium adsorption capacity of adsorbent for removal of Cr(VI) in batch mode upon reusing the adsorbent after 4 cycles of regeneration

# Chapter 7

## SUMMARY

### AND

## CONCLUSION

## Summary and conclusion

The current study has been performed to evaluate the performance of a novel biosorbent for its Cr(VI) removal capacity. Pollution of natural water sources by wastewater of industrial effluent has been a major factor responsible for serious health problems in human and deleterious effect on ecosystem. These wastewaters contain several types of organic and inorganic, soluble and insoluble compounds which needs to be removed so that natural systems can be safeguarded. Among the major culprits are the salts of heavy metals like Cr, Cd, As, Pb, Cu. Cr(VI) released from leather, paint, and metal processing industries is the focus problem of current study. Current study aims to evaluate the performance of a novel adsorbent prepared from combination of nZVI and Cr(VI) tolerant bacteria for removing Cr(VI) from wastewater.

Cr(VI) tolerant bacteria was isolated from wastewater receiving effluent water from various industries. The water nearby to the banks of the channel was expected to be enriched with such microbes which are capable to survive in high Cr(VI) concentration. The isolated bacteria was found to tolerate Cr(VI) upto 400 ppm. More places can be explored to prospect for bacteria with even higher MIC of Cr(VI). The bacterial morphological characterization revealed that it was a gram positive rod shaped bacteria. Molecular characterization confirmed that it was a strain of *Bacillus subtilis*. The species was found to be tolerant to Cr(VI) by other groups as well. We used this bacteria for encapsulating it into calcium alginate beads along with nZVI. We expected the synergism of bacteria and nZVI will give a better Cr(VI) removal efficiency.

nZVI was purchased and characterized for physical and chemical properties. SEM examination revealed spherical homogenous particles with smooth surfaces. Particles tend to aggregate together in the aqueous phase as seen in TEM examination. This was expected as the particles are of metallic nature with no charge on surfaces. XRD analysis was performed which gave very sharp peaks attributed to high purity of the sample. Zeta potential of the sample was 12.09 in aqueous solution and this value is

suggests the colloid to be unstable and the solute tends to aggregate in this region. DLS scattering results revealed a smooth, symmetric, and narrow distribution that suggests a smaller difference in average size of particles and homogeneity in particles.

Four different types of NBA were synthesized using the components. Blank calcium alginate beads (CA), beads with bacteria only (BCA), beads with nZVI only (NCA), and beads with both bacteria and nZVI (BNCA). All four were used in batch experiments to evaluate their performances over % Cr(VI) removal and adsorption capacity under varying conditions i.e. initial pH of solution, initial solute concentration, adsorbent dosage, and time of incubation. Batch data revealed that in all the condition tested, BNCA was found to have maximum % Cr(VI) removal and adsorption capacity. This goes well with our hypothesis where we expected that due of synergetic effect of nZVI and bacteria and adsorption shall get better.

The capacities were found to be best at pH 7. While varying initial Cr(VI) concentration it was found that removal percentage decreased with increase in Cr(VI) concentration. With more amount of solute the total amount adsorbed was getting higher, but percentage of the total adsorption was falling as the amount adsorbed does not increase in a linear manner. However in the case, adsorption capacities increased as more amount of solute was bound to the adsorbent at equilibrium. So this suggests that the binding sites on the adsorbent are available but due to thermodynamic constraints the filling of these sites was inhibited. Cr(VI) adsorption was found to increase with time and got saturated after around 90 min for BNCA. This time is the time required by the adsorbent to get saturated with the solute. Cr(VI) removal % was increased with increase in adsorbent dosage but the same trend was not observed in the case of adsorption capacity. Adding more adsorbent resulted in more amount of solute to be adsorbed on it in a fixed time and fixed initial concentration. But at higher dosage the time required for reaching equilibrium was not enough (90 min). This resulted in loss of adsorption capacity. Through these experiments it was concluded that BNCA, bead with both bacteria and nZVI is showing highest capacity to remove Cr(VI). Further experiments were performed with this NBA only. In a study by Samuel et al. (2013), they experimented using sodium alginate to encapsulate *Bacillus subtilis*, *Escherichia coli*, and *Acinetobacter johnsonii* in order to remove Cr(VI) from



wastewater. Next, the immobilized bacterial biomass's efficiency was contrasted with that of the unfixed/free bacteria. The highest Cr(VI) adsorption capacity (657 mg/g) was noted. In another study (Wi et al. 2019), Cr(VI) tolerant strain were immobilized in calcium alginate beads that were able to remove nearly all the Cr(VI) from a solution of 150 mg/L.

Batch experiments with BNCA were performed to plot and analyze the isotherms. Three types of isotherm viz. Langmuir, Freundlich, and Sips were used to model the data obtained and it was found that Sips model shall be the best fit model and that assumes adsorption in non ideal, reversible manner. The heterogeneous nature of adsorption sites is also explained with the help of this model.

Kinetics of the batch adsorption was studied using Pseudo first order (PFO), Pseudo second order (PSO), and Vermeulen model and analytical studies suggested that the current system can be explained best by assuming Vermeulen model and its further analysis reveals that intra particle diffusion limits the adsorption process. This can be improved by further optimizing the concentrations of sodium alginate and operating parameters.

The BNCA was further evaluated in fixed bed columns by preparing breakthrough curves under varying bed height and varying flow rates. The modeling of these curves was done with Adams Bohart model and Yoon Nelson model. The breakthrough time was found to increase with increase in bed height as more adsorbent was available for adsorption at a given flow rate and thus elution is delayed. With flow rate, the breakthrough time decreased. This is attributed to the fact that with high flow rates more solute is entering the column per unit time that saturates the bed quicker and hence elution is observed early. Some deviation is the actual results and model predicted values were observed in fixed bed columns. It can be attributed to the fact that the column was not packed homogeneously. The radial diffusion in the column may also limit the predicted curve to be exactly followed. It is a good practice to see that equal amount of adsorbent is being packed in every unit of the column. Real WW spiked with Cr(VI) was also used further in fixed bed column. In this case, due to

presence of few more ions, the breakthrough was achieved earlier as compared to synthetic WW.

Adsorbent was regenerated by exposing the spent adsorbent to desorption solution and curing in  $\text{CaCl}_2$ . The regenerated adsorbent has shown a remarkable capacity to remove Cr(VI) from WW without any significant loss up to four cycles . This suggests that the BNCA can be used in the system again and again thus reducing the disposal related problems.

SNo	Adsorbent	Contaminant	Maximum adsorption capacity	Reference
1	<i>Yarrowialipolytica</i> immobilized in calcium alginate	Uranium	2.25 mg/g	Kolhe et al. (2020)
2	Bentonite supported nZVI	Total Cr	7.3 mg/g	Shi et al. (2011)
		Pb <sup>2+</sup>	1.3 mg/g	
		Cu <sup>2+</sup>	3.0 mg/g	
		Zn <sup>2+</sup>	16.8 mg/g	
3	nZVI composite	Cr(VI)	199.46 mg/g	Zhou et al. (2022)
4	Polyethylene glycol-stabilized nano zero-valent iron	Cr(VI)	125.22 mg/g	Wu et al. (2020)
5	Biochar supported nZVI	Cr(VI)	24.08 mg/g	Cao and Zhang (2024)
6	Immobilized nZVI with bacteria	Cr(VI)	0.58mg/g (wet weight)	This study

Table 7.1: Adsorption capacities of similar adsorbents

This entire study have established that Cr(VI) tolerant bacteria along of nZVI can be used to prepared an adsorbent which can be utilized efficiently for Cr(VI) from WW in the prevalent conditions. The adsorbent can be used in fixed bed that can be used in industrial scales as well when scaled up appropriately. The adsorbent can be reused and have a significant capacity to hold the solute. Table 7.1 comprehends a comparison of capacities of few similar adsorbents

This research has revealed a novel design of adsorbent where the properties of two materials can be synergistically captured to remove Cr(VI) from WW. The study has added the knowledge of capacity and reusability of the material as well as has analyzed the kinetics in batch and continuous mode of operation. The study can be utilized further for creating a suitable large scale equipment which can handle a larger volumetric flow rate. Also, the study provides a framework for other similar studies.

# **BIBLIOGRAPHY**

## References

- Alvarez, C. C., M. E. Bravo Gómez and A. Hernández Zavala (2021). "Hexavalent chromium: Regulation and health effects." Journal of Trace Elements in Medicine and Biology 65: 126729.
- Arthy, M. and B. Phanikumar (2016). "Efficacy of Iron-Based Nanoparticles and Nanobiocomposites in Removal of Cr 3+." Journal of Hazardous, Toxic, and Radioactive Waste 20(3): 04016005.
- Ayob, A., S. Alias, F. A. Dahalan, R. Santiagoo, A. Z. Abdullah and T. T. Teng (2015). "Kinetic removal of Cr6+ by carboxymethyl cellulose-stabilized nano zerovalent iron particles." Macedonian Journal of Chemistry and Chemical Engineering 34(2): 295-308.
- Bharagava, R. N. and S. Mishra (2018). "Hexavalent chromium reduction potential of *Cellulosimicrobium sp.* isolated from common effluent treatment plant of tannery industries." Ecotoxicology and Environmental Safety 147: 102-109.
- Breida, M., S. A. Younssi, M. Ouammou, M. Bouhria and M. Hafsi (2019). "Pollution of water sources from agricultural and industrial effluents: special attention to NO<sub>3</sub><sup>-</sup>, Cr (VI), and Cu (II)." Water Chemistry: 39.
- Cao, M., & Zhang, Y. (2024). Removal of Cr (Vi) by phosphorylated biochar supported nanoscale zero-valent iron. Available at SSRN 4696624.
- Chen, J. and Y. Tian (2021). "Hexavalent chromium reducing bacteria: mechanism of reduction and characteristics." Environmental Science and Pollution Research 28: 20981-20997.
- Cherifi, M., S. Hazourli, S. Pontvianne, F. Lopicque and J.-P. Leclerc (2016). "Electrokinetic removal of aluminum and chromium from industrial wastewater electrocoagulation treatment sludge." Desalination and water treatment 57(39): 18500-18515.
- Chiew, C. S. C., H. K. Yeoh, P. Pasbakhsh, P. E. Poh, B. T. Tey and E. S. Chan (2016). "Stability and reusability of alginate-based adsorbents for repetitive lead (II) removal." Polymer Degradation and Stability 123: 146-154.
- Chowdhury, M., M. G. Mostafa, T. K. Biswas, A. Mandal and A. K. Saha (2015). "Characterization of the Effluents from Leather Processing Industries." Environmental Processes 2(1): 173-187.

Coetzee, J. J., N. Bansal and E. M. Chirwa (2020). "*Chromium in environment, its toxic effect from chromite-mining and ferrochrome industries, and its possible bioremediation.*" Exposure and health 12: 51-62.

Crini, G. and E. Lichtfouse (2019). "*Advantages and disadvantages of techniques used for wastewater treatment.*" Environmental Chemistry Letters 17: 145-155.

Dalal, U. and S. N. Reddy (2019). "*A novel nano zero-valent iron biomaterial for chromium (Cr 6+ to Cr 3+) reduction.*" Environmental Science and Pollution Research 26: 10631-10640.

Debnath, A., K. Deb, N. S. Das, K. K. Chattopadhyay and B. Saha (2016). "*Simple chemical route synthesis of Fe<sub>2</sub>O<sub>3</sub> nanoparticles and its application for adsorptive removal of Congo red from aqueous media: artificial neural network modeling.*" Journal of Dispersion Science and Technology 37(6): 775-785.

DesMarias, T. L. and M. Costa (2019). "*Mechanisms of chromium-induced toxicity.*" Current opinion in toxicology 14: 1-7.

Dong, H., J. Deng, Y. Xie, C. Zhang, Z. Jiang, Y. Cheng, K. Hou and G. Zeng (2017). "*Stabilization of nanoscale zero-valent iron (nZVI) with modified biochar for Cr (VI) removal from aqueous solution.*" Journal of Hazardous Materials 332: 79-86.

Dong, H., L. Li, Y. Lu, Y. Cheng, Y. Wang, Q. Ning, B. Wang, L. Zhang and G. Zeng (2019). "*Integration of nanoscale zero-valent iron and functional anaerobic bacteria for groundwater remediation: A review.*" Environment International 124: 265-277.

Engwa, G. A., P. U. Ferdinand, F. N. Nwalo and M. N. Unachukwu (2019). "*Mechanism and health effects of heavy metal toxicity in humans.*" In IntechOpen eBooks. <https://doi.org/10.5772/intechopen.82511>.

Enniya, I., L. Rghioui and A. Jourani (2018). "*Adsorption of hexavalent chromium in aqueous solution on activated carbon prepared from apple peels.*" Sustainable Chemistry and Pharmacy 7: 9-16.

Fan, Z., Q. Zhang, B. Gao, M. Li, C. Liu and Y. Qiu (2019). "*Removal of hexavalent chromium by biochar supported nZVI composite: Batch and fixed-bed column evaluations, mechanisms, and secondary contamination prevention.*" Chemosphere 217: 85-94.

Fila, D. and D. Kołodyńska (2023). "Fixed-Bed Column Adsorption Studies: Comparison of Alginate-Based Adsorbents for La(III) Ions Recovery." Materials 16(3): 1058.

Foo, K. Y. and B. H. Hameed (2010). "Insights into the modeling of adsorption isotherm systems." Chemical Engineering Journal 156(1): 2-10.

Franguelli, F. P., K. Tannous and C. Cione Coppi (2019). "Biosorption of hexavalent chromium from aqueous solutions using raw coconut fiber as a natural adsorbent." Chemical Engineering Communications 206(11): 1426-1439.

Fu, F., J. Ma, L. Xie, B. Tang, W. Han and S. Lin (2013). "Chromium removal using resin supported nanoscale zero-valent iron." Journal of Environmental Management 128: 822-827.

Fu, F. and Q. Wang (2011). "Removal of heavy metal ions from wastewaters: a review." Journal of environmental management 92(3): 407-418.

Gan, H., J. Liu, H. Zhang, Y. Qian, H. Jin and K. Zhang (2018). "Enhanced photocatalytic removal of hexavalent chromium and organic dye from aqueous solution by hybrid bismuth titanate  $Bi_4Ti_3O_{12}/Bi_2Ti_2O_7$ ." Research on Chemical Intermediates 44: 2123-2138.

Hanchang, S. (2009). "Industrial wastewater-types, amounts and effects." Point sources of pollution: Local effects and their control 2: 191.

Holmes, A. L., S. Wise and J. Wise (2008). "Carcinogenicity of hexavalent chromium." Indian journal of medical research 128(4): 353-372.

Honetschlägerová, L., R. Škarohlíd, M. Martinec, M. Šír and V. Luciano (2018). "Interactions of nanoscale zero valent iron and iron reducing bacteria in remediation of trichloroethene." International Biodeterioration & Biodegradation 127: 241-246.

Islam, M. A., M. J. Angove and D. W. Morton (2019). "Recent innovative research on chromium (VI) adsorption mechanism." Environmental Nanotechnology, Monitoring & Management 12: 100267.

Jangra, V. (2016). "Green Printing: Inevitability for Printing Industry Sustainability." International Journal of Engineering and Management Research (IJEMR) 6(4): 16-19.

Jin, W., H. Du, S. Zheng and Y. Zhang (2016). "Electrochemical processes for the environmental remediation of toxic Cr (VI): A review." Electrochimica Acta 191: 1044-1055.



- Jindal, R. and K. Handa (2019). "Hexavalent chromium-induced toxic effects on the antioxidant levels, histopathological alterations and expression of Nrf2 and MT2 genes in the branchial tissue of *Ctenopharyngodon idellus*." Chemosphere 230: 144-156.
- Jobby, R., P. Jha, A. K. Yadav and N. Desai (2018). "Biosorption and biotransformation of hexavalent chromium [Cr (VI)]: a comprehensive review." Chemosphere 207: 255-266.
- Jung, K.-W., T.-U. Jeong, J.-W. Choi, K.-H. Ahn and S.-H. Lee (2017). "Adsorption of phosphate from aqueous solution using electrochemically modified biochar calcium-alginate beads: Batch and fixed-bed column performance." Bioresource Technology 244: 23-32.
- Jyothi, N. R. (2020). "Heavy metal sources and their effects on human health." In IntechOpen eBooks. <https://doi.org/10.5772/intechopen.95370>.
- Kabdaşlı, I. and O. Tünay (2023). "Hexavalent chromium removal from water and wastewaters by electrochemical processes." Molecules 28(5): 2411.
- Kargar, M. and G. Zolfaghari (2018). "Hybrid nano-filtration and micro-filtration pilot processes for the removal of chromium from water." Journal of Water and Wastewater; Ab va Fazilab (in persian) 29(5): 41-50.
- Kazemi, M., M. Jahanshahi and M. Peyravi (2018). "Hexavalent chromium removal by multilayer membrane assisted by photocatalytic couple nanoparticle from both permeate and retentate." Journal of hazardous materials 344: 12-22.
- Kocur, C. M. D., L. Lomheim, H. K. Boparai, A. I. A. Chowdhury, K. P. Weber, L. M. Austrins, E. A. Edwards, B. E. Sleep and D. M. O'Carroll (2015). "Contributions of Abiotic and Biotic Dechlorination Following Carboxymethyl Cellulose Stabilized Nanoscale Zero Valent Iron Injection." Environmental Science & Technology 49(14): 8648-8656.
- Kolhe, N., Zinjarde, S. & Acharya, C (2020). Removal of uranium by immobilized biomass of a tropical marine yeast *Yarrowia lipolytica*. Journal of Environmental Radioactivity, **223**, 106419.
- Kumar, V. and S. Dwivedi (2019). "Hexavalent chromium reduction ability and bioremediation potential of *Aspergillus flavus* CR500 isolated from electroplating wastewater." Chemosphere 237: 124567.

- Kumar, V., P. Kumar, J. Singh and P. Kumar (2020). "Current status of water pollution by integrated industrial hubs (IIHs) in India." Environmental Degradation: Causes and Remediation Strategies 1: 104.
- Lace, A., D. Ryan, M. Bowkett and J. Cleary (2019). "Chromium monitoring in water by colorimetry using optimised 1, 5-diphenylcarbazide method." International journal of environmental research and public health 16(10): 1803.
- Li, Y., A. B. Cundy, J. Feng, H. Fu, X. Wang and Y. Liu (2017). "Remediation of hexavalent chromium contamination in chromite ore processing residue by sodium dithionite and sodium phosphate addition and its mechanism." Journal of environmental management 192: 100-106.
- Liu, J., K. Huang, K. Xie, Y. Yang and H. Liu (2016). "An ecological new approach for treating Cr (VI)-containing industrial wastewater: photochemical reduction." Water research 93: 187-194.
- Madhavi, V., T. Prasad, A. V. B. Reddy, B. R. Reddy and G. Madhavi (2013). "Application of phyto-genic zerovalent iron nanoparticles in the adsorption of hexavalent chromium." Spectrochimica Acta Part A: Molecular and Biomolecular Spectroscopy 116: 17-25.
- Mahurpawar, M. (2015). "Effects of heavy metals on human health." Int J Res Granthaalayah 530(516): 1-7.
- Maity, J. P., G.-S. Chen, Y.-H. Huang, A.-C. Sun and C.-Y. Chen (2019). "Ecofriendly heavy metal stabilization: microbial induced mineral precipitation (MIMP) and biomineralization for heavy metals within the contaminated soil by indigenous bacteria." Geomicrobiology Journal 36(7): 612-623.
- Malaviya, P. and A. Singh (2016). "Bioremediation of chromium solutions and chromium containing wastewaters." Critical reviews in microbiology 42(4): 607-633.
- Mansour, S. A. and M. F. Gad (2010). "Risk assessment of pesticides and heavy metals contaminants in vegetables: a novel bioassay method using *Daphnia magna* Straus." Food and chemical toxicology 48(1): 377-389.
- Mao, Z., Q. Wu, M. Wang, Y. Yang, J. Long and X. Chen (2014). "Tunable synthesis of SiO<sub>2</sub>-encapsulated zero-valent iron nanoparticles for degradation of organic dyes." Nanoscale Research Letters 9: 1-9.

- Mata, Y. N., M. L. Blázquez, A. Ballester, F. González and J. A. Muñoz (2010). "Studies on sorption, desorption, regeneration and reuse of sugar-beet pectin gels for heavy metal removal." Journal of Hazardous Materials 178(1): 243-248.
- Mella, B., A. C. Glanert and M. Gutterres (2015). "Removal of chromium from tanning wastewater and its reuse." Process Safety and Environmental Protection 95: 195-201.
- Mortazavian, S., H. An, D. Chun and J. Moon (2018). "Activated carbon impregnated by zero-valent iron nanoparticles (AC/nZVI) optimized for simultaneous adsorption and reduction of aqueous hexavalent chromium: Material characterizations and kinetic studies." Chemical Engineering Journal 353: 781-795.
- Němeček, J., P. Pokorný, O. Lhotský, V. Knytl, P. Najmanová, J. Steinová, M. Černík, A. Filipová, J. Filip and T. Cajthaml (2016). "Combined nano-biotechnology for in-situ remediation of mixed contamination of groundwater by hexavalent chromium and chlorinated solvents." Science of The Total Environment 563-564: 822-834.
- Pavesi, T. and J. C. Moreira (2020). "Mechanisms and individuality in chromium toxicity in humans." Journal of applied toxicology 40(9): 1183-1197.
- Pena-Caballero, V., R. Aguilar-López, P. A. López-Pérez and M. I. Neria-González (2016). "Reduction of Cr (VI) utilizing biogenic sulfide: an experimental and mathematical modeling approach." Desalination and Water Treatment 57(28): 13056-13065.
- Peng, H. and J. Guo (2020). "Removal of chromium from wastewater by membrane filtration, chemical precipitation, ion exchange, adsorption electrocoagulation, electrochemical reduction, electrodialysis, electrodeionization, photocatalysis and nanotechnology: a review." Environmental Chemistry Letters 18: 2055-2068.
- Phillips, I., J. Acar, T. Bergan, J. Degener, F. Baquero, A. Forsgren, G. Schito and B. Wiedemann (1998). "Methods for the determination of susceptibility of bacteria to antimicrobial agents. Terminology, EUCAST Definitive Document." Clinical Microbiology and Infection, 4: 291-296.
- Pradhan, D. and L. B. Sukla (2019). "Bioreduction of hexavalent chromium using microalgae." In Springer eBooks (pp. 65–73). [https://doi.org/10.1007/978-981-13-1586-2\\_5](https://doi.org/10.1007/978-981-13-1586-2_5)

- Pradhan, D., L. B. Sukla, M. Sawyer and P. K. Rahman (2017). "Recent bioreduction of hexavalent chromium in wastewater treatment: A review." Journal of Industrial and Engineering Chemistry 55: 1-20.
- Rahman, Z. and L. Thomas (2021). "Chemical-assisted microbially mediated chromium (Cr)(VI) reduction under the influence of various electron donors, redox mediators, and other additives: an outlook on enhanced Cr (VI) removal." Frontiers in Microbiology 11: 619766.
- Ramakrishnaiah, C. and B. Prathima (2012). "Hexavalent chromium removal from industrial wastewater by chemical precipitation method." International Journal of Engineering Research and Applications 2(2): 599-603.
- Sharma, P., V. Bihari, S. K. Agarwal, V. Verma, C. N. Kesavachandran, B. S. Pangtey, N. Mathur, K. P. Singh, M. Srivastava and S. K. Goel (2012). "Groundwater contaminated with hexavalent chromium [Cr (VI)]: a health survey and clinical examination of community inhabitants (Kanpur, India)." PloS one 7(10): e47877.
- Sharma, P., S. P. Singh, S. K. Parakh and Y. W. Tong (2022). "Health hazards of hexavalent chromium (Cr (VI)) and its microbial reduction." Bioengineered 13(3): 4923-4938.
- Shaw, P., P. Mondal, A. Bandyopadhyay and A. Chattopadhyay (2019). "Environmentally relevant concentration of chromium activates Nrf2 and alters transcription of related XME genes in liver of zebrafish." Chemosphere 214: 35-46.
- Shi, L., Zhang, X. & Chen, Z. Removal of chromium (VI) from wastewater using bentonite-supported nanoscale zero-valent iron. (2011) Water Res 45, 886–892
- Shi, Z., W. Shen, K. Yang, N. Zheng, X. Jiang, L. Liu, D. Yang, L. Zhang, Z. Ai and B. Xie (2019). "Hexavalent chromium removal by a new composite system of dissimilatory iron reduction bacteria *Aeromonas hydrophila* and nanoscale zero-valent iron." Chemical Engineering Journal 362: 63-70.
- Sibi, G. (2016). "Biosorption of chromium from electroplating and galvanizing industrial effluents under extreme conditions using *Chlorella vulgaris*." Green Energy & Environment 1(2): 172-177.
- Singh, J., P. Yadav, A. K. Pal and V. Mishra (2020). "Water pollutants: Origin and status." Sensors in water pollutants monitoring: Role of material: 5-20.

- Sivaram, N. M. and D. Barik (2019). Chapter 5 - Toxic Waste From Leather Industries. In Elsevier eBooks (pp. 55–67). <https://doi.org/10.1016/b978-0-08-102528-4.00005-5>.
- Srivastava, V. and Y. Sharma (2014). "Synthesis and characterization of Fe<sub>3</sub>O<sub>4</sub>@n-SiO<sub>2</sub> nanoparticles from an agrowaste material and its application for the removal of Cr (VI) from aqueous solutions." Water, Air, & Soil Pollution 225: 1-16.
- Srivastava, V., Y. Sharma and M. Sillanpää (2015). "Response surface methodological approach for the optimization of adsorption process in the removal of Cr (VI) ions by Cu<sub>2</sub>(OH)<sub>2</sub>CO<sub>3</sub> nanoparticles." Applied Surface Science 326: 257-270.
- Sun, Y.-P., X.-q. Li, J. Cao, W.-x. Zhang and H. P. Wang (2006). "Characterization of zero-valent iron nanoparticles." Advances in colloid and interface science 120(1-3): 47-56.
- Tan, K. L. and B. H. Hameed (2017). "Insight into the adsorption kinetics models for the removal of contaminants from aqueous solutions." Journal of the Taiwan Institute of Chemical Engineers 74: 25-48.
- Tarekegn, M. M., A. M. Hiruy and A. H. Dekebo (2021). "Nano zero valent iron (nZVI) particles for the removal of heavy metals (Cd<sup>2+</sup>, Cu<sup>2+</sup> and Pb<sup>2+</sup>) from aqueous solutions." RSC advances 11(43): 27084-27084.
- Toli, A., K. Chalastara, C. Mystrioti, A. Xenidis and N. Papassiopi (2016). "Incorporation of zero valent iron nanoparticles in the matrix of cationic resin beads for the remediation of Cr (VI) contaminated waters." Environmental pollution 214: 419-429.
- Tsybulskaya, O., T. Ksenik, A. Yudakov and V. Slesarenko (2019). "Reagent decontamination of liquid chrome-containing industrial wastes." Environmental Technology & Innovation 13: 1-10.
- Vaiopoulou, E. and P. Gikas (2020). "Regulations for chromium emissions to the aquatic environment in Europe and elsewhere." Chemosphere 254: 126876.
- Vakili, M., S. Deng, T. Li, W. Wang, W. Wang and G. Yu (2018). "Novel crosslinked chitosan for enhanced adsorption of hexavalent chromium in acidic solution." Chemical Engineering Journal 347: 782-790.

Varjani, S., P. Rakholiya, T. Shindhal, A. V. Shah and H. H. Ngo (2021). "Trends in dye industry effluent treatment and recovery of value added products." Journal of Water Process Engineering 39: 101734.

Wang, T., S. Liu, W. Mao, Y. Bai, K. Chiang, K. Shah and J. Paz-Ferreiro (2020). "Novel Bi<sub>2</sub>WO<sub>6</sub> loaded N-biochar composites with enhanced photocatalytic degradation of rhodamine B and Cr (VI)." Journal of hazardous materials 389: 121827.

Wu, H., Wei, W., Xu, C., Meng, Y., Bai, W., Yang, W., & Lin, A. (2020). Polyethylene glycol-stabilized nano zero-valent iron supported by biochar for highly efficient removal of Cr (VI). Ecotoxicology and Environmental Safety, 188, 109902.

Xiu, Z.-m., Z.-h. Jin, T.-l. Li, S. Mahendra, G. V. Lowry and P. J. J. Alvarez (2010). "Effects of nano-scale zero-valent iron particles on a mixed culture dechlorinating trichloroethylene." Bioresource Technology 101(4): 1141-1146.

Xu, H., C. Qin, H. Zhang and Y. Zhao (2024). "New insights into long-lasting Cr(VI) removal from groundwater using in situ biosulfidated zero-valent iron with sulfate-reducing bacteria." Journal of Environmental Management 355: 120488.

Yoshinaga, M., H. Ninomiya, M. A. Al Hossain, M. Sudo, A. A. Akhand, N. Ahsan, M. A. Alim, M. Khalequzzaman, M. Iida and I. Yajima (2018). "A comprehensive study including monitoring, assessment of health effects and development of a remediation method for chromium pollution." Chemosphere 201: 667-675.

Younas, F., A. Mustafa, Z. U. R. Farooqi, X. Wang, S. Younas, W. Mohy-Ud-Din, M. Ashir Hameed, M. Mohsin Abrar, A. A. Maitlo and S. Noreen (2021). "Current and emerging adsorbent technologies for wastewater treatment: trends, limitations, and environmental implications." Water 13(2): 215.

Zablon, H. A., A. VonHandorf and A. Puga (2019). "Chromium exposure disrupts chromatin architecture upsetting the mechanisms that regulate transcription." Experimental Biology and Medicine 244(9): 752-757.

Zhao, Y., D. Kang, Z. Chen, J. Zhan and X. Wu (2018). "Removal of chromium using electrochemical approaches: a review." International journal of electrochemical science 13(2): 1250-1259.

Zhou, H., Ye, M., Zhao, Y., Baig, S. A., Huang, N., & Ma, M.. Sodium citrate and biochar synergistic improvement of nanoscale zero-valent iron composite for the removal of chromium in aqueous solutions. (2022) Journal of Environmental Sciences **115**, 227–239

# **APPENDICES**



	CA		BCA		NCA		BNCA	
pH	Cr(VI) Removal %	SD	Cr(VI) Removal %	SD	Cr(VI) Removal %	SD	Cr(VI) Removal %	SD
5	3	0.5	45	2.39	24	1.91	43	5.11
6	8.6	1.6	50	3.56	63	4.93	78	6.53
7	14.5	1.59	62	7.31	79	6.93	89	6.98
8	11	0.87	52	4.93	55	3.33	85	5.97
9	7.5	1.12	42	3.53	31	2.91	66	6.43

Table A.1: Cr(VI) removal percentage for different adsorbents in study under varying pH

	CA		BCA		NCA		BNCA	
Initial Cr(VI) concentration (ppm)	Cr(VI) Removal %	SD	Cr(VI) Removal %	SD	Cr(VI) Removal %	SD	Cr(VI) Removal %	SD
10	14	1	10	66	82	5.5	91	5.8
20	11	0.8	20	60	76	4.8	87	5.1
30	9.5	0.7	30	54	62	5.9	82	6.8
40	7.8	1.1	40	50	59	3.7	81	4.7
50	5.7	0.7	50	45	56	2.9	78	3.9

Table A.2: Cr(VI) removal percentage for different adsorbents in study under varying initial Cr(VI) concentration

	CA		BCA		NCA		BNCA	
<b>Time (min)</b>	<b>Cr(VI) Removal %</b>	<b>SD</b>	<b>Cr(VI) Removal %</b>	<b>SD</b>	<b>Cr(VI) Removal %</b>	<b>SD</b>	<b>Cr(VI) Removal %</b>	<b>SD</b>
<b>0</b>	0	0	0	0	0	0	0	0
<b>30</b>	9	2.3	33	1.9	58	3.2	67	5.5
<b>60</b>	13.5	1.9	57	4.5	73	6.5	79	5.9
<b>90</b>	15	1.3	64	3.9	78	4.4	90	7.1
<b>120</b>	15.5	1.8	63	4.2	77	3.9	91	7.5
<b>150</b>	15.8	1.5	65	3.5	79	3.2	88	5.45

Table A.3: Cr(VI) removal percentage for different adsorbents in study with time

	CA		BCA		NCA		BNCA	
<b>Dosage (g)</b>	<b>Cr(VI) Removal %</b>	<b>SD</b>	<b>Cr(VI) Removal %</b>	<b>SD</b>	<b>Cr(VI) Removal %</b>	<b>SD</b>	<b>Cr(VI) Removal %</b>	<b>SD</b>
<b>0</b>	0	0	0	0	0	0	0	0
<b>0.5</b>	4.5	0.8	9	1.1	45	4.3	58	5.1
<b>1.0</b>	7.6	1.1	25	3.5	62	5.1	69	4.2
<b>1.5</b>	14.3	2.3	49	4.2	72	6.4	75	4.3
<b>2.0</b>	15.1	2.5	63	5.3	77	6.6	89	5.5
<b>2.5</b>	14.9	1.8	63	5.5	80	8.2	93	6.2

Table A.4: Cr(VI) removal percentage for different adsorbents in study under varying adsorbent dosage

Input Variable	pH			
<b>Two-way RM ANOVA</b>				
Source of Variation	% of total variation	P value	P value summary	Significant?
Interaction	7.85	P<0.0001	***	Yes
pH	17.77	P<0.0001	***	Yes
Adsorbent Type	71.61	P<0.0001	***	Yes
Subjects (matching)	2.5496	P<0.0001	***	Yes
Source of Variation	Df	Sum-of-squares	Mean square	F
Interaction	12	3450	287.5	94.07
pH	4	7804	1951	638.4
Adsorbent Type	3	31460	10490	74.90
Subjects (matching)	8	1120	140.0	45.81
Residual	32	97.80	3.056	
<b>Bonferroni posttests</b>				
<b>Blank vs BCA</b>				
pH	Difference	t	P value	Summary
5	42.00	9.323	P<0.001	***
6	41.40	9.189	P<0.001	***
7	47.50	10.54	P<0.001	***
8	41.00	9.101	P<0.001	***
9	34.50	7.658	P<0.001	***
<b>Blank vs NCA</b>				
pH	Difference	t	P value	Summary
5	21.00	4.661	P<0.001	***
6	54.40	12.08	P<0.001	***
7	64.50	14.32	P<0.001	***
8	44.00	9.767	P<0.001	***
9	23.50	5.216	P<0.001	***
<b>Blank vs BNCA</b>				
pH	Difference	t	P value	Summary
5	40.00	8.879	P<0.001	***
6	69.40	15.40	P<0.001	***
7	74.50	16.54	P<0.001	***
8	74.00	16.43	P<0.001	***
9	58.50	12.99	P<0.001	***
<b>BCA vs NCA</b>				
pH	Difference	t	P value	Summary
5	-21.00	4.661	P<0.001	***
6	13.00	2.886	P < 0.05	*
7	17.00	3.773	P<0.01	**
8	3.000	0.6659	P > 0.05	ns
9	-11.00	2.442	P > 0.05	ns
<b>BCA vs BNCA</b>				
pH	Difference	t	P value	Summary

<b>5</b>	-2.000	0.4439	P > 0.05	ns
<b>6</b>	28.00	6.215	P<0.001	***
<b>7</b>	27.00	5.993	P<0.001	***
<b>8</b>	33.00	7.325	P<0.001	***
<b>9</b>	24.00	5.327	P<0.001	***
<b>NCA vs BNCA</b>				
<b>pH</b>	<b>Difference</b>	<b>t</b>	<b>P value</b>	<b>Summary</b>
<b>5</b>	19.00	4.217	P<0.001	***
<b>6</b>	15.00	3.330	P<0.01	**
<b>7</b>	10.00	2.220	P > 0.05	ns
<b>8</b>	30.00	6.659	P<0.001	***
<b>9</b>	35.00	7.769	P<0.001	***

Table A.5: Two way ANOVA analysis for effect of pH and adsorbent type on Cr(VI) removal percentage

<b>Input variable analyzed</b>	<b>Initial Cr(VI) concentration</b>			
<b>Two-way RM ANOVA</b>				
<b>Source of Variation</b>	<b>% of total variation</b>	<b>P value</b>	<b>P value summary</b>	<b>Significant?</b>
<b>Interaction</b>	1.01	P<0.0001	***	Yes
<b>Initial Cr(VI) Concentration</b>	4.67	P<0.0001	***	Yes
<b>Type of adsorbent</b>	92.05	P<0.0001	***	Yes
<b>Subjects (matching)</b>	2.1778	P<0.0001	***	Yes
<b>Source of Variation</b>	<b>Df</b>	<b>Sum-of-squares</b>	<b>Mean square</b>	<b>F</b>
<b>Interaction</b>	12	498.0	41.50	30.26
<b>Initial Cr(VI) Concentration</b>	4	2306	576.4	420.3
<b>Type of adsorbent</b>	3	45440	15150	112.7
<b>Subjects (matching)</b>	8	1075	134.4	97.99
<b>Residual</b>	32	43.88	1.371	
<b>Bonferroni posttests</b>				
<b>Blank vs BCA</b>				
<b>Initial Cr(VI) Concentration</b>	<b>Difference</b>	<b>t</b>	<b>P value</b>	<b>Summary</b>
<b>10</b>	52.00	12.04	P<0.001	***
<b>20</b>	49.00	11.35	P<0.001	***
<b>30</b>	44.50	10.30	P<0.001	***
<b>40</b>	42.20	9.772	P<0.001	***
<b>50</b>	39.30	9.101	P<0.001	***
<b>Blank vs NCA</b>				
<b>Initial Cr(VI) Concentration</b>	<b>Difference</b>	<b>t</b>	<b>P value</b>	<b>Summary</b>
<b>10</b>	68.00	15.75	P<0.001	***
<b>20</b>	65.00	15.05	P<0.001	***
<b>30</b>	52.50	12.16	P<0.001	***
<b>40</b>	51.20	11.86	P<0.001	***
<b>50</b>	50.30	11.65	P<0.001	***
<b>Blank vs BNCA</b>				
<b>Initial Cr(VI) Concentration</b>	<b>Difference</b>	<b>t</b>	<b>P value</b>	<b>Summary</b>
<b>10</b>	77.00	17.83	P<0.001	***
<b>20</b>	76.00	17.60	P<0.001	***
<b>30</b>	72.50	16.79	P<0.001	***
<b>40</b>	73.20	16.95	P<0.001	***
<b>50</b>	72.30	16.74	P<0.001	***
<b>BCA vs NCA</b>				
<b>Initial Cr(VI) Concentration</b>	<b>Difference</b>	<b>t</b>	<b>P value</b>	<b>Summary</b>
<b>10</b>	16.00	3.705	P<0.01	**
<b>20</b>	16.00	3.705	P<0.01	**
<b>30</b>	8.000	1.853	P > 0.05	ns
<b>40</b>	9.000	2.084	P > 0.05	ns
<b>50</b>	11.00	2.547	P > 0.05	ns

<b>BCA vs BNCA</b>				
<b>Initial Cr(VI) Concentration</b>	<b>Difference</b>	<b>t</b>	<b>P value</b>	<b>Summary</b>
<b>10</b>	25.00	5.789	P<0.001	***
<b>20</b>	27.00	6.252	P<0.001	***
<b>30</b>	28.00	6.484	P<0.001	***
<b>40</b>	31.00	7.179	P<0.001	***
<b>50</b>	33.00	7.642	P<0.001	***
<b>NCA vs BNCA</b>				
<b>Initial Cr(VI) Concentration</b>	<b>Difference</b>	<b>t</b>	<b>P value</b>	<b>Summary</b>
<b>10</b>	9.000	2.084	P > 0.05	ns
<b>20</b>	11.00	2.547	P > 0.05	ns
<b>30</b>	20.00	4.631	P<0.001	***
<b>40</b>	22.00	5.094	P<0.001	***
<b>50</b>	22.00	5.094	P<0.001	***

Table A.6: Two way ANOVA analysis for effect of initial Cr(VI) concentration and adsorbent type on Cr(VI) removal percentage

Input variable	Time			
<b>Two-way RM ANOVA</b>				
Source of Variation	% of total variation	P value	P value summary	Significant?
Interaction	9.78	P<0.0001	***	Yes
Time	44.75	P<0.0001	***	Yes
Adsorbent type	44.02	P<0.0001	***	Yes
Subjects (matching)	1.1567	P<0.0001	***	Yes
Source of Variation	Df	Sum-of-squares	Mean square	F
Interaction	15	7781	518.7	89.71
Time	5	35590	7118	1231
Adsorbent type	3	35020	11670	101.5
Subjects (matching)	8	920.0	115.0	19.89
Residual	40	231.3	5.782	
<b>Bonferroni posttests</b>				
<b>Blank vs BCA</b>				
Time	Difference	t	P value	Summary
0.0000	0.0000	0.0000	P > 0.05	Ns
30.00	24.00	6.002	P<0.001	***
60.00	43.50	10.88	P<0.001	***
90.00	49.00	12.25	P<0.001	***
120.0	47.50	11.88	P<0.001	***
150.0	49.20	12.30	P<0.001	***
<b>Blank vs NCA</b>				
Time	Difference	t	P value	Summary
0.0000	0.0000	0.0000	P > 0.05	Ns
30.00	49.00	12.25	P<0.001	***
60.00	59.50	14.88	P<0.001	***
90.00	63.00	15.75	P<0.001	***
120.0	61.50	15.38	P<0.001	***
150.0	63.20	15.80	P<0.001	***
<b>Blank vs BNCA</b>				
Time	Difference	t	P value	Summary
0.0000	0.0000	0.0000	P > 0.05	Ns
30.00	58.00	14.50	P<0.001	***
60.00	65.50	16.38	P<0.001	***
90.00	75.00	18.76	P<0.001	***
120.0	75.50	18.88	P<0.001	***
150.0	72.20	18.06	P<0.001	***
<b>BCA vs NCA</b>				
Time	Difference	t	P value	Summary
0.0000	0.0000	0.0000	P > 0.05	ns
30.00	25.00	6.252	P<0.001	***
60.00	16.00	4.001	P<0.01	**
90.00	14.00	3.501	P<0.01	**
120.0	14.00	3.501	P<0.01	**

150.0	14.00	3.501	P<0.01	**
<b>BCA vs BNCA</b>				
<b>Time</b>	<b>Difference</b>	<b>t</b>	<b>P value</b>	<b>Summary</b>
0.0000	0.0000	0.0000	P > 0.05	ns
30.00	34.00	8.503	P<0.001	***
60.00	22.00	5.502	P<0.001	***
90.00	26.00	6.502	P<0.001	***
120.0	28.00	7.002	P<0.001	***
150.0	23.00	5.752	P<0.001	***
<b>NCA vs BNCA</b>				
<b>Time</b>	<b>Difference</b>	<b>t</b>	<b>P value</b>	<b>Summary</b>
0.0000	0.0000	0.0000	P > 0.05	ns
30.00	9.000	2.251	P > 0.05	ns
60.00	6.000	1.500	P > 0.05	ns
90.00	12.00	3.001	P < 0.05	*
120.0	14.00	3.501	P<0.01	**
150.0	9.000	2.251	P > 0.05	ns

Table A.7: Two way ANOVA analysis for effect of time and adsorbent type on Cr(VI) removal percentage



Input variable	Adsorbent Dosage			
<b>Two-way RM ANOVA</b>				
<b>Source of Variation</b>	<b>% of total variation</b>	<b>P value</b>	<b>P value summary</b>	<b>Significant?</b>
Interaction	11.65	P<0.0001	***	Yes
Adsorbent dosage	44.51	P<0.0001	***	Yes
Adsorbent type	42.26	P<0.0001	***	Yes
Subjects (matching)	1.2231	P<0.0001	***	Yes
<b>Source of Variation</b>	<b>Df</b>	<b>Sum-of-squares</b>	<b>Mean square</b>	<b>F</b>
Interaction	15	8884	592.3	88.10
Adsorbent dosage	5	33950	6790	1010
Adsorbent type	3	32230	10740	92.14
Subjects (matching)	8	932.8	116.6	17.34
Residual	40	268.9	6.723	
<b>Bonferroni posttests</b>				
<b>Blank vs BCA</b>				
<b>Adsorbent Dosage</b>	<b>Difference</b>	<b>t</b>	<b>P value</b>	<b>Summary</b>
0.0000	0.0000	0.0000	P > 0.05	Ns
0.0500	4.500	1.101	P > 0.05	Ns
0.1000	17.40	4.259	P<0.001	***
0.1500	34.70	8.494	P<0.001	***
0.2000	47.90	11.72	P<0.001	***
0.2500	48.10	11.77	P<0.001	***
<b>Blank vs NCA</b>				
<b>Adsorbent Dosage</b>	<b>Difference</b>	<b>t</b>	<b>P value</b>	<b>Summary</b>
0.0000	0.0000	0.0000	P > 0.05	ns
0.0500	40.50	9.913	P<0.001	***
0.1000	54.40	13.32	P<0.001	***
0.1500	57.70	14.12	P<0.001	***
0.2000	61.90	15.15	P<0.001	***
0.2500	65.10	15.93	P<0.001	***
<b>Blank vs BNCA</b>				
<b>Adsorbent Dosage</b>	<b>Difference</b>	<b>t</b>	<b>P value</b>	<b>Summary</b>
0.0000	0.0000	0.0000	P > 0.05	ns
0.0500	53.50	13.10	P<0.001	***
0.1000	61.40	15.03	P<0.001	***
0.1500	60.70	14.86	P<0.001	***
0.2000	73.90	18.09	P<0.001	***
0.2500	78.10	19.12	P<0.001	***
<b>BCA vs NCA</b>				
<b>Adsorbent Dosage</b>	<b>Difference</b>	<b>t</b>	<b>P value</b>	<b>Summary</b>
0.0000	0.0000	0.0000	P > 0.05	ns
0.0500	36.00	8.812	P<0.001	***
0.1000	37.00	9.057	P<0.001	***
0.1500	23.00	5.630	P<0.001	***

<b>0.2000</b>	14.00	3.427	P<0.01	**
<b>0.2500</b>	17.00	4.161	P<0.001	***
<b>BCA vs BNCA</b>				
<b>Adsorbent Dosage</b>	<b>Difference</b>	<b>t</b>	<b>P value</b>	<b>Summary</b>
<b>0.0000</b>	0.0000	0.0000	P > 0.05	ns
<b>0.0500</b>	49.00	11.99	P<0.001	***
<b>0.1000</b>	44.00	10.77	P<0.001	***
<b>0.1500</b>	26.00	6.364	P<0.001	***
<b>0.2000</b>	26.00	6.364	P<0.001	***
<b>0.2500</b>	30.00	7.343	P<0.001	***
<b>NCA vs BNCA</b>				
<b>Adsorbent Dosage</b>	<b>Difference</b>	<b>t</b>	<b>P value</b>	<b>Summary</b>
<b>0.0000</b>	0.0000	0.0000	P > 0.05	ns
<b>0.0500</b>	13.00	3.182	P < 0.05	*
<b>0.1000</b>	7.000	1.713	P > 0.05	ns
<b>0.1500</b>	3.000	0.7343	P > 0.05	ns
<b>0.2000</b>	12.00	2.937	P < 0.05	*
<b>0.2500</b>	13.00	3.182	P < 0.05	*

Table A.8: Two way ANOVA analysis for effect of adsorbent dosage and adsorbent type on Cr(VI) removal percentage

Time (m)	C/Co (H=4 cm)	C/Co (H=8 cm)	C/Co (H=12 cm)
0	0	0	0
10	0	0	0
20	0	0	0
30	0	0	0
40	0.024	0	0
50	0.04	0	0
60	0.1	0	0
70	0.189	0.025	0
80	0.228	0.04	0
90	0.288	0.089	0
100	0.309	0.15	0
110	0.349	0.21	0
120	0.359	0.25	0.049
130	0.388	0.28	0.1
140	0.409	0.32	0.125
150	0.459	0.36	0.185
160	0.48	0.37	0.212
170	0.508	0.39	0.269
180	0.529	0.398	0.31
190	0.558	0.412	0.369
200	0.59	0.46	0.375
210	0.66	0.487	0.385
220	0.71	0.496	0.388
230	0.778	0.526	0.389
240	0.849	0.556	0.412
250	0.88	0.587	0.42
260	0.888	0.622	0.456
270	0.909	0.687	0.489
280	0.93	0.698	0.523
290	0.948	0.723	0.558
300	0.98	0.756	0.589
310	1	0.789	0.598
320	1	0.816	0.612
330	1	0.835	0.635

Time (m)	C/Co (H=4 cm)	C/Co (H=8 cm)	C/Co (H=12 cm)
340	-	0.867	0.669
350	-	0.897	0.698
360	-	0.921	0.725
370	-	0.935	0.754
380	-	0.956	0.778
390	-	0.98	0.802
400	-	0.985	0.812
410	-	0.992	0.821
420	-	0.997	0.823
430	-	1	0.856
440	-	1	0.887
450	-	1	0.898
460	-	-	0.889
470	-	-	0.91
480	-	-	0.926
490	-	-	0.935
500	-	-	0.956
510	-	-	0.966
520	-	-	0.989
530	-	-	0.991
540	-	-	0.995
550	-	-	1
560	-	-	1
570	-	-	1
580	-	-	1
590	-	-	1

Table A.9: Variation of C/C0 with time for fixed bed column under variable bed height with synthetic wastewater

Time (m)	C/Co (F=0.5 ml/min)	C/Co (F=1.0 ml/min)	C/Co (F=1.5 ml/min)
0	0	0	0
10	0	0	0
20	0	0	0
30	0	0	0
40	0	0	0.049
50	0	0	0.125
60	0	0	0.185
70	0	0.025	0.269
80	0	0.04	0.31
90	0	0.089	0.375
100	0	0.15	0.432
110	0	0.21	0.455
120	0	0.25	0.456
130	0.019476	0.28	0.489
140	0.04	0.32	0.589
150	0.085	0.36	0.635
160	0.118	0.37	0.698
170	0.143	0.39	0.724
180	0.178	0.398	0.735
190	0.205	0.412	0.778
200	0.209	0.46	0.812
210	0.216	0.487	0.856
220	0.241	0.496	0.898
230	0.252	0.526	0.966
240	0.277	0.556	0.995
250	0.298	0.587	1
260	0.309	0.622	1
270	0.318	0.687	1
280	0.341	0.698	-
290	0.353	0.723	-
300	0.376	0.756	-
310	0.409	0.789	-
320	0.422	0.816	-
330	0.447	0.835	-

Time (m)	C/Co (F=0.5 ml/min)	C/Co (F=1.0 ml/min)	C/Co (F=1.5 ml/min)
340	0.451	0.867	-
350	0.452	0.897	-
360	0.478	0.921	-
370	0.488	0.935	-
380	0.498	0.956	-
390	0.524	0.98	-
400	0.544	0.985	-
410	0.573	0.992	-
420	0.618	0.997	-
430	0.628	1	-
440	0.645	1	-
450	0.685	1	-
460	0.708	-	-
470	0.732	-	-
480	0.756	-	-
490	0.776	-	-
500	0.766	-	-
510	0.809	-	-
520	0.845	-	-
530	0.868	-	-
540	0.876	-	-
550	0.907	-	-
560	0.918	-	-
570	0.92	-	-
580	0.92	-	-
590	0.92	-	-
600	0.95	-	-
610	0.975	-	-
620	1	-	-
630	1	-	-
640	1	-	-

Table A.10: Variation of C/C0 with time for fixed bed column under variable flow rate with synthetic wastewater

Time (m)	C/Co (H=4 cm)	C/Co (H=8 cm)	C/Co (H=12 cm)
0	0	0	0
10	0	0	0
20	0	0	0
30	0.022	0	0
40	0.055	0	0
50	0.087	0.019	0
60	0.12	0.043	0
70	0.128	0.0932	0.036
80	0.226	0.134	0.078
90	0.229	0.166	0.112
100	0.35	0.223	0.178
110	0.41	0.298	0.222
120	0.47	0.356	0.265
130	0.53	0.412	0.298
140	0.58	0.468	0.334
150	0.672	0.5	0.367
160	0.712	0.567	0.398
170	0.768	0.582	0.466
180	0.823	0.634	0.49
190	0.866	0.678	0.563
200	0.892	0.706	0.59
210	0.923	0.734	0.632
220	0.954	0.792	0.675
230	0.987	0.834	0.734
240	0.99	0.887	0.756
250	0.99	0.892	0.782
260	0.99	0.924	0.812
270	1	0.934	0.847
280	1	0.967	0.872
290	-	0.985	0.89
300	-	0.99	0.912

Time (m)	C/Co (H=4 cm)	C/Co (H=8 cm)	C/Co (H=12 cm)
310	-	0.99	0.919
320	-	0.99	0.922
330	-	0.99	0.934
340	-	1	0.968
350	-	1	0.98
360	-	-	0.99
370	-	-	0.99
380	-	-	0.99
390	-	-	0.999
400	-	-	1
410	-	-	1

Table A.11: Variation of C/C0 with time for fixed bed column under variable bed height with spiked real wastewater

Time (m)	C/Co (F=0.5 ml/min)	C/Co (F=1.0 ml/min)	C/Co (F=1.5 ml/min)
0	0	0	0
10	0	0	0
20	0	0	0
30	0	0	0
40	0	0	0.076
50	0	0.019	0.12
60	0	0.043	0.192
70	0	0.0932	0.245
80	0	0.134	0.276
90	0.021	0.166	0.312
100	0.053	0.223	0.376
110	0.093	0.298	0.434
120	0.134	0.356	0.49
130	0.168	0.412	0.564
140	0.198	0.468	0.612
150	0.225	0.5	0.676
160	0.278	0.567	0.73
170	0.312	0.582	0.77
180	0.336	0.634	0.845
190	0.364	0.678	0.9
200	0.38	0.706	0.935
210	0.423	0.734	0.98
220	0.468	0.792	0.99
230	0.493	0.834	0.99
240	0.523	0.887	1
250	0.555	0.892	1
260	0.575	0.924	1
270	0.589	0.934	-
280	0.612	0.967	-
290	0.634	0.985	-
300	0.648	0.99	-

Time (m)	C/Co (F=0.5 ml/min)	C/Co (F=1.0 ml/min)	C/Co (F=1.5 ml/min)
310	0.656	0.99	-
320	0.678	0.99	-
330	0.709	0.99	-
340	0.724	1	-
350	0.744	1	-
360	0.767	-	-
370	0.77	-	-
380	0.79	-	-
390	0.834	-	-
400	0.848	-	-
410	0.873	-	-
420	0.893	-	-
430	0.922	-	-
440	0.936	-	-
450	0.976	-	-
460	0.983	-	-
470	0.99	-	-
480	0.99	-	-
490	0.99	-	-
500	1	-	-
510	1	-	-
520	1	-	-

Table A.12: Variation of C/C0 with time for fixed bed column under variable flow rate with spiked real wastewater

No of cycle	% Cr(VI) removal	SD
Cycle 1	92	1.5
Cycle 2	89	1.2
Cycle 3	91	1.1
Cycle 4	87	0.89

Table A.13: Cr(VI) removal percentage under four cycles of adsorbent regeneration

One-way ANOVA for reuse of adsorbent			
P value	0.9998		
P value summary	ns		
Are means signif. different? (P < 0.05)	No		
Number of groups	4		
F	0.002262		
R squared	0.0008474		
ANOVA Table			
	SS	df	MS
Treatment (between columns)	17.36	3	5.785
Residual (within columns)	20460	8	2558
Total	20480	11	

Table A.14: ANOVA table for effect of adsorbent reuse on Cr(VI) removal percentage

### **List of publications**

1. **Shashank Garg**, Simranjeet Singh, Nadeem A. Khan, Justin Samuel, Praveen C. Ramamurthy & Joginder Singh. (2023). Equilibrium and kinetic modeling of Cr(VI) removal by novel tolerant bacteria species along with zero-valent iron nanoparticles. Scientific Reports, **Accepted**, <https://doi.org/10.1038/s41598-024-57835-z>
2. Garg, Shashank, Simranjeet Singh, Nabila Shehata, HariBhakta Sharma, Justin Samuel, Nadeem A. Khan, Praveen C. Ramamurthy et al. "Aerogels in wastewater treatment: A review." Journal of the Taiwan Institute of Chemical Engineers (2023): 105299. <https://doi.org/10.1016/j.jtice.2023.105299>





OPEN **Equilibrium and kinetic modeling of Cr(VI) removal by novel tolerant bacteria species along with zero-valent iron nanoparticles**

Shashank Garg<sup>1,6</sup>, Simranjeet Singh<sup>2,6</sup>, Nadeem A. Khan<sup>3</sup>, Jastin Samuel<sup>4</sup>, Praveen C. Ramamurthy<sup>2</sup> & Joginder Singh<sup>5</sup>

This work describes the study of the removal of a refractory contaminant, i.e., Hexavalent chromium (Cr(VI)) from aqueous systems by a novel adsorbent comprising Cr(VI) tolerant bacteria and zero valent iron nanoparticle (nZVI). A gram-positive, rod-shaped bacteria used in the study were isolated from wastewater (WW) received from the effluent of leather industries. The adsorbents were prepared with bacteria, nZVI alone, and a combination of both. The adsorbent comprising both elements was found to remove Cr(VI) with a higher percentage (93%) and higher capacities (0.58 mg/g) as compared to adsorbent with bacteria (Cr(VI) removal = 63%,  $q_s = 0.163$  mg/g) or nanoparticles (Cr(VI) removal = 80%,  $q_s = 0.45$  mg/g) alone. The adsorbent worked best at neutral pH, and the removal became saturated after 90 min of incubation. Equilibrium studies with isotherm modeling suggested that the adsorption process follows sips isotherm ( $R^2 = 0.9955$ ), which is expected to be an intra-particle diffusion process before the actual adsorption. Process kinetics was modeled with pseudo-first order, pseudo-second order, and Vermeulen model. The diffusion coefficient determined by fitting the kinetic data to Vermeulen model was found to be  $0.0000314$  cm<sup>2</sup>/s. The adsorbent can be tested further for continuous flow processes to find more insights about the usage on a large scale.

**Keywords** Hexavalent chromium, Nanobioadsorbent, Zerovalent iron, Isotherm, Modeling, Kinetics

The main reasons for increasing environmental pollution levels are the expanding population and industrialization<sup>1,2</sup>. Researchers are primarily concerned about water contamination resulting from industrial waste emissions containing significant amounts of organic and inorganic contaminants from industries like textile, food, dye, and paint<sup>3-5</sup>. Hexavalent chromium Cr(VI) is now regarded amongst the significant environmental pollutants due to its increasing use in the majority of industrial processes (leather processing, electroplating, printing, dyeing, and metallurgy), which causes disease in life forms<sup>6-8</sup>. Several industry unit operations produce chromium-containing chemical species, of which trivalent chromium Cr(III) and Cr(VI) are the most common. These chromium species are accumulating in natural waters due to improper disposal of these industries' effluent water, which is deadly for plants and animals because chromium is carcinogenic and mutagenic to a certain extent<sup>9</sup>. This addresses the uproaring demand for sustainable, easy, and economical methods for properly disposing Cr(VI) bearing wastewater. A study on inhabitants of Kanpur, India (an area with a lot of tanneries and chromium salts manufacturing industries), has revealed that impaired hemoglobin function and gastrointestinal and dermatological symptoms are linked to elevated concentrations of Cr(VI) in groundwater<sup>10</sup>.

<sup>1</sup>Department of Biotechnology, Lovely Professional University, Phagwara, Punjab 144411, India. <sup>2</sup>Interdisciplinary Centre for Water Research (ICWaR), Indian Institute of Science, Bangalore 560012, India. <sup>3</sup>Interdisciplinary Research Center for Membranes and Water Security, King Fahd University of Petroleum and Minerals, Dhahran, 31261, Saudi Arabia. <sup>4</sup>Waste Valorization Research Lab, Lovely Professional University, Phagwara, Punjab 144411, India. <sup>5</sup>Department of Botany, Nagaland University, HQRS: Lumami, Nagaland 798627, India. <sup>6</sup>These authors contributed equally: Shashank Garg and Simranjeet Singh. ✉email: er.nadimcivil@gmail.com; onegroup203@gmail.com; joginder@nagalanduniversity.ac.in



ELSEVIER

Contents lists available at ScienceDirect

Journal of the Taiwan Institute of Chemical Engineers

journal homepage: [www.journals.elsevier.com/journal-of-the-taiwan-institute-of-chemical-engineers](http://www.journals.elsevier.com/journal-of-the-taiwan-institute-of-chemical-engineers)

## Aerogels in wastewater treatment: A review

Shashank Garg<sup>a,1</sup>, Simranjeet Singh<sup>b,1</sup>, Nabila Shehata<sup>c</sup>, HariBhakta Sharma<sup>d</sup>, Jastin Samuel<sup>e</sup>, Nadeem A Khan<sup>f,1</sup>, Praveen C Ramamurthy<sup>b,\*</sup>, Joginder Singh<sup>g,\*</sup>, Muhammad Mubashir<sup>h,1</sup>, Awais Bokhari<sup>i,k</sup>, Der Jiun Ooi<sup>l</sup>, Pau Loke Show<sup>m,2</sup>

<sup>a</sup> Department of Biotechnology, Lovely Professional University, Phagwara 144411, Punjab, India

<sup>b</sup> Interdisciplinary Centre for Water Research (ICWaR), Indian Institute of Science, Bangalore 560012, India

<sup>c</sup> Environmental Science and Industrial Development Department, Faculty of Postgraduate Studies for Advanced Sciences, Beni-Suef University, Egypt

<sup>d</sup> Department of Civil Engineering, Sikkim Manipal Institute of Technology, Sikkim -737136, India

<sup>e</sup> Waste Valorization Research Lab, Lovely Professional University, Phagwara - 144411, Punjab, India

<sup>f</sup> Interdisciplinary Research Center for Membranes and Water Security, King Fahd University of Petroleum and Minerals, Saudi Arabia

<sup>g</sup> Department of Botany, Nagaland University, HQRS: Lumami, Nagaland 798627, India

<sup>h</sup> Saline Water Conversion Corporation (SWCC)- Water Technologies Innovation Institute & Research Advancement-WTIIRA, Saudi Arabia

<sup>i</sup> Faculty of Science, Technology and Medicine, University of Luxembourg, 2, Avenue de l'Université, Esch-sur-Alzette, Luxembourg

<sup>j</sup> School of Engineering, Lebanese American University, Byblos, Lebanon

<sup>k</sup> Sustainable Process Integration Laboratory, SPIL, NETME Centre, Faculty of Mechanical Engineering, Brno University of Technology, VUT Brno, Technická 2896/2, Brno 61600, Czech Republic

<sup>l</sup> Department of Oral Biology and Biomedical Sciences, Faculty of Dentistry, MAHSA University, Jenjarom, Selangor 42610, Malaysia

<sup>m</sup> Department of Chemical Engineering, Khalifa University, Shakhboub Bin Sultan St - Zone 1 - Abu Dhabi - United Arab Emirates

## ARTICLE INFO

## Keywords:

Aerogels  
Water/wastewater treatment  
Adsorption  
Isotherms  
Kinetics  
Life cycle assessment

## ABSTRACT

**Background:** Aerogels are highly porous and light-weighted materials with extensive surface areas. The remarkable thermal, mechanical, and chemical properties render them ideally suited as adsorbents in water/wastewater treatment.

**Methods:** Specific search queries were used to retrieve research articles from several databases like Scopus, PubMed, and Google Scholar. The papers explicitly related to the treatment of water/wastewater by different aerogels were then screened and used to collect information related to the mechanism, kinetics, isotherms, removal efficiencies, and life cycle assessments of aerogels. This review discussed the recent advances in aerogels preparation as well.

**Significant Findings:** Aerogels prepared using natural, synthetic or hybrid materials could be loaded with different functional nanoparticles or subjected to chemical surface modification for efficiency enhancement. Significant advances have been made to remove various contaminants from wastewater using aerogels. Particularly, these functions are highly dependent on the pH of the medium and initial adsorbate concentration. The mechanism of adsorption is mainly chemisorption with ion exchange as a mediating process, where the adsorption process generally follows Langmuir isotherm and reaction kinetics of adsorption is mostly pseudo-second-order. It was found that solution pH, pKa of adsorbate, pH value at zero charges of adsorbent, and specific surface area of adsorbent are the major factors influencing the adsorption capabilities of aerogels from the perspective of kinetics and isotherms. Future research could investigate the unique structure of aerogels for surface engineering and functionalization to enhance overall efficiencies, as well as explore the use of waste materials to produce aerogels, thereby lowering costs and improving sustainability.

## 1. Introduction

Water contamination by industrial and municipal wastewater has

been a long-standing issue. The contamination of water bodies directly or indirectly causes detrimental impacts on all types of biological forms. Heavy metals are a major source of chronic and non-biodegradable

\* Corresponding authors.

E-mail addresses: [praveen@iisc.ac.in](mailto:praveen@iisc.ac.in) (P.C. Ramamurthy), [joginder@nagalanduniversity.ac.in](mailto:joginder@nagalanduniversity.ac.in) (J. Singh), [PauLoke.Show@ku.ac.ae](mailto:PauLoke.Show@ku.ac.ae) (P.L. Show).

<sup>1</sup> These authors equally contributed equally to this work.

<https://doi.org/10.1016/j.jtice.2023.105299>


Received 2 May 2023; Received in revised form 20 November 2023; Accepted 11 December 2023

1876-1070/© 2023 Published by Elsevier B.V. on behalf of Taiwan Institute of Chemical Engineers.

### **List of conferences**


1. Oral Presentation on the topic entitled **Studies on removal of hexavalent chromium from aqueous environment with novel hybrid adsorbent** in the **International Conference on Bioengineering and Biosciences (ICBB-2022)** held on **18-19 November 2022** organized by the Department of Biotechnology, School of Bio-engineering and Biosciences in association with the Society of Bioinformatics for Experimenting Scientists (Bioclues) organized at Lovely Professional University, Punjab.
2. Presented a paper entitled “**Fixed-Bed Column Adsorption Studies: Evaluation Of Alginate-Based Nanobioadsorbents Removal Of Cr(VI)**” in the **International Conference on Sustainable Experimentation and Modeling in Civil Engineering (SEMCE- 2023)** held on **August 10-11, 2023**, organized by the School of Civil Engineering, Lovely Professional University, Punjab in association with the Department of Civil Engineering, Dr B R Ambedkar National Institute of Technology, Jalandhar

Certificate No.257761



**L**OVELY  
**P**ROFESSIONAL  
**U**NIVERSITY


*Transforming Education Transforming India*





## Certificate of Participation

This is to certify that **Prof./Dr./Mr./Ms. Shashank Garg** of **Lovely Professional University** has participated in **Oral Presentation** on the topic entitled **Studies on removal of hexavalent chromium from aqueous environment with novel hybrid adsorbent** in the International Conference on **Bioengineering and Biosciences (ICBB-2022)** held on **18-19 November 2022** organized by the Department of Biotechnology, School of Bio-engineering and Biosciences in association with the Society of Bioinformatics for Experimenting Scientists (Bioclues) organized at Lovely Professional University, Punjab.


Date of Issue : 07-12-2022  
Place: Phagwara (Punjab), India

  
 Prepared by  
(Administrative Officer-Records)

  
 Dr. Himanshu Singh  
Organizing Secretary, ICBB, 2022


  
 Dr. Neeta Raj Sharma  
Convener, ICBB, 2022

Certificate No. 287489



**L**OVELY  
**P**ROFESSIONAL  
**U**NIVERSITY


*Transforming Education Transforming India*





## Certificate of Paper Presentation


This is to certify that **Dr./Mr./Ms. Shashank Garg** of **Lovely Professional University, Phagwara** has presented a paper entitled **"Fixed-Bed Column Adsorption Studies: Evaluation Of Alginate-Based Nanobioadsorbents Removal Of Cr(VI)"** in the International Conference on **Sustainable Experimentation and Modeling in Civil Engineering (SEMCE-2023)** held on **August 10-11, 2023**, organized by the School of Civil Engineering, Lovely Professional University, Punjab in association with the Department of Civil Engineering, Dr B R Ambedkar National Institute of Technology, Jalandhar.

Date of Issue : 29-08-2023  
Place : Phagwara (Punjab), India

  
 Prepared by  
(Administrative Officer-Records)

  
 Program chair  
(SEMCE-2023)

  
 General Chair  
(SEMCE-2023)

  
 Organizing Secretary  
(SEMCE-2023)